Deployable Stable Lasers for Gravitational Wave Interferometers

by

David J. Hosken

Thesis submitted for the degree of
Doctor of Philosophy
in
The University of Adelaide
School of Chemistry and Physics
September, 2008

Appendix A

Publications

This appendix contains publications both associated with and arising as a result of this work.

A.1 Publications associated with this work

A.1.1 Development of Power Scalable Lasers for Gravitational Wave Interferometry

D. J. Hosken, D. Mudge, C. Hollitt, K. Takeno, P. J. Veitch, M. W. Hamilton and J. Munch, *Prog. Theor. Phys. Supp.*, **151**, 216-220 (May, 2003)

Hosken, D.J., Mudge, D., Hollitt, C., Takeno, K., Veitch, P.J., Hamilton, M.W. and Munch, J. (2003) Development of power scalable lasers for gravitational wave interferometry.
Progress of Theoretical Physics Supplement, no. 151, pp. 216-220

A.2 Publications arising as a result of this thesis

A.2.1 Compensation of Strong Thermal Lensing in High-Optical-Power Cavities

C. Zhao, J. Degallaix, L. Ju, Y. Fan, D. G. Blair, B. J. J. Slagmolen, M. B. Gray, C.M. Mow Lowry, D. E. McClelland, D. J. Hosken, D. Mudge, A. Brooks, J. Munch, P. J. Veitch, M. A. Barton and G. Billingsley, *Phys. Rev. Lett.*, **96**, 231101(4), (Jun., 2006)

C. Zhao, J. Degallaix, L. Ju, Y. Fan, D. G. Blair, B. J. Slagmolen, M. B. Gray, C. M. Lowry, D. E. McClelland, D. J. Hosken, D. Mudge, A. Brooks, J. Munch, P. J. Veitch, M. A. Barton, and G. Billingsley (2006) Compensation of Strong Thermal Lensing in High-Optical-Power Cavities
Physical Review Letters, v. 96 (23) , pp. 231101-1 - 231101-4, June 2006

A.2.2 Gingin High Optical Power Test Facility

C. Zhao, D.G. Blair, P. Barrigo, J. Degallaix, J-C Dumas, Y. Fan, S. Gras, L. Ju, B. Lee, S. Schediwy, Z. Yan, D.E. McClelland, S.M. Scott, M.B. Gray, A.C. Searle, S. Gossler, B.J.J. Slagmolen, J. Dickson, K. McKenzie, C. Mow-Lowry, A. Moylan, D. Rabeling, J. Cumpston, K. Wette, J. Munch, P.J. Veitch, D. Mudge, A. Brooks, and D. Hosken, *J. Phys.: Conf. Ser.*, **32**, 368-373, (2006)

Institute of Physics Publishing
doi:10.1088/1742-6596/32/1/056

Journal of Physics: Conference Series **32** (2006) 368–373
Sixth Edoardo Amaldi Conference on Gravitational Waves

Gingin High Optical Power Test Facility

C. Zhao, D.G. Blair, P. Barrigo, J. Degallaix, J-C Dumas, Y. Fan, S. Gras, L. Ju, B. Lee, S. Schediwy, Z. Yan

School of Physics, The University of Western Australia, Crawley, Western Australia, 6009 Australia

D.E. McClelland, S.M. Scott, M.B. Gray, A.C. Searle, S. Gossler, B.J.J. Slagmolen, J. Dickson, K. McKenzie, C. Mow-Lowry, A. Moylan, D. Rabeling, J. Cumpston, K. Wette

Centre for Gravitational Physics, The Australian National University, Canberra, 0200, Australia

J. Munch, P.J. Veitch, D. Mudge, A. Brooks, and D. Hosken

Deaprtment of Physics, The University of Adelaide, Adelaide, South Australia, 5005 Australia

zhao@physics.uwa.edu.au

Abstract. The Australian Consortium for Gravitational Wave Astronomy (ACIGA) in collaboration with LIGO is developing a high optical power research facility at the AIGO site, Gingin, Western Australia. Research at the facility will provide solutions to the problems that advanced gravitational wave detectors will encounter with extremely high optical power. The problems include thermal lensing and parametric instabilities. This article will present the status of the facility and the plan for the future experiments.

A.2.3 Observation of three-mode parametric interactions in long optical cavities

C. Zhao, L. Ju, Y. Fan, S. Gras, B. J. J. Slagmolen, H. Miao, P. Barriga, D. G. Blair, D. J. Hosken, A. F. Brooks, P. J. Veitch, D. Mudge and J. Munch, *Phys. Rev. A*, **78**, 023807(6), (Aug., 2008)

PHYSICAL REVIEW A **78**, 023807 (2008)

Observation of three-mode parametric interactions in long optical cavities

C. Zhao,* L. Ju, Y. Fan, S. Gras, B. J. J. Slagmolen,† H. Miao, P. Barriga, and D. G. Blair
School of Physics, University of Western Australia, 35 Stirling Highway, Crawley, Western Australia 6009, Australia

D. J. Hosken, A. F. Brooks,‡ P. J. Veitch, D. Mudge, and J. Munch
Department of Physics, The University of Adelaide, Adelaide, South Australia, 5005 Australia
(Received 17 December 2007; published 6 August 2008)

We report the observation of three-mode optoacoustic parametric interactions of the type predicted to cause parametric instabilities in a 77-m-long, high-optical-power cavity that uses suspended sapphire mirrors. Resonant interaction occurs between two distinct optical modes and an acoustic mode of one mirror when the difference in frequency between the two optical cavity modes is close to the frequency of the acoustic mode. Experimental results validate the theory of parametric instability in high-power optical cavities, and demonstrate tunable parametric gain $\sim 10^{-2}$ and more than 20 dB amplification of a high-order optical mode power generated by an applied acoustic signal.

A.2.4 The Science benefits and Preliminary Design of the Southern hemisphere Gravitational Wave Detector AIGO

D. G. Blair, P. Barriga, A. F. Brooks, P. Charlton, D. Coward, J-C. Dumas, Y. Fan, D. Galloway, S. Gras, D. J. Hosken, E. Howell, S. Hughes, L. Ju1, D. E. McClelland, A. Melatos, H. Miao, J. Munch, S. M. Scott, B. J. J. Slagmolen, P. J. Veitch, L. Wen, J. K. Webb, A. Wolley, Z. Yan and C. Zhao, *J. Phys.: Conf. Ser.*, **122**, 012001(6), (2008)

7th Edoardo Amaldi Conference on Gravitational Waves (Amaldi7) IOP Publishing
Journal of Physics: Conference Series **122** (2008) 012001 doi:10.1088/1742-6596/122/1/012001

The Science benefits and Preliminary Design of the Southern hemisphere Gravitational Wave Detector AIGO

D. G. Blair[1], P. Barriga[1], A. F. Brooks[2], P. Charlton[7], D. Coward[1], J-C. Dumas[1], Y. Fan[1], D. Galloway[6] S. Gras[1], D. J. Hosken[2], E. Howell[1], S. Hughes[8], L. Ju[1], D. E. McClelland[3], A. Melatos[4], H. Miao[1], J. Munch[2], S. M. Scott[3], B. J. J. Slagmolen[3], P. J. Veitch[2], L. Wen[1], J. K. Webb[5], A. Wolley[1], Z. Yan[1], C. Zhao[1]

[1]School of Physics, University of Western Australia, Perth, WA 6009, Australia

[2]Department of Physics, The University of Adelaide, Adelaide, SA, 5005 Australia

[3]Department of Physics, Australian National University, Canberra, ACT 0200, Australia

[4]School of Physics University of Melbourne, Parkville Vic 3010 Australia

[5]School of Physics, The University of New South Wales, Sydney 2052, Australia

[6]School of Mathematical Sciences, Monash University, Vic 3800, Australia

[7]School of Computing and Mathematics, Charles Sturt University, NSW 2678, Australia

[8]Departmentof Physics, Massachusetts Institute of Technology, Cambridge, MA 02139-4307, USA

dgb@physics.uwa.edu.au

Abstract. The proposed southern hemisphere gravitational wave detector AIGO increases the projected average baseline of the global array of ground based gravitational wave detectors by a factor ~4. This allows the world array to be substantially improved. The orientation of AIGO allows much better resolution of both wave polarisations. This enables better distance estimates for inspiral events, allowing unambiguous optical identification of host galaxies for about 25% of neutron star binary inspiral events. This can allow Hubble Law estimation without optical identification of an outburst, and can also allow deep exposure imaging with electromagnetic telescopes to search for weak afterglows. This allows independent estimates of cosmological acceleration and dark energy as well as improved understanding of the physics of neutron star and black hole coalescences. This paper reviews and summarises the science benefits of AIGO and presents a preliminary conceptual design.

A.2.5 Observation of optical torsional stiffness in a high optical power cavity

Y. Fan, L. Merrill, C. Zhao, L. Ju, D.G. Blair, B.J.J. Slagmolen, D. J. Hosken, A. F. Brooks, P. J. Veitch, D. Mudge, and J. Munch, *to be submitted to Appl. Opt.* (2008)

Observation of optical torsional stiffness in a high optical power cavity

Y. Fan,* L. Merrill, C. Zhao, L. Ju, D.G. Blair and B.J.J. Slagmolen †

School of Physics, University of Western Australia, 35 Stirling Highway, Crawley, WA 6009, Australia

† *Currently with Center for Gravitational Physics, The Australian National University, Canberra, 0200, Australia*

D. J. Hosken, A. F. Brooks ‡, P. J. Veitch, D. Mudge, J. Munch

Department of Physics, The University of Adelaide, Adelaide, South Australia, 5005 Australia

‡ *Currently with LIGO, California Institute of Technology, Pasadena, California, USA*

*Corresponding author: fanyh@physics.uwa.edu.au

We have observed negative optical torsional rigidity in an 80m suspended high optical power cavity that will induce the Sidle-Sigg instability as a result of sufficient circulating power. The magnitude of the negative optical spring constant per unit power is a few $\mu N \cdot m/rad/W$ as the result of optical torsional stiffness in the yaw mode of a suspended mirror Fabry-Perot cavity. It is observed to depend on the optical power and g-factor of the cavity, which is in agreement with Sidles-Sigg theory.

A.2.6 Direct Measurement of Absorption-Induced Wavefront Distortion in Cavities with High Optical Power

Aidan F. Brooks, David Hosken, Jesper Munch, Peter J. Veitch, Zewu Yan, Chunnong Zhao, Yaohui Fan, Ju Li, David Blair, Phil Willems, Bram Slagmolen and Jerome Degallaix, *Appl. Opt.,* **48**, 355-364, (Jan., 2009)

Direct measurement of absorption-induced wavefront distortion in high optical power systems

Aidan F. Brooks,[1,2,*] David Hosken,[1] Jesper Munch,[1] Peter J. Veitch,[1] Zewu Yan,[3] Chunnong Zhao,[3] Yaohui Fan,[3] Li Ju,[3] David Blair,[3] Phil Willems,[2] Bram Slagmolen,[4] and Jerome Degallaix[3,5]

[1]Department of Physics, The University of Adelaide, Adelaide, South Australia 5005, Australia

[2]LIGO Laboratory, California Institute of Technology, 1200 East California Boulevard, Pasadena, California 91125, USA

[3]School of Physics, The University of Western Australia, 35 Stirling Highway, Nedlands, Western Australia 6009, Australia

[4]Centre for Gravitational Physics, The Australian National University, Canberra, ACT, 0200 Australia

[5]Max-Planck-Institut für Gravitationsphysik (Albert-Einstein-Institut) und Universität Hannover, Callinstr. 38, D-30167 Hannover, Germany

*Corresponding author: brooks_a@ligo.caltech.edu

Received 10 October 2008; accepted 21 November 2008; posted 9 December 2008 (Doc. ID 102498); published 7 January 2009

Wavefront distortion due to absorption in the substrates and coatings of mirrors in advanced gravitational wave interferometers has the potential to compromise the operation and sensitivity of these interferometers [Opt. Lett. **29**, 2635–2637 (2004)]. We report the first direct spatially-resolved measurement, to our knowledge, of such wavefront distortion in a high optical power cavity. The measurement was made using an ultrahigh sensitivity Hartmann wavefront sensor on a dedicated test facility. The sensitivity of the sensor was $\lambda/730$, where $\lambda = 800$ nm.

OCIS codes: 280.4788, 350.6830, 120.2230.

Appendix B

CPFS gain medium schematics

The schematics in this appendix are of the Nd:YAG laser crystals that were produced and used for the experiments described in this thesis.

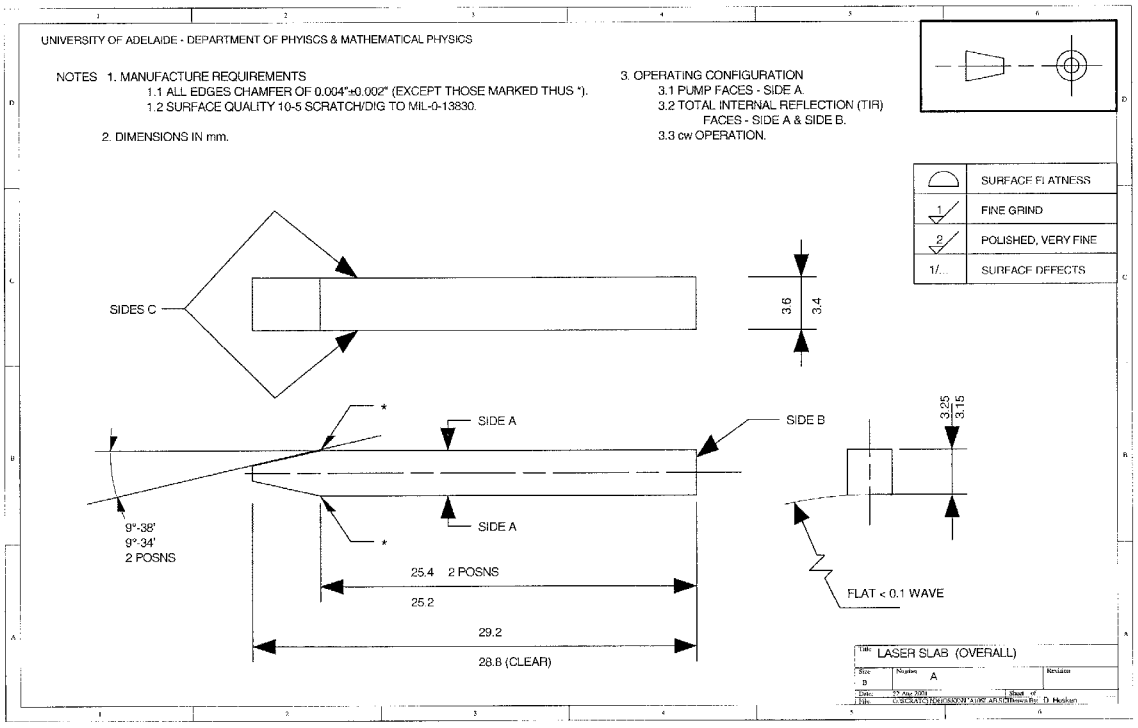

Figure B.1: Slab schematic 1 of 3.

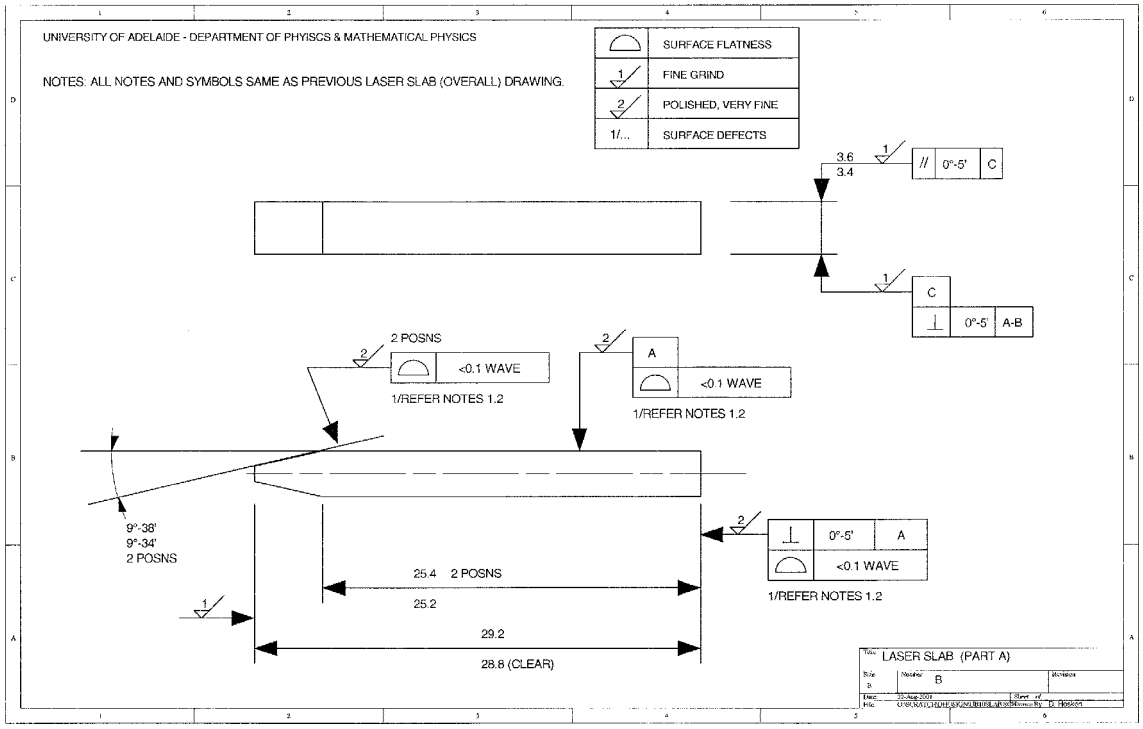

Figure B.2: Slab schematic 2 of 3.

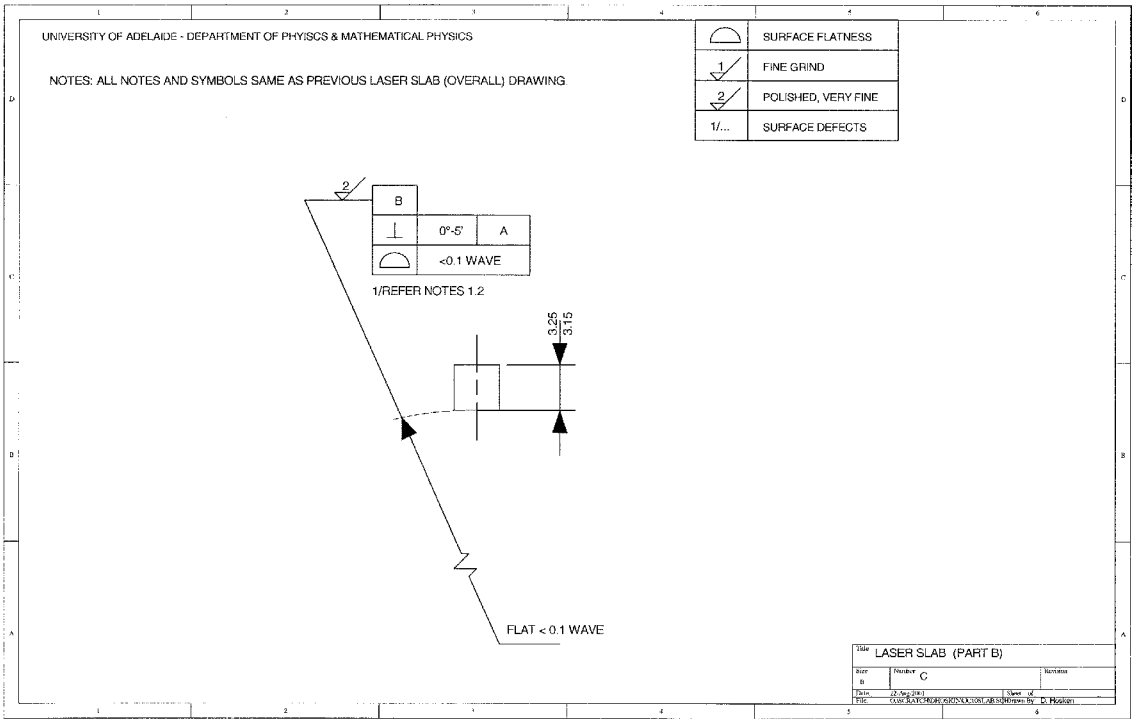

Figure B.3: Slab schematic 3 of 3.

Appendix C

Laser diode pump module properties

The pump laser diode arrays used on the final 10 W slave lasers were purchased from Cutting Edge Optronics (CEO), with the specifications and performance of these arrays found in this appendix.

C.1 Specifications and tolerances

Specifications for the Cs double laser diode packages.

- Height tolerance: $< \pm 50$ μm (in fast axis)
- 2×34 W lensed 1-bar laser diode arrays
- Rated at 22 W at 35 °C heatsink for each bar
- $2 - 3$ mm gap between bars, total emitting length ~ 23 mm
- 45° cut from the front corner of the package. 5 mm in from either side on the left when looking from the emission side
- 1-bar diode arrays to be connected electrically in series
- Diode arrays collimated in both near field (first 50 mm from emitters) and in the far field

- Collimation parallel to the laser diode package base
- Symmetric intensity lobe of both stripes in the fast-axis direction

Specifications for each array used in the Cs double package were:

- Beam divergence of the lensed bar: 1×10^{o} (with fast axis lensing)
- Spectral Width : 1.9 nm
- Slope Efficiency : 0.9 W/A
- Total Output Power : 34 W
- Maximum Operating Current : 55 A
- Wavelength : 808 ± 2 nm (at the rated output power and heatsink temperature for the Cs double package : 22 W at 35 °C heatsink temperature)
- The centre wavelengths of each of the stripes are to be matched and the smiles minimised
- Polarisation : TM

The tolerances required for the manufacture and collimation of the 1-bar laser diode arrays are shown in Figure C.1. This shows that the collimated output from each of the laser diode arrays was required to be at the same height and parallel to the package base, so that both arrays would pump the same plane within the Nd:YAG slab.

C.2 Custom package schematic

A schematic of the CEO Cs double laser diode package which was used on the final 10 W slave lasers is shown in Figure C.2.

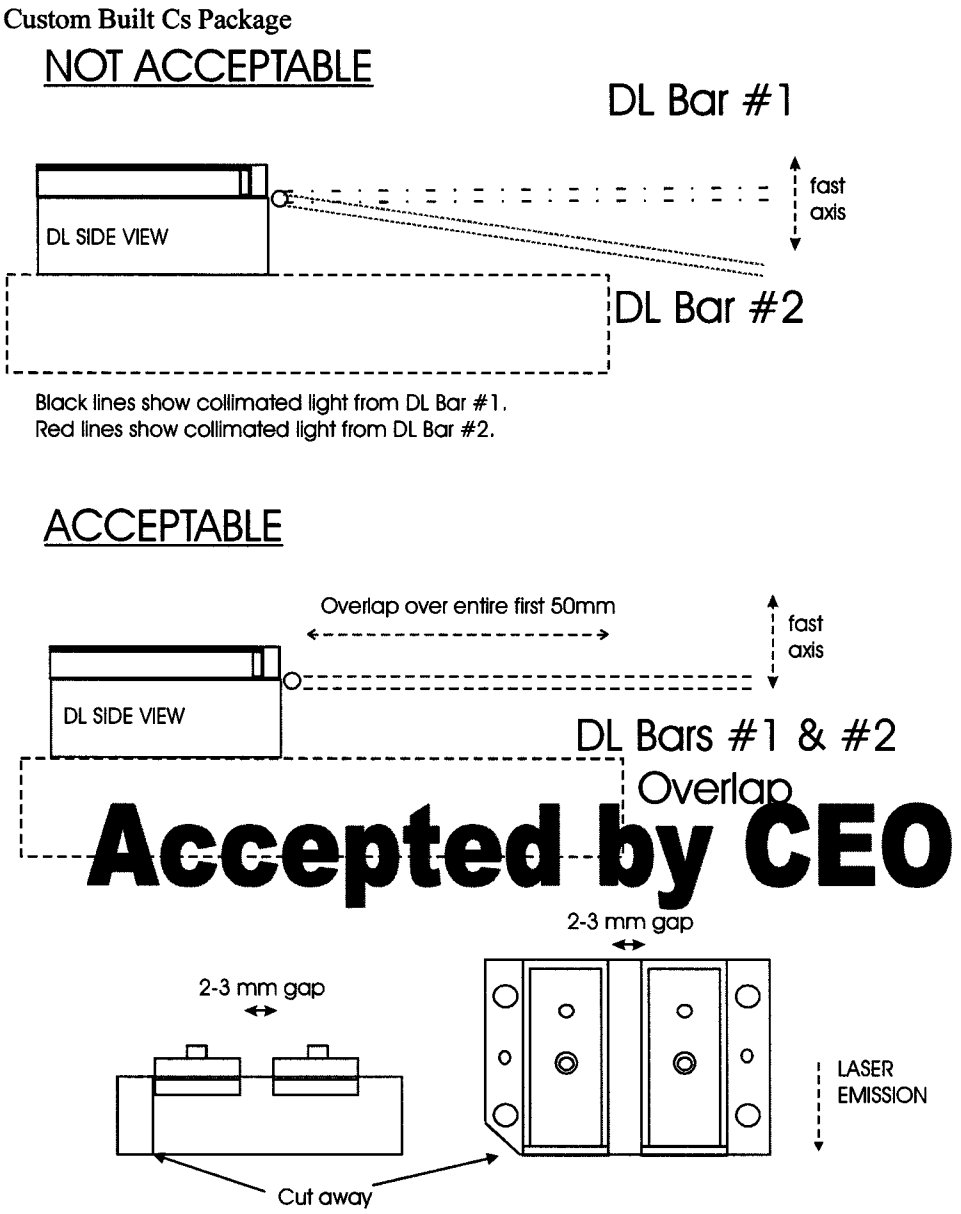

- Two 34W lensed 1-bar diode arrays
- Total emitting length ~23mm (2-3mm gap between bars)
- 45 degree cut from the front corner of the package. 5mm in from either side on the left when viewing from the emission side. (See diagram above)

1. Height of DL Bar #2 above package base should be the same as DL Bar #1 to within < ± 50 μm (in fast axis).
2. Diodes collimated in both nearfield (first 50mm from DL) and farfield. Collimation should be parallel to DL base.
3. Symmetric intensity lobe of both stripes in the fast axis direction.
4. Diode bullets to be connected electrically in series.

David Hosken
University of Adelaide

Figure C.1: Diagram of the tolerances required for the collimation of the laser diode arrays.

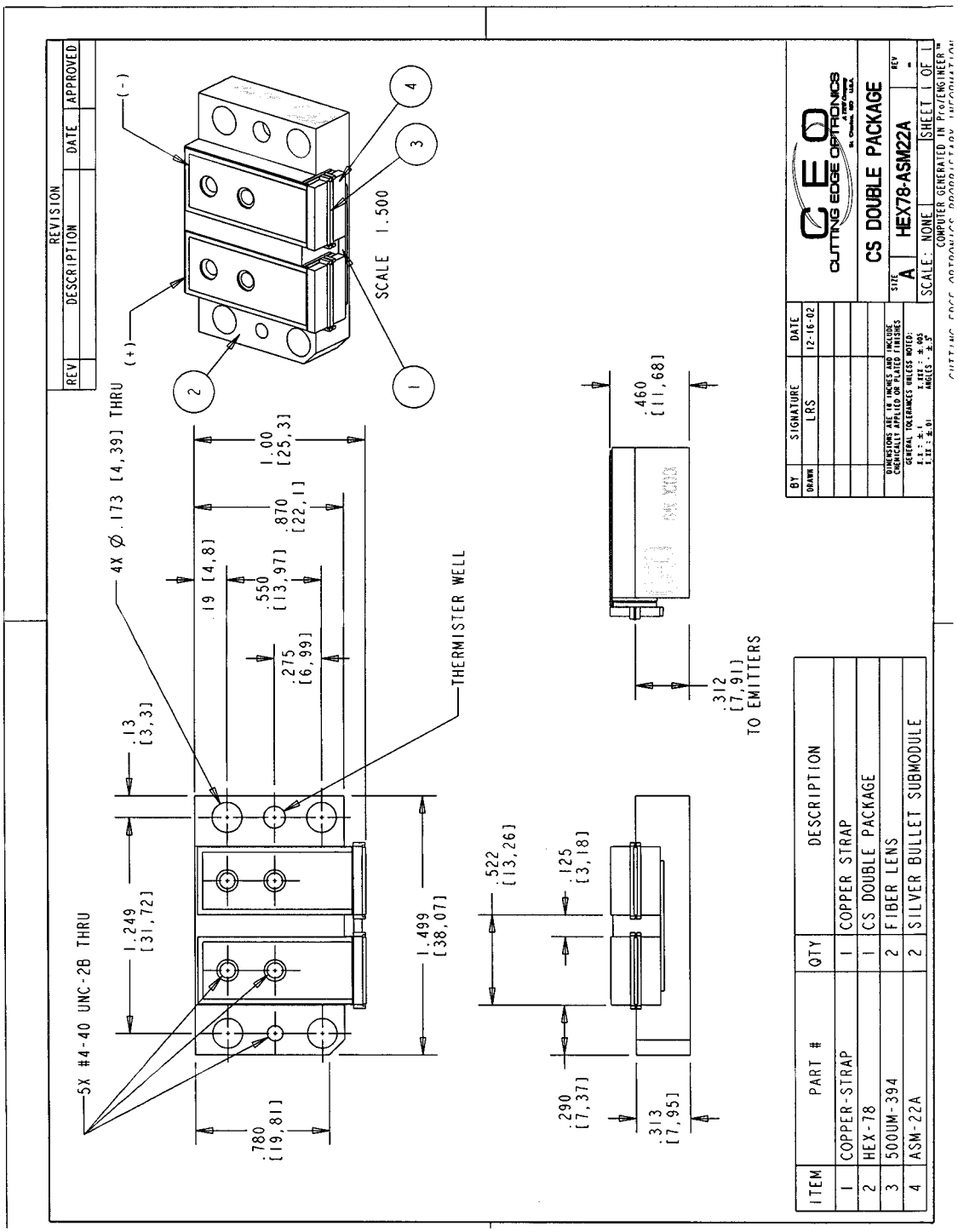

Figure C.2: Schematic of the CEO Cs double package which was used on the final 10 W lasers.

C.3 Custom package performance

The two double laser diode array packages that were purchased from CEO had serial numbers 17817 and 17820, and have been referred to as package A and package B respectively throughout this thesis. Performance specifications (supplied by CEO) for these packages are shown in Figures C.3 and C.4.

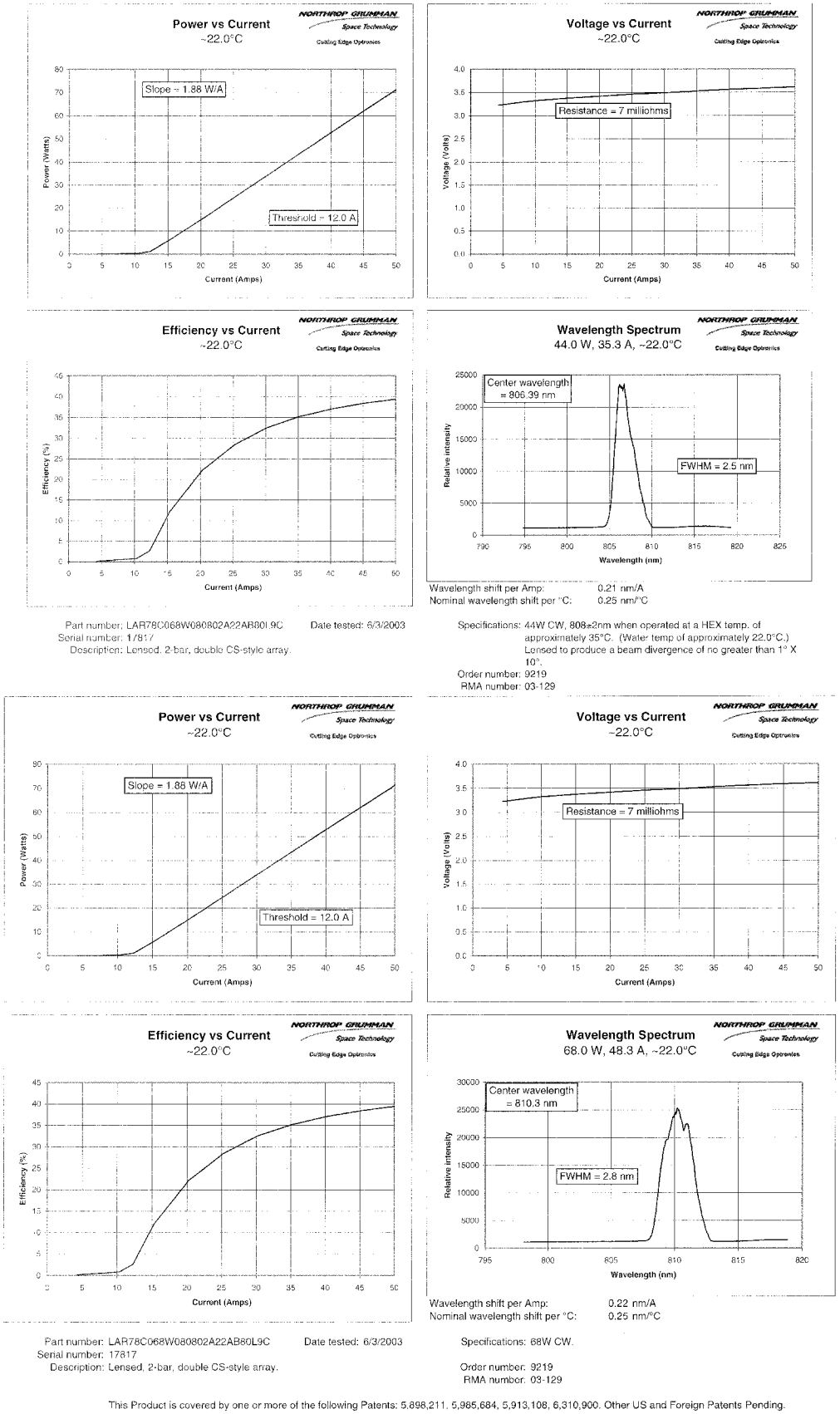

Figure C.3: Performance of laser diode array package A.

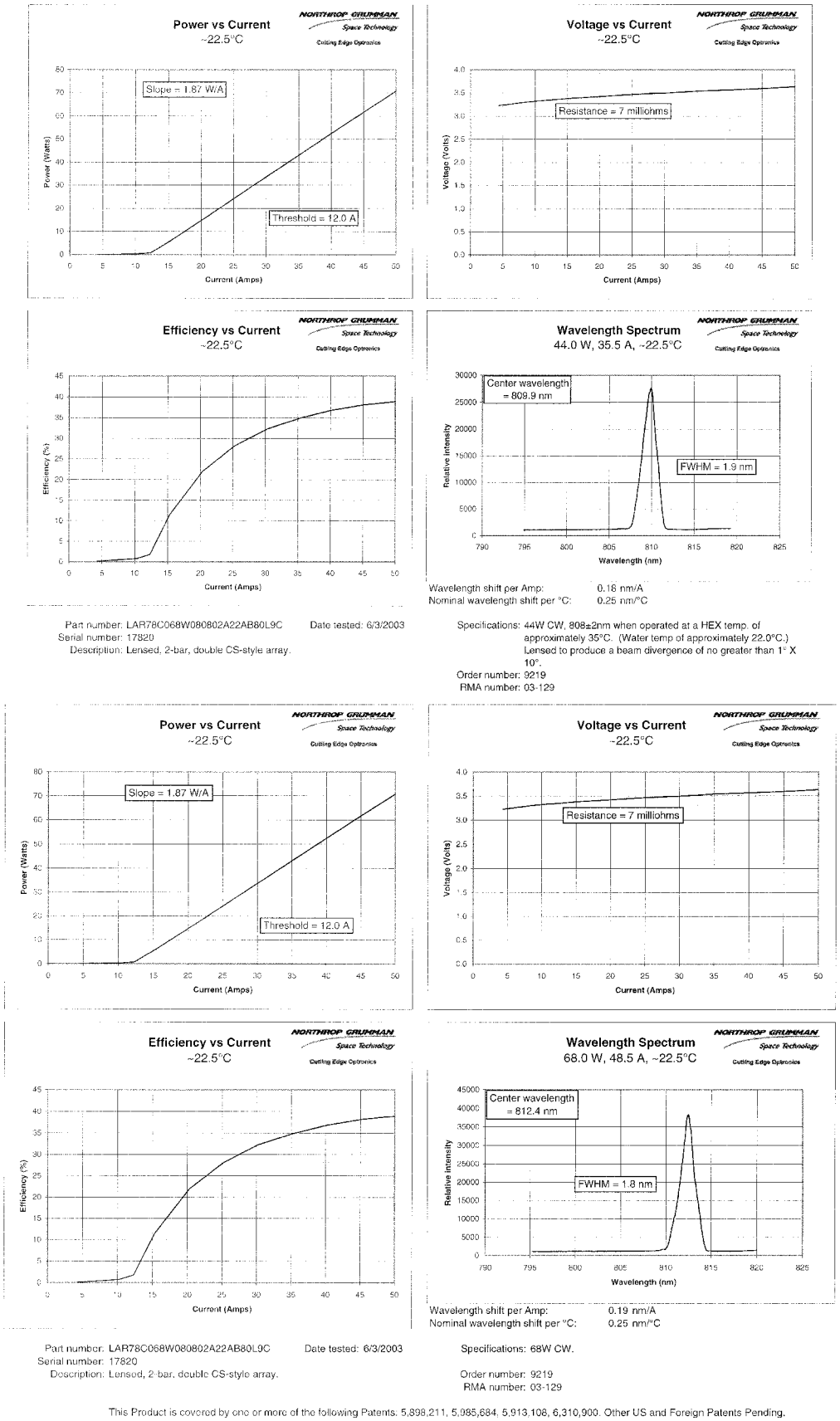

Figure C.4: Performance of laser diode array package B.

Appendix D

Temperature stabilisation circuit diagrams

Circuit diagrams used during the course of this work together with descriptions of the methods used for temperature control are found in this appendix. Unless otherwise stated, all resistor values are in ohms.

D.1 Laser diode temperature stabilisation

The circuit diagram for laser diode cooling and temperature stabilisation is shown in Figure D.1. This circuit consists of an error signal stage, pre-amp gain stage and a power op-amp output stage. The pre-amp stage incorporates a PID stage followed by a summing op-amp. An instrumentation amplifier with a gain of twenty one precedes the pre-amp stage, the output of which is buffered by a power op-amp output stage with a gain of five.

Initial and intermediate 10 W laser heads used a single, independent temperature servo and a single TEC (Melcor CP2-127-06L) to stabilise each laser diode array. The TEC hotside was bolted to a copper heatsink, initially using water cooling for efficient heat removal. The intermediate laser used this copper heatsink attached to another air-cooled aluminium heatsink.

The final 10 W laser uses a single, temperature stabilised copper block on which the pump laser diode array is mounted. A single feedback servo independently drives

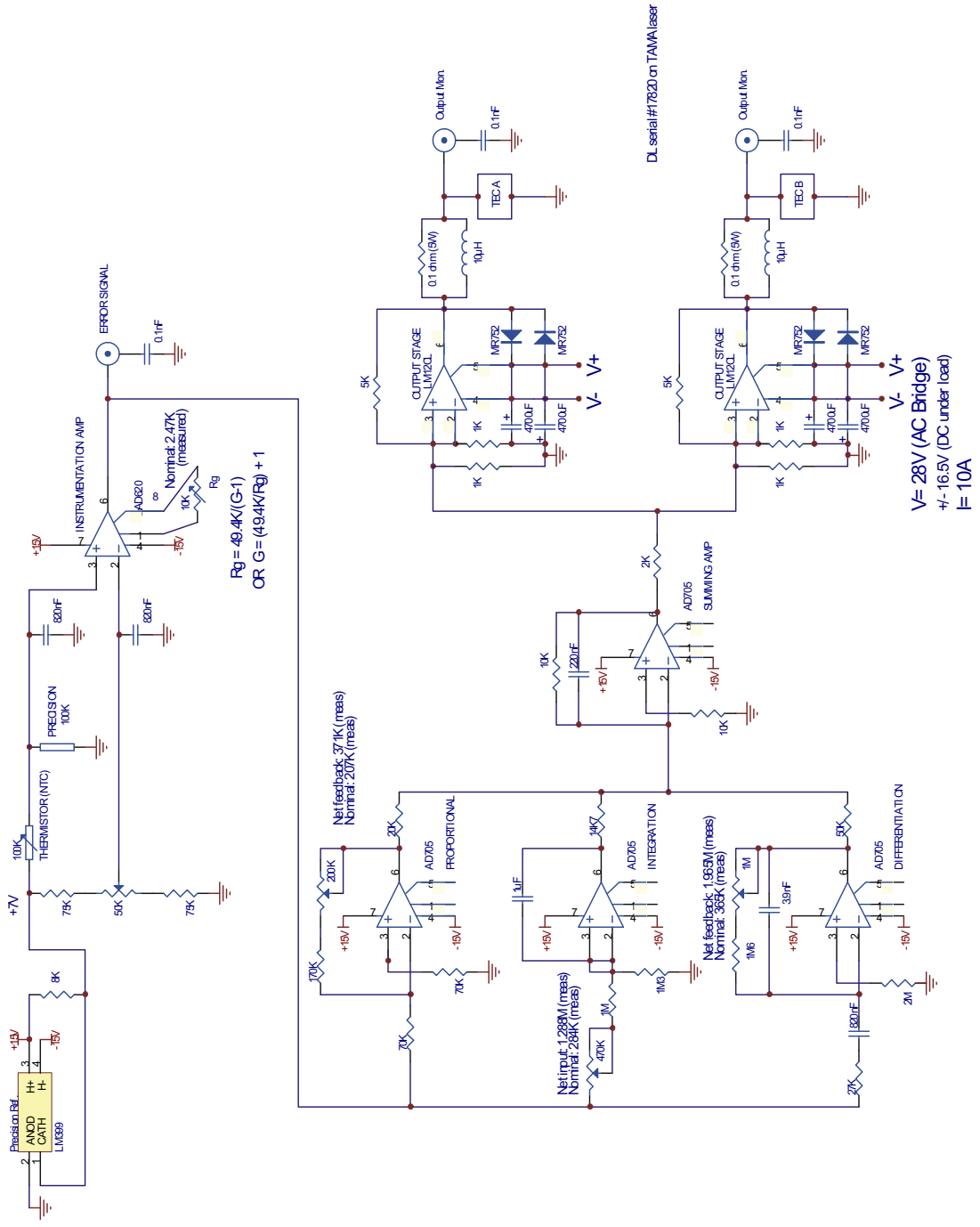

Figure D.1: Schematic of the laser diode temperature feedback servo.

two TECs (Melcor UT15-12-40-F2-T2-RTV), located side-by-side. Here, the TEC hot side is cooled by the integrated air-cooled heatsink.

D.2 Slab temperature stabilisation

Slab cooling and temperature stabilisation requires the use of two feedback servos, with circuit diagrams for the top and bottom servos shown in Figures D.2 and D.3 respectively. Each of these circuits consists of an error signal stage, pre-amp gain stage and a power op-amp output stage. The pre-amp stage incorporates a PID stage followed by a summing op-amp. The bottom servo also incorporates a temperature input stage, which allows feedback to the resonator base for long-term injection locking. Additionally, instrumentation amplifiers precede these pre-amp stages, with gains of seventeen and twenty eight for the slab top and slab bottom servos respectively. The output of these are then buffered by power op-amp output stages, each with a gain of five.

The slab is mounted on a large aluminium block (the resonator base), which itself is mounted on three TECs (Melcor UT6-7-30-F1-T2-RTV), connected electrically in series to control the slab bottom temperature. This bottom feedback servo uses a single thermistor as the temperature sensor, located immediately below the slab. The hot side of the TECs is cooled by the integrated air-cooled heatsink (details in Chapter 4).

The slab mounting aluminium block is much smaller than the bottom (resonator base) block. This top block clamps down on the slab by connecting to the heatsink using a single TEC (Melcor UT6-12-40-F1-T1-RTV). Thermal isolation between top and bottom blocks is essential to ensure the only thermal connection between the blocks is through the slab. This is necessary since slab thermal shorts create difficulties when adjusting thermal servos.

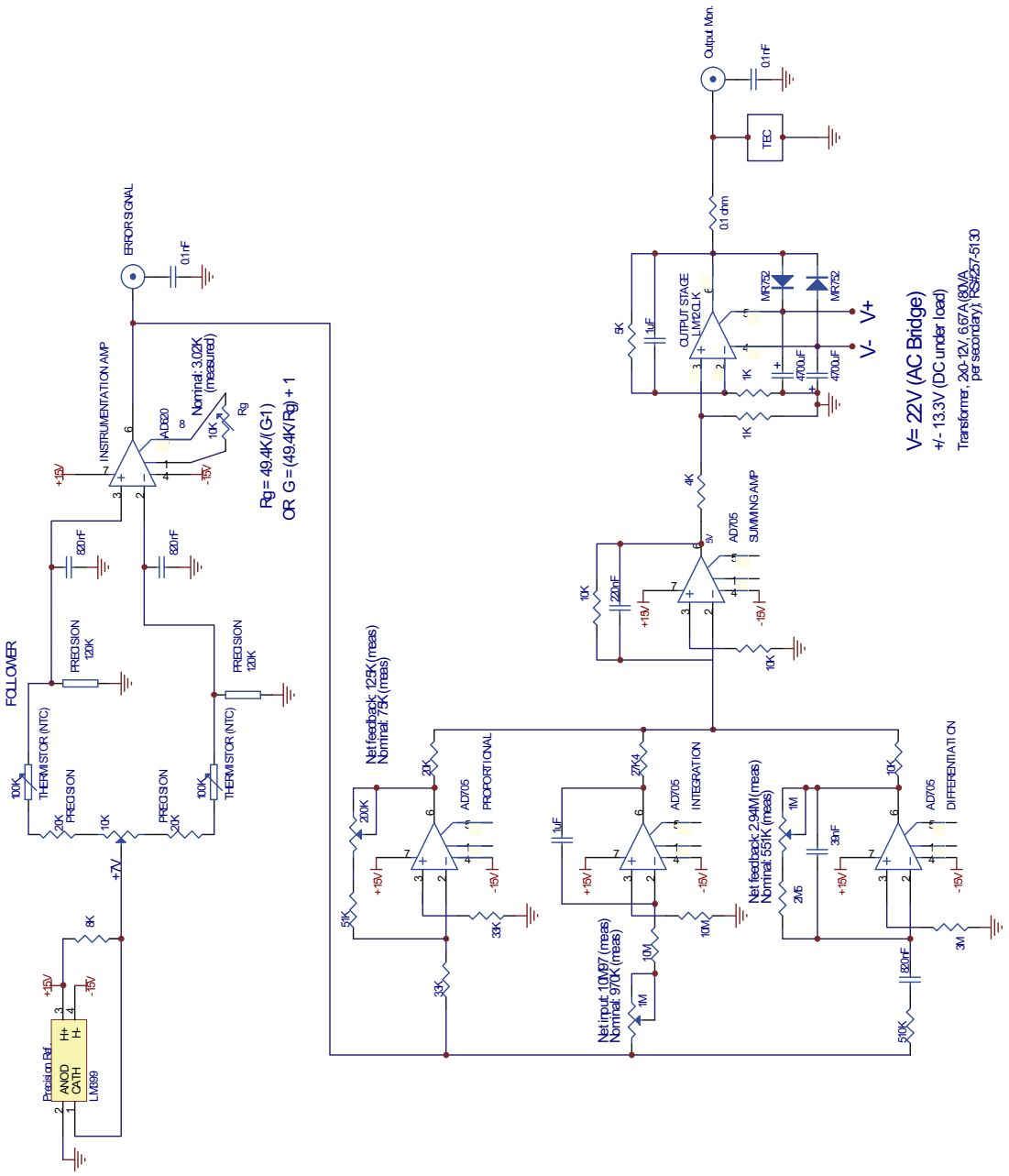

Figure D.2: Schematic of the slab top temperature feedback servo.

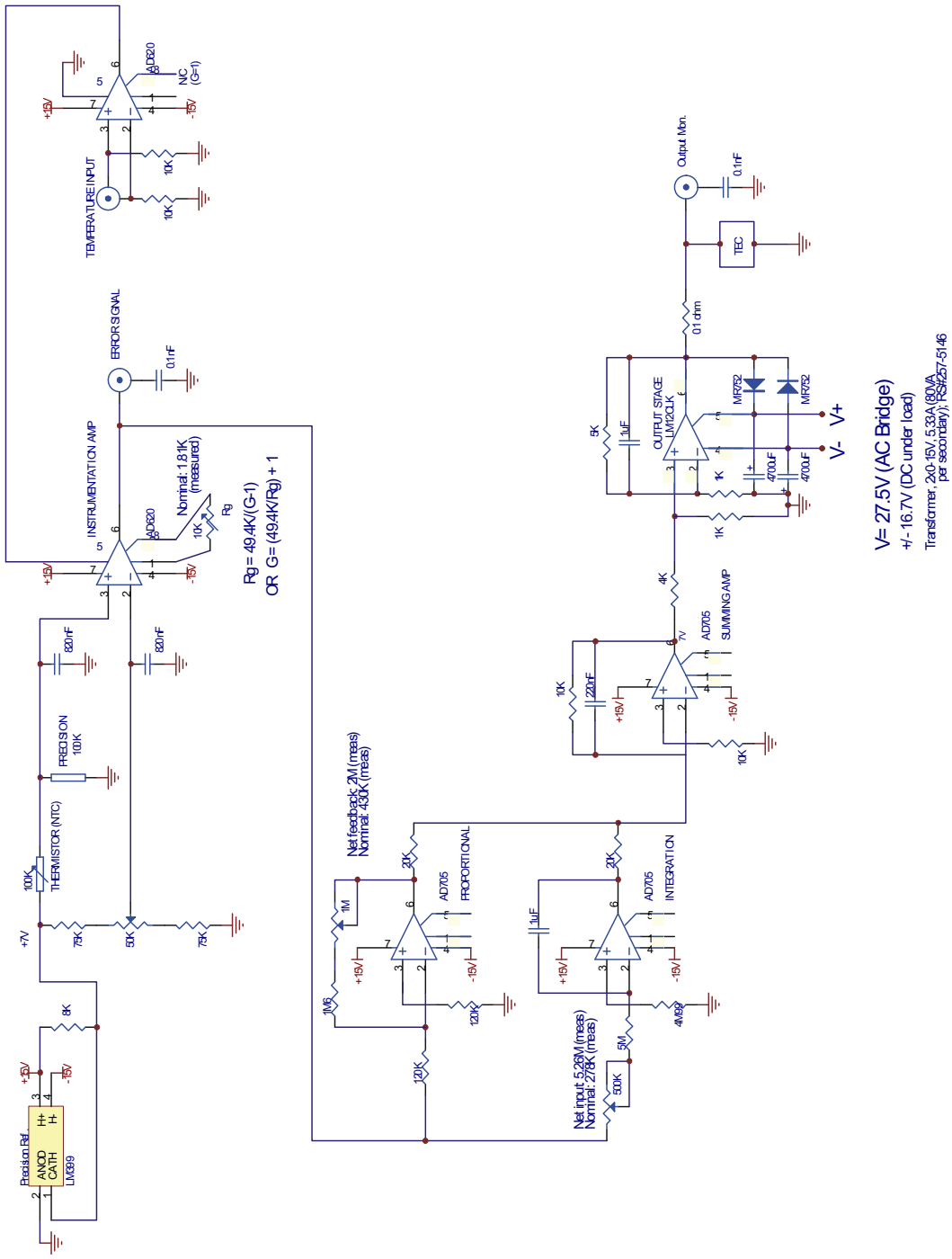

Figure D.3: Schematic of the slab bottom temperature feedback servo.

D.3 Setting the resonator temperature offset

Setting the resonator temperature offset is easily achieved, and is especially important during resonator alignment (see Chapter 3). Setting of the offset is achieved by:

1. Turning off all temperature controllers for an extended period of time (overnight if possible), to allow the slab and top/bottom blocks to reach the same temperature.

2. Disconnecting the resonator TEC controller (slab temperature control) feedback connectors from the laser head, then turning on this TEC controller.

3. Measuring the top error signal, then zeroing this signal by adjusting the temperature offset potentiometer.

This potentiometer setting ensures that both the top and bottom thermistors measure the same temperature, and allow the temperatures of the top and bottom blocks to be matched.

Appendix E

Thermal lensing measurement technique

This appendix describes in detail the thermal lensing measurement technique.

E.1 Description of the IDL program

An IDL program was written by Dr Mudge [98] to analyse the interferograms during thermal lensing analysis. This program was modified for use during the course of this work, with the program used to analyse interferograms shown in Figure E.1.

This program reads in a fringe pattern (.tif file) and produces sets of cross sectional data by averaging three vertical lines in this image (location of the central line is determined by the operator, so that it is positioned in the middle of the acquired image). This data is written to a intensity profile file (v.dat), while files containing the maxima (m.dat) and the maxima of splines (s.dat) are also produced. This is in addition to the raw data file (.dat).

E.2 Analysis using fringe peak positions

The analysis was performed using a spreadsheet program, using the acquired raw data (.dat) and spline data (s.dat) files. These data files were produced for each of the recorded interferograms that were described in Section 3.8.1, in addition to a

IDL program: Fringv4.pro

```
;program (2/2/00) to read in a fringe pattern as a tiff file and then average 3 vertical
;lines in it to produce a set of y-data. The program then finds the peaks of the fringes and
;writes this data to a file. vertical data.

Output=INTARR(480,480)
Output2=INTARR(480)
maxar=INTARR(480)

close, 1; just in case they are already open
close, 2
close, 3
close, 4
set_plot,'win'

Result=READ_TIFF("o:\dhosken\Mach Zehnder\lens measurement\110302\N110302.tif", R, G, B)
TV, Result
for loop1=0,(479) do begin
 for loop2=0,(479) do begin
  Output(loop1,loop2)=Result(loop1,loop2)
 endfor
endfor

;Output(270,*)=250
; intensity profile(cross section)
openw, 1, 'o:\dhosken\Mach Zehnder\lens measurement\110302\N110302v.dat'
for loop3=0,(479) do begin
  Output2(loop3)=(Output(149,loop3)+Output(150,loop3)+Output(151,loop3))/3
  printf, 1, Output2(loop3)
endfor
close, 1

;look for maximums
openw, 2, 'o:\dhosken\Mach Zehnder\lens measurement\110302\N110302m.dat'
loop4=0
for loop3=1,(478) do begin
  if(output2(loop3) GT output2(loop3-1)) and (output2(loop3) GE output2(loop3+1)) then begin
    loop4=loop4 + 1
    maxar(loop4)=loop3+1
    printf, 2, maxar(loop4), output2(loop3)
  endif
endfor
close, 2

openw, 3, 'o:\dhosken\Mach Zehnder\lens measurement\110302\N110302.dat'

x=fltarr(480)
t=fltarr(2000)
for i=0, (479) do x(i)=i
for i=0, (1999) do t(i)=i* 480.0/2000.0

new_y=fltarr(2000)
new_y=spline(x,output2,t)
for i=0, (1994) do begin
  printf, 3, t(i+5), new_y(i)
endfor
close, 3

;look for maximums of spline
openw, 4, 'o:\dhosken\Mach Zehnder\lens measurement\110302\N110302s.dat'
loop4=0
for loop3=1,(1995) do begin
  if(new_y(loop3) GT new_y(loop3-1)) and (new_y(loop3) GE new_y(loop3+1)) then begin
    loop4=loop4 + 1
    maxar(loop4)=loop3+1
    printf, 4, t(loop3+5), new_y(loop3)
  endif
endfor
close, 4

shade_surf,Output,shades=bytscl(Output,top=!D.table_size),az=0,ax=90

end
```

Figure E.1: The IDL program used to analyse interferograms.

single unpumped interferogram for each set of measurements, where these interferograms are

- The unpumped zero fringe interferogram (*Zero_Unpumped*).
- The unpumped tilted reference interferogram (*Tilted_Reference*).
- The pumped interferogram (*Pumped_Output*).

Each fringe peak represents a phase shift of 2π, with the procedure used to analyse the tilted interferograms being as follows:

1. Compare the raw and spline data to confirm that the peaks are correctly determined for each of the interferograms, and then examine just the spline data to see if these have all been correctly determined (*slab_ position*).
2. Each fringe peak corresponds to a 2π phase shift. This is the change in phase between consecutive peaks (*phase_shift*).
3. Calculate the magnification factor, *MAG_Factor*. Using *Zero_Unpumped*, locate the slab edge pixel numbers, and then convert from pixels to the actual size on the CCD. This is determined by the number of pixels multiplied by the size of the pixels, then divided by the actual slab height.
4. Conversion of *slab_position* to *corrected_peak_positions* within the slab, for *Tilted_Reference* and *Pumped_Output*. These used the known pixel sizes and *MAG_Factor*, determined in step 2. These are found by multiplying the *slab_position* data by the pixel size, then dividing by *MAG_Factor*.
5. Calculation of the magnitude of the introduced tilt, using *Tilted_Reference*. Plotting *corrected_peak_positions* against *phase_shift* produces a linear relationship, with slope *TILT*.
6. Determine wavefront distortion due to pumping of the slab. This is the *corrected_phase_shift* and is given by *(TILT*corrected_peak_positions - phase_shift)*.
7. Plot *corrected_peak_positions* against *corrected_phase_shift*.

8. This shows a plot with both linear regions and a lens region. Fit a parabola to the lens region using Equation E.5 (discussed in Section E.3) and extract the γ fit parameter. This allows the effective focal length to be calculated (as discussed in Chapter 4).

E.3 Parabolic fit to the measured wavefront

The measurement of thermal lensing in the pumped region of the slab requires a parabola to be fitted to the measured wavefront.

As discussed in Chapter 4, beam propagation through the pumped slab is considered as a Gaussian lens duct, with the refractive index *n(r,z)* given by

$$n(r,z) = n_0\left(1 - \frac{1}{2}\gamma^2 r^2\right); \quad \text{where } \gamma^2 \equiv \frac{n_2(z)}{n_0(z)} \tag{E.1}$$

By considering the pumped slab as a lens duct, the optical pathlength seen by a ray at a distance *b(r,z)* from the axis ($r = 0$) varies such that

$$b(r,z) = z\ n(r,z) \tag{E.2}$$

Where l is the total pathlength in the slab, the associated phase shift (compared to a ray at the axis) seen by propagation through a duct of length l is written as

$$\begin{aligned} 2\pi\frac{b(r,l) - b(0,l)}{\lambda_{probe}} &= (2\pi)\,\frac{(l\ n(r,l) - l\ n(0,l))}{\lambda_{probe}} \\ &= (2\pi)\,\frac{\left[n_0\left(1 - \frac{1}{2}\gamma^2 r^2\right) - n_0\right] l}{\lambda_{probe}} \\ &= -\frac{(2\pi)\,n_0 l\gamma^2 r^2}{2\lambda_{probe}}\ , \end{aligned} \tag{E.3}$$

which is in the form of a parabola ($y \propto x^2$), with a vertex at (0,0).

A parabola with its axis parallel to the y-axis, vertex at *A(x_0,y_0)* and with the distance from A to the focus F being $a > 0$, the general equation is given by [166]

$$(x - x_0)^2 = \pm 4a\,(y - y_0) \tag{E.4}$$

with the ± depending on if the parabola opens up or down.

Fitting to the measured wavefront uses a parabola with a vertex at $A(P_3,P_1)$. By comparing Equations E.3 and E.4 the phase shift is written as

$$y = P_1 \pm \frac{(2\pi)\, n_0 l \gamma^2 (x - P_3)^2}{2\lambda_{probe}} \ , \tag{E.5}$$

where

$$\frac{1}{4a} = \frac{(2\pi)\, n_0 l \gamma^2}{2\lambda_{probe}} \tag{E.6}$$

Once Equation E.5 is fitted to the measured wavefront, the γ parameter is used to calculate the effective focal length of the lens duct. This is discussed in Section 4.3.4.

Appendix F

Heatsink thermal resistance calculations

This appendix details the method and formulae used to calculate the heat sink thermal resistance for both natural convection (Section F.1) and forced-air convection (Section F.2).

F.1 Natural convection

Calculation of the heatsink thermal resistance using natural convection required both convection and radiation heat dissipation to be considered, together with the expected average temperature of the heatsink to be known. This allowed the thermal resistance to be calculated using [119]

$$\Theta_{sa} = \left[\frac{1}{h_c A_c + h_r A_r}\right] \ , \tag{F.1}$$

where h_c and h_r are the convection and radiation heat transfer coefficients (each having units of W/m^2.^{o}C), while A_c and A_r are the convection and radiation surface areas (in m^2).

F.1.1 Radiative area and heat transfer coefficient

Radiative heat transfer coefficient

Heatsink cooling due to radiation is most useful when the temperature of the heatsink is considerably higher than the ambient temperature. When performing calculations involving h_r, a temperature difference between the heatsink and the surroundings of 20 °C was assumed, for an ambient temperature of 20 °C. This corresponded to a h_r value of approximately 5.68 W/m^2.°C [119] for black anodised aluminium.

Radiative area

When a heatsink consists of numerous parallel surfaces (fins), the surface area able to dissipate heat to the surroundings via radiative means is considerably less than the actual heatsink surface area. For a heatsink with the dimensions shown in Figure F.1, the radiative area can be approximated by [119]

$$A_r = 2H_f\left(W + L_f\right) + WL_f \ , \tag{F.2}$$

for cases where the fin height from the base (H_f) is over four times the width of the space between fins (S_f). Here, L_f is the vertical length of the heatsink and W is the overall width of the heatsink.

F.1.2 Conductive area and heat transfer coefficient

Conductive heat transfer coefficient

For a single isolated vertically mounted surface h_c is given by [119]

$$h_c = 1.41\left(\frac{\Delta T}{L_f}\right)^{1/4} \ , \tag{F.3}$$

where ΔT is the assumed difference between the heatsink and ambient temperatures.

Equation F.3 can be modified for a parallel surface heatsink by multiplication by the heat transfer coefficient correction factor h_c^*, given by [119]

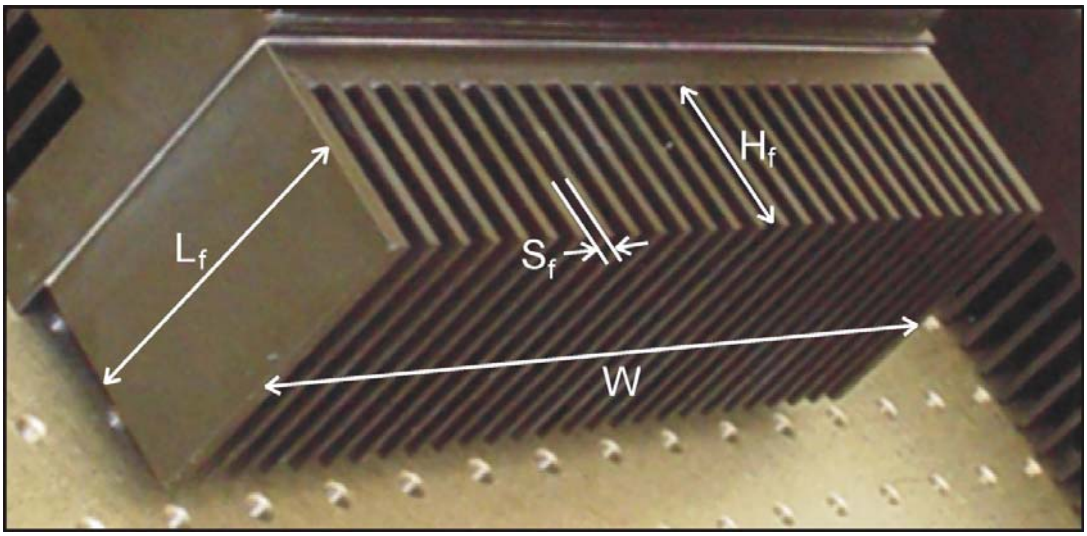

Figure F.1: Heatsink dimensions, measured in metres.

$$h_c^* = \frac{1.68F^3}{24}\left[1 - \exp\left(\frac{-24}{1.68F^3}\right)\right] \ , \tag{F.4}$$

where F is the fin spacing parameter, given by

$$F = 100.7S_f\left(\frac{\Delta T}{L_f}\right)^{1/4} \tag{F.5}$$

Conductive area

The conductive area of the heatsink is calculated by determining the total surface area of the heatsink fins and spacings, while the flat, back mounting surface is excluded since it does not see the ambient conditions.

F.2 Forced-air convection

When cooling a heatsink using forced-air convection, radiation is not a significant heat dissipation method. Therefore, Equation F.1 can be simplified and written as

$$\Theta_{sa} = \frac{1}{h_c A_c} \tag{F.6}$$

where A_c is calculated as for natural convection (Section F.1.2).

Calculation of the conductive heat transfer coefficient requires the airflow velocity to be known, allowing h_c to be written as [119]

$$h_c = 3.86\sqrt{\frac{V}{L_f}}\ , \tag{F.7}$$

where V is the linear air velocity (in ms^{-1}) and L_f is the length of the fin parallel to the airflow.

Appendix G

Slave laser alignment procedure

Correct slave laser operation requires careful alignment to the gain region. A carefully aligned HeNe alignment laser is used to align both standing-wave and travelling-wave resonators.

Angles between beams are measured using four thin, sharp alignment spikes placed in these beams. Measurement of distances between spikes allows calculation of angles using the cosine rule

$$a^2 = b^2 + c^2 - 2bc\cos A \tag{G.1}$$

G.1 Alignment to the CPFS gain medium

The following procedures are used to align the HeNe laser beam to the CPFS gain medium.

G.1.1 Horizontal

Horizontal HeNe alignment is achieved with the slab unpumped.

1. Transmit the collimated HeNe beam through the slab. No clipping of this beam by slab apertures should be observed.

2. Measure the total beam separation angle (θ_{beam}) between the incident and transmitted HeNe beams. Alignment spikes placed in this beam (S1, S2, S3

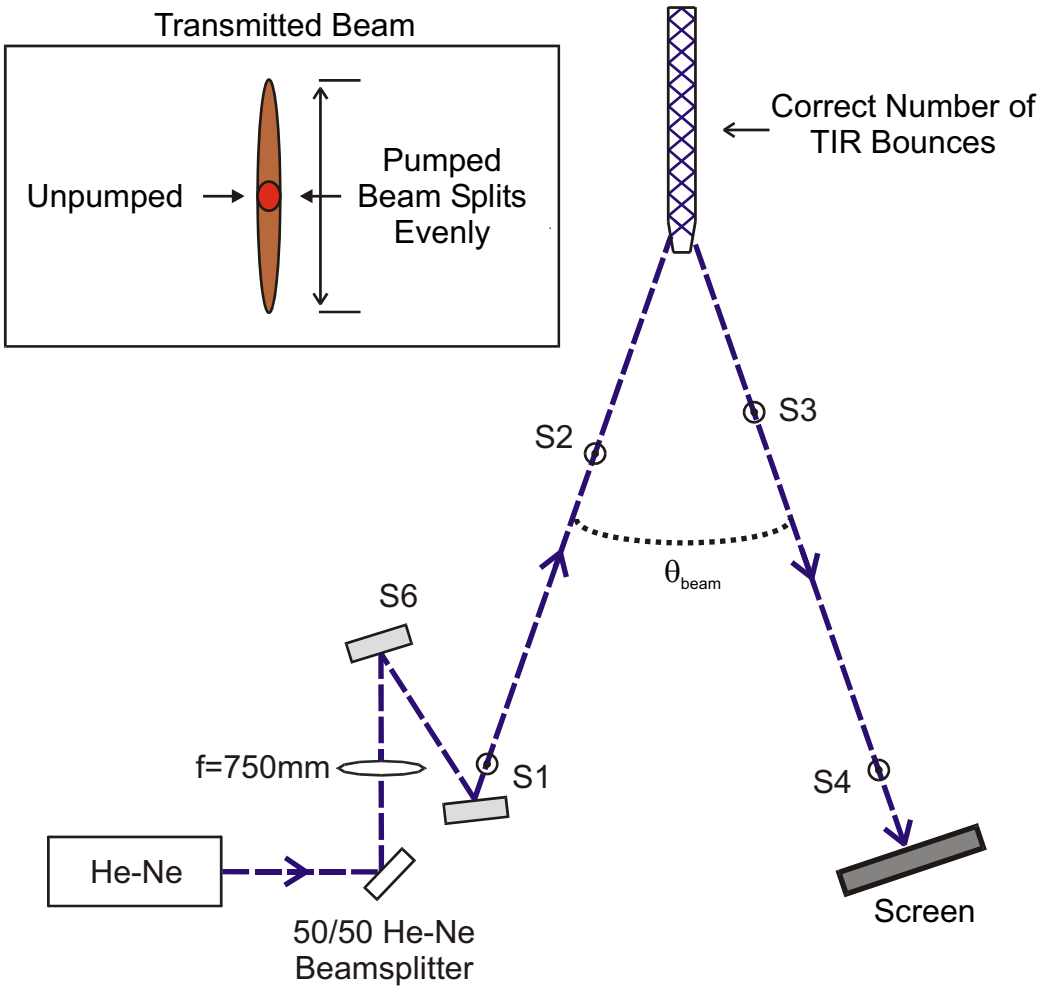

Figure G.1: Schematic of the layout used for aligning the HeNe beam to the CPFS gain medium. The effect of slab pumping on the transmitted beam is shown in the boxed region at the top of this figure.

and S4) are used to determine this angle, as shown in Figures G.1 and G.2. Calculation of θ_{214} and θ_{341} using Equation G.1 allows θ_{beam} to be determined.

3. Adjust the beam separation angle until $\theta_{beam} = 38.4^{o}$ is achieved.

4. Once achieved, confirm that there are 10 evenly spaced TIR bounces along the slab side, between the slab blunt end and the Brewster window shoulder. Fine adjustment of the HeNe alignment may be required. The HeNe beam must enter and exit through the Brewster windows, extremely close to the shoulder.

5. Confirm the transmitted beam is not clipping on slab apertures.

6. Repeat steps $2-5$ as necessary.

Correct horizontal alignment is achieved when 10 evenly spaced TIR bounces are observed, with the correct total beam separation angle, and when no clipping of the transmitted beam is observed.

G.1.2 Vertical

Vertical HeNe alignment requires the slab to be both unpumped and pumped.

1. With the slab unpumped, transmit the HeNe beam through the slab and mark the position on a screen, as shown in Figure G.1.

2. Pump the slab, observing the position of the transmitted beam on the screen. The beam will stretch vertically, caused by the dominant vertical thermal lens. Vertical translation of this beam position, and/or an uneven split indicates incorrect vertical alignment.

3. Adjust the vertical alignment of the HeNe beam, then compare the unpumped and pumped transmitted beam positions. Figure G.1 shows the result of correct vertical alignment.

4. Confirm correct horizontal alignment is still achieved. Repeat procedure G.1.1 if required.

5. Repeats steps $1-4$ as necessary.

Correct vertical alignment is achieved when the transmitted HeNe beam splits evenly and without vertical or horizontal translation.

G.2 Standing-wave alignment

Flat standing-wave mirrors are aligned to the gain medium using the HeNe alignment beam. An iris placed in the alignment beam, on the input side of the slab, is used to align mirror back reflections. Mirrors need to be perpendicular to this beam.

Once cavity mirrors are aligned, output power optimisation is able to be performed. The HeNe beam can then be realigned to the optimised mirror positions. The procedure described in Section G.1 is able to confirm the correct bounce solution is retained after realignment to the standing-wave cavity mirrors.

G.3 Travelling-wave alignment

Alignment of the travelling-wave resonator uses the alignment beam described in Section G.1. A second alignment beam is retro aligned to the first, enabling preservation of the optimised alignment. Alignment beams are referred to as the RW and FW beams, as shown in Figure G.2.

Initially, the output coupler position and angle needs to be set, before positioning the Max-R mirror. Positioning of these optics is shown schematically in Figure G.3. The incidence angle on the output coupler is 10.8°, while that on the Max-R mirror is 60°.

G.3.1 Output coupler positioning

The following procedure is used to position the output coupler, with the slab remaining unpumped.

1. Position the output coupler at the desired distance from the Brewster window and lightly clamp.

2. Using the transmitted FW alignment beam through the slab, horizontally centre this beam on the output coupler. Vertical height should be checked

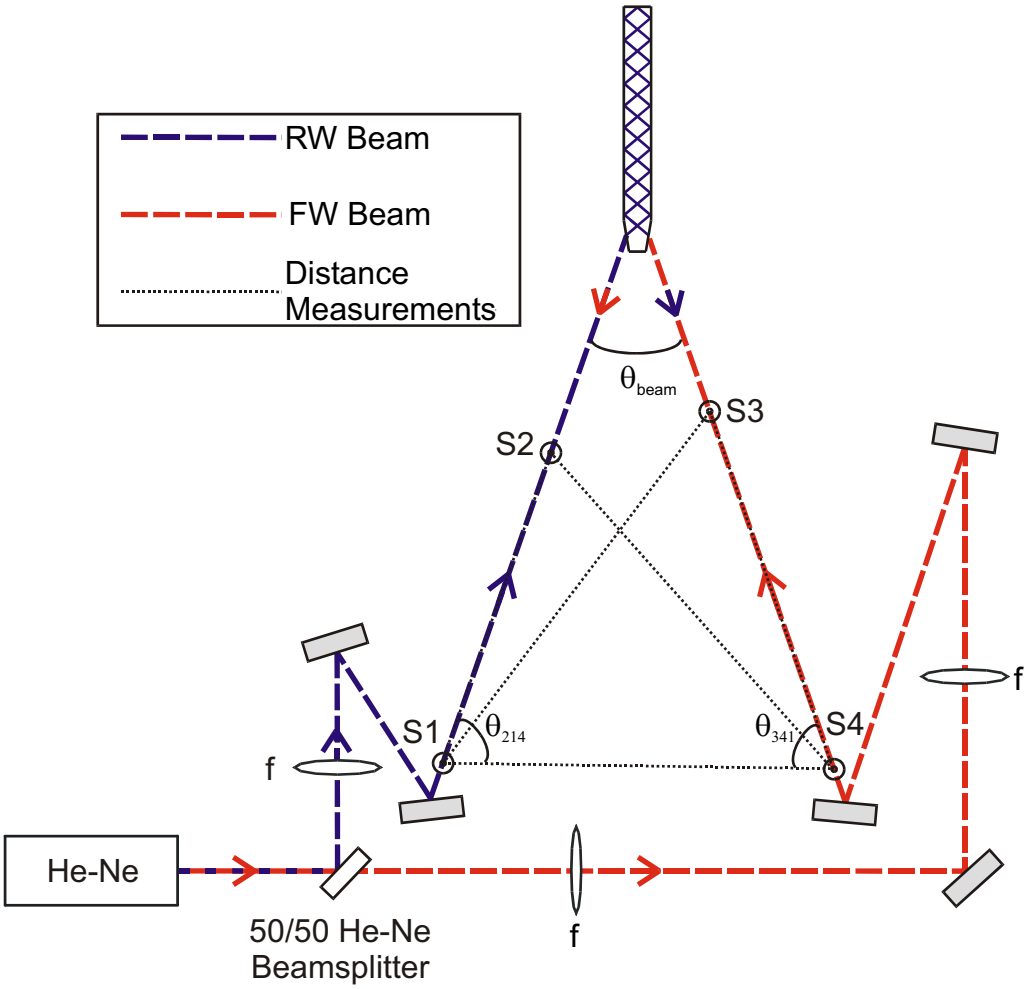

Figure G.2: The RW and FW HeNe alignment beams are shown, together with the placement of the alignment spikes to allow the calculation of the separation angle.

prior to assembly, with appropriate changes being made to the mount when required. Rotate the output coupler horizontally until an incident angle of approximately 10.8° is achieved, with the FW beam remaining centred.

3. Setting the correct horizontal output coupler angle uses the back reflection of the RW beam off the output coupler. This is shown in Figure G.3 (A). This angle is calculated using alignment spikes in the incident and reflected RW beams (S1, S2, S5 and S6). θ_{OCback} should be set to 21.6°.

4. Rotate the output coupler base to keep the FW beam centred, since course actuator adjustment usually shifts the FW beam off centre.

5. Repeat steps $2-4$ until the correct angle for θ_{OCback} is found. Ensure the output coupler base is clamped securely and that the correct Brewster window to output coupler distance has been retained. If not, then return to step 1.

6. Inserting the output coupler translates the RW beam. Using adjustable irises in the FW beam, retro align the RW to the FW beam. Correct RW beam vertical alignment can be checked by repeating the procedure in Section G.1.2.

7. Vertical tilt of the output coupler needs to be set approximately. The HeNe alignment beam is usually flat through the slab with respect to the optical table. Setting the height of the RW back reflection off the output coupler to be the same height as the incident RW beam at comparable distances is usually sufficient. However, if the transmitted RW beam is seen to slope down slightly, then the RW reflection off the output coupler should slope up slightly over a comparable distance, and vice versa.

8. If necessary, repeat steps 6 and 7 after adjusting the vertical tilt.

With the output coupler correctly positioned, the FW alignment beam can be blocked. The FW beam retains the correct slab alignment, should further output coupler adjustment be required.

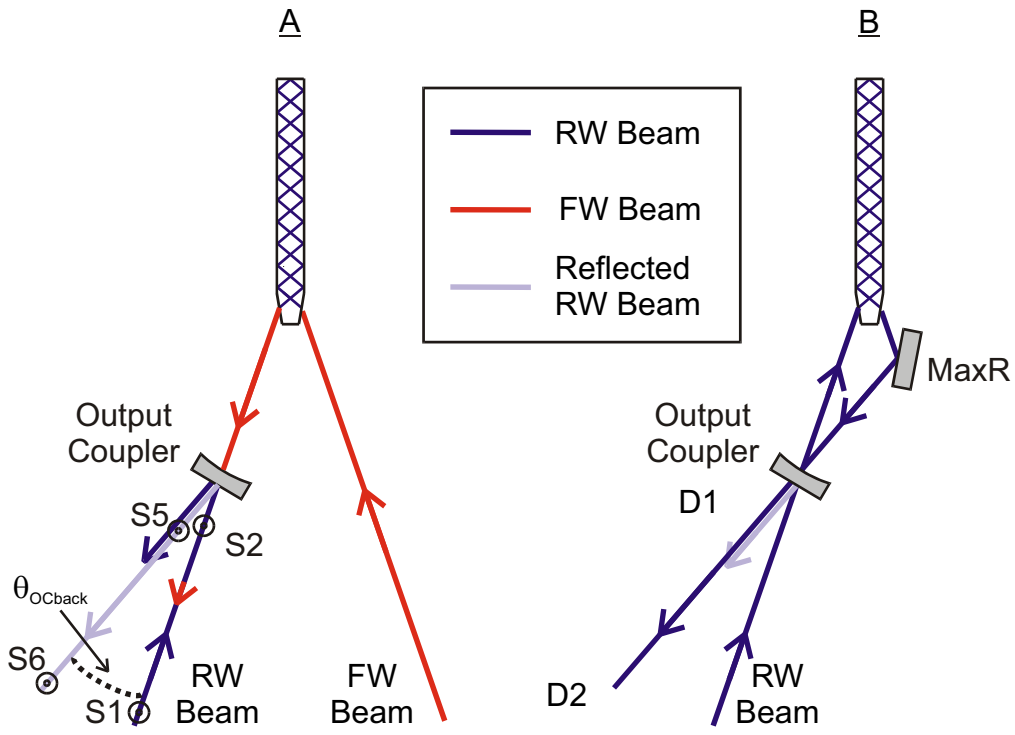

Figure G.3: (A) Schematic showing how to position the output coupler, and (B), alignment of the Max-R mirror.

G.3.2 Max-R mirror positioning

The following procedure is used to position the Max-R mirror. Steps $1-5$ require the slab to remain unpumped.

1. Position the Max-R mount on the resonator base, insert the securing bolts and lightly tighten. Rotation and translation will still be allowed.

2. Reflect the transmitted RW HeNe beam off the Max-R mirror, ensuring the HeNe spot is centred. This beam overlaps the reflection of the RW beam off the front surface of the output coupler. Placing a screen at positions D1 and D2 (in Figure G.3 (B)) is used to check beam overlap. Maximise the distance between D1 and D2.

3. Vertical Max-R mirror adjustment requires the clamping screw on the mount to be loosened. The tilt adjustment screw is then adjusted to allow the transmitted RW HeNe beam off the Max-R mirror to overlap the reflected RW output coupler beam. Re-tighten the clamping screw to set the vertical tilt.

4. With the clamping bolts loose, carefully rotate and translate the Max-R mount horizontally.

5. Repeat steps $2-4$ as necessary. Interference is observed when correctly aligned. The Max-R base should be bolted down just tight enough to prevent unwanted movement, but loose enough to allow it to be shifted, if required.

6a. Insert powermeters in the RW and FW beams. Pump the slab at a level just above laser diode threshold (approximately $12-14$ amps). Using an IR viewer, look for lasing. Correct alignment should produce a low threshold with an even power split in the RW and FW directions.

6b. Confirm the beam is centred on both the Max-R and output couplers. If not, then return to step 1.

7a. If not lasing, the threshold is high or the output power is not evenly split in the RW and FW directions, then repeat steps $2-6$ before continuing.

7b. If the threshold is low, but the power split is not even, very careful horizontal adjustment of the Max-R mirror is used to even up the power split. This should only be performed at a laser diode current level slightly above threshold. Once power is evened up with mirror spots remaining centred the laser diode current can be increased once again.

7c. Otherwise, slowly increase the laser diode current while measuring the output power in both the RW and FW directions. Even power split should be retained. Continue to increase the laser diode current until the desired pump power is achieved.

8. Turn down the laser diode current to just above threshold. Pick off a small fraction of either the RW or FW output beam and align a CCD (or an M^2 measuring device).

9. Slowly increase the laser diode current. The vertical mode should be seen to split evenly about the centre with increased pump power, with an even output power split. Measure the M^2, if applicable.

10. Tighten the Max-R mirror base bolts. Slight output coupler vertical and horizontal adjustment can then be performed to improve the mode, if required.

Note 1. On occasions, an additional Max-R mirror mounted on a small adjustable mount was used to achieve the correct position and alignment. This allowed minor alignment changes/improvements to be made, while measuring the M^2. Once the desired M^2 and output power was achieved, the final Max-R mount could be easily positioned using alignment irises and an additional reflected alignment beam (if necessary).

Note 2. If the vertical mode does not split evenly, or if output decreases with time, then vertical alignment is incorrect. Vertical adjustment of the output coupler can often improve this. Max-R mirror vertical adjustment should not be adjusted, but if required, procedures G.3.1 and G.3.2 should be repeated.

Note 3. Horizontal multimode operation indicates either incorrect slab alignment, or that the resonator is too short. Procedures G.3.1 and G.3.2 need to be repeated, possibly with an increased Brewster window to output coupler distance. Once horizontal single transverse mode operation is achieved, the vertical mode can be adjusted, if necessary.

Note 4. Single transverse mode operation in the vertical plane requires the vertical thermal lens to be appropriate for the resonator length. The vertical mode can be improved by either changing the pump power, or by altering the laser diode heatsink temperature. This changes the amount of absorbed pump power, and thus, the vertical thermal lens.

Appendix H

Injection-locking circuit diagrams

Circuit diagrams of the detectors and the feedback servo used for injection-locking the slave laser are found in this appendix. Unless otherwise stated, all resistor values are in ohms.

H.1 FW and RW detectors

Chapter 5 describes injection-locking of the 10 W slave laser, which uses the PDH stabilisation technique. Schematics of the detectors used to are shown in Figure H.1.

H.2 Feedback servo for injection locking

A schematic of the injection-locking electronics is shown in Figure H.2. This servo contains feedback loops for the three actuators described in Section 5.5.

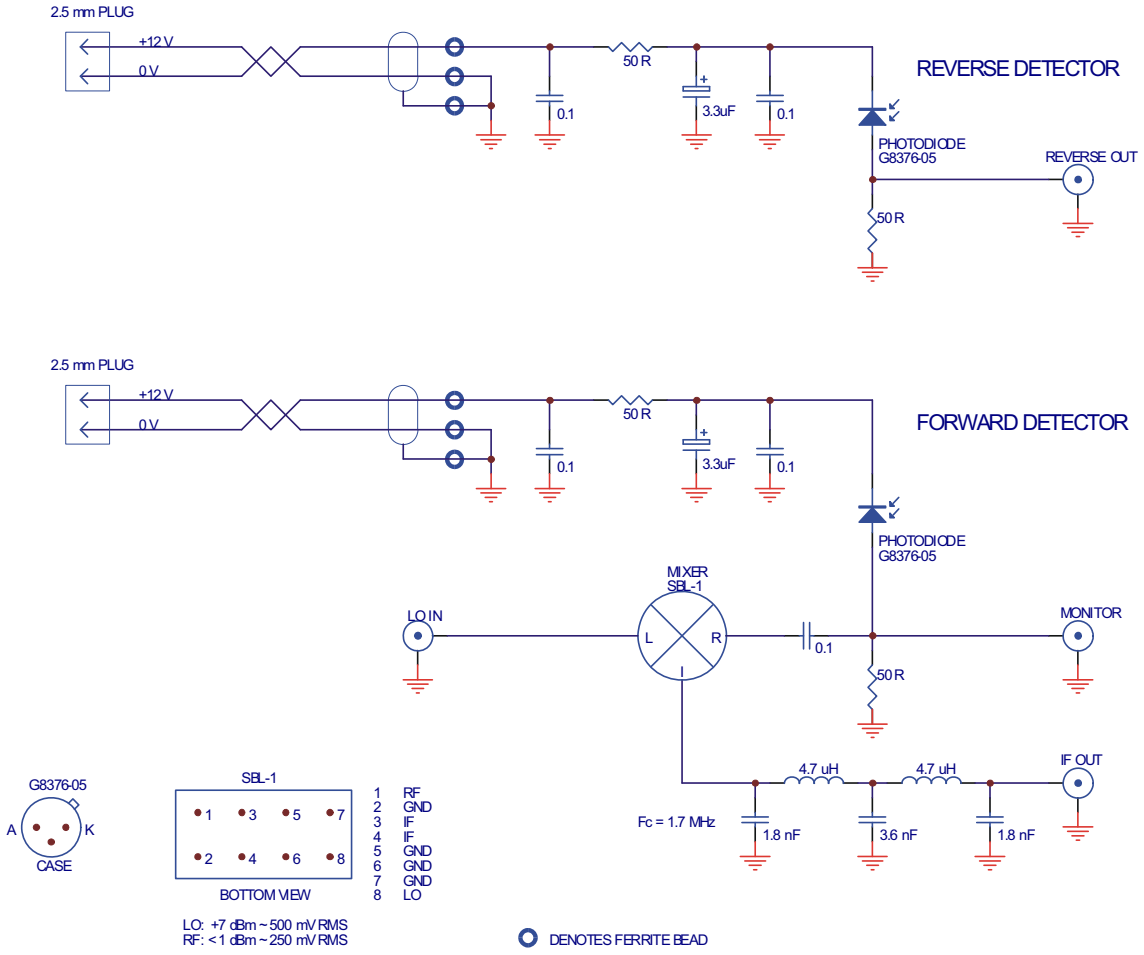

Figure H.1: Schematics of the FW and RW detectors which are used for injection-locking of the 10 W slave laser.

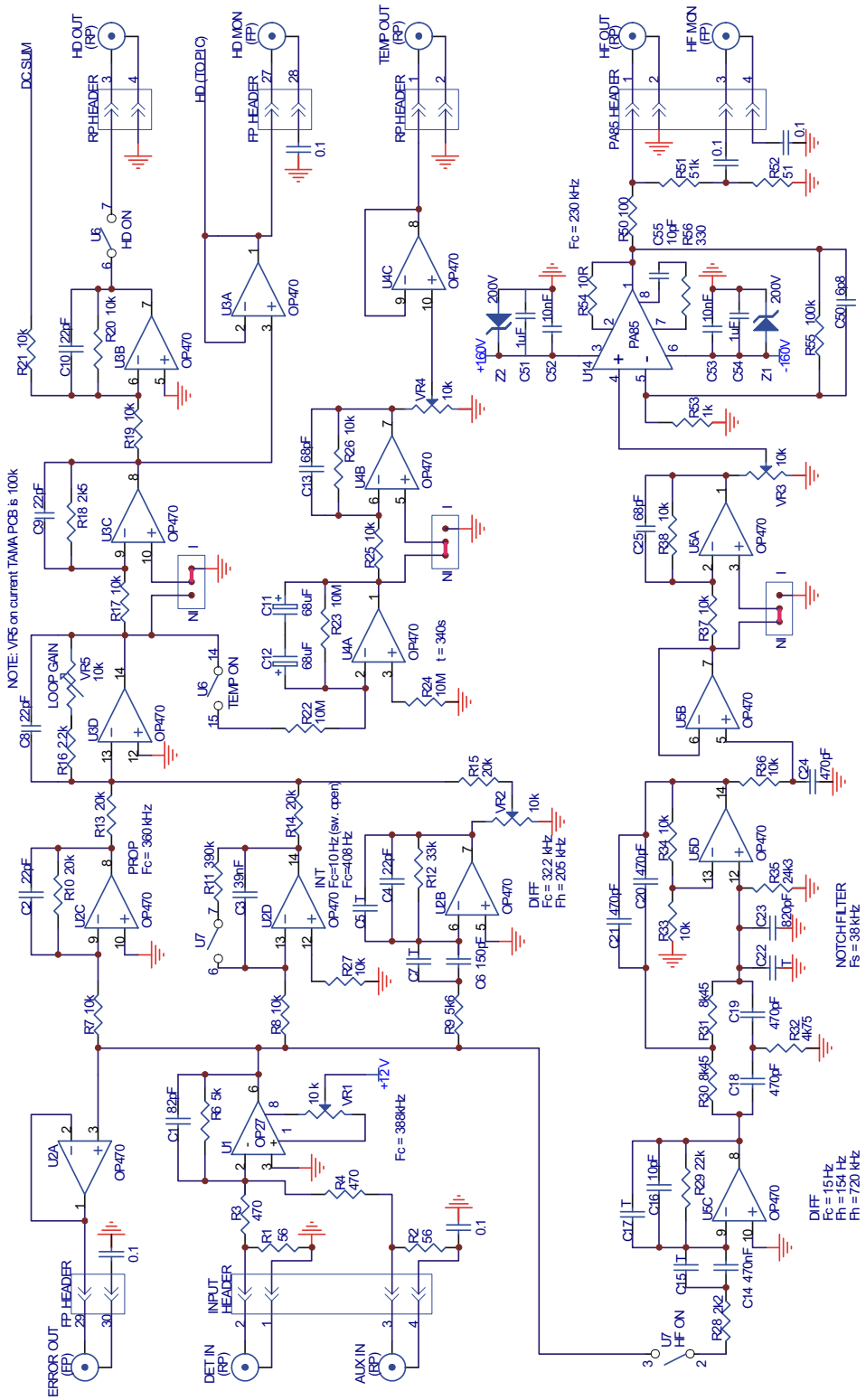

Figure H.2: Schematic of the injection-locking servo.

Appendix I

10 W injection-locked laser manual

As has been described in this thesis, injection-locked 10 W slave lasers were produced and installed at both TAMA 300 and the ACIGA HPTF. An operating manual was produced for each of these lasers, and contains circuit diagrams and operational information.

This appendix contains a copy of the 10 W laser manual for the laser installed at TAMA 300 (Version 1.1). This document was written and complied by the author and Dr Damien Mudge. Unless otherwise stated, all resistor values shown in circuit diagrams are in ohms.

THE UNIVERSITY OF ADELAIDE
AUSTRALIA

SUB CRUCE LUMEN

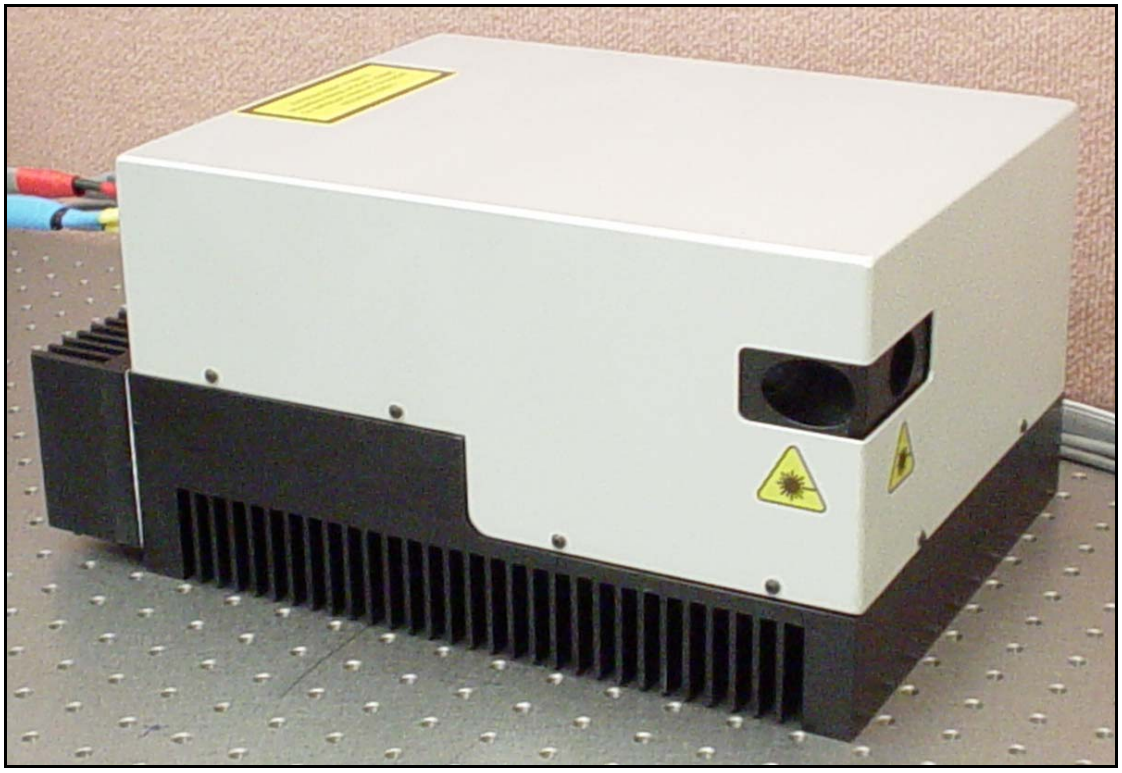

10W LASER

(TAMA 300)

Written by David Hosken / Damien Mudge

Version 1.1 (13/12/05)

CONTENTS:

GLOSSARY OF TERMS:

- **A/D** : Analogue / Digital
- **ESD** : Electro-Static Discharge
- **FW** : Forward-Wave
- **RW** : Reverse-Wave
- **HD** : High Dynamic Range
- **HF** : High Frequency Range
- **HV** : High Voltage
- **NTC** : Negative Temperature Coefficient
- **PDH** : Pound-Drever-Hall
- **PICOLOG** : Analogue / Digital Converter (Brand Name)
- **PID** : Proportional Integration Differentiation
- **PZT** : Piezoelectric Transducer
- **TEC** : Thermoelectric Cooler
- **n/c** : Not connected

WARNING: The pin connections have been described as accurately as possible. Check before making any changes!!!!

1. 10W SLAVE LASER OPERATIONAL SETTINGS

NEWPORT LASER DIODE DRIVER:

I_0 = 25.50 Amps

LIGHTWAVE NPRO 125/126 SERIES

DC = 1.98 Amps
DT = 21.8 ^{0}C
LT = 47.6 ^{0}C
T+ = 45.2 ^{0}C
Pwr = 223 mW
(Shown on controller)

DIODE TEC POWER SUPPLY:

Set Temp = 4.38

RESONATOR TEC POWER SUPPLY:

Temp. Offset = 5.53
Set Temp = 6.50

DIODE LASER EMISSION CHARACTERISTICS

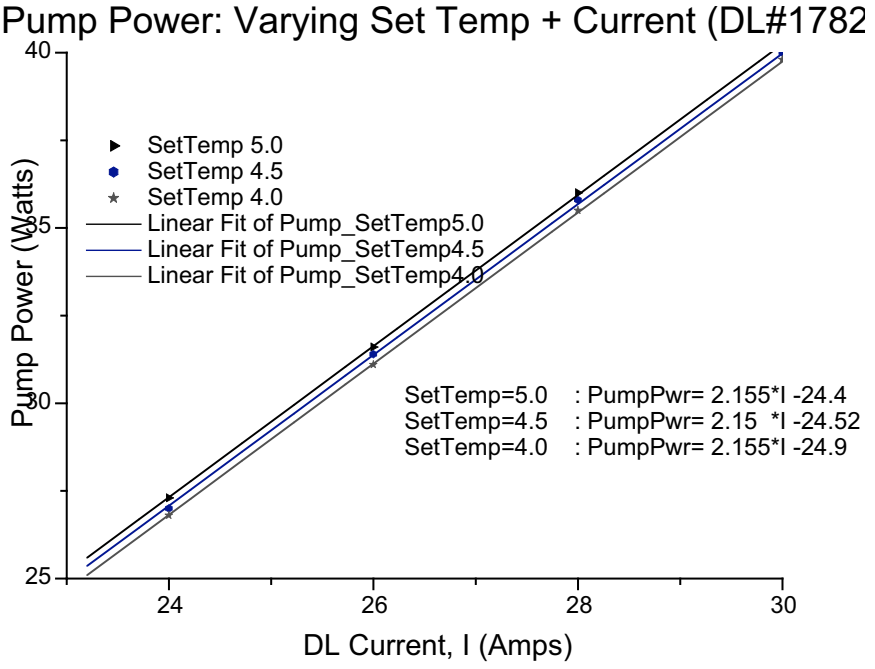

2. 10 W LASER TURN ON/OFF PROCEDURE

TURN ON

- Turn the mains plug on (This will power the entire 10W laser rack).

Note: The Diode Laser relies on the earth connection to prevent ESD

- Reset the SUPPLY FAIL by pressing the button switch on the INTERLOCK CONTROLLER. This will turn the red LED off.

(Note: In the event of momentary or permanent power failures this LED will turn on and the laser will not operate. The NEWPORT LASER DIODE DRIVER will need to be turned off and the turn on procedure needs to be repeated starting with resetting the SUPPLY FAIL).

- Clear any faults indicated by the orange FAULT STATUS LEDs on the INTERLOCK CONTROLLER by pressing the toggle switch down once.

*** If any of the fault LED's remain on, there is a problem that needs to be addressed ***

- Turn on the SERVO LOCK POWER unit (the switch on the left of the lowest silver unit in the LASER RACK). Each of the small toggle switches on the right should be turned on (LED's indicate on). This powers the AUTO LOCK unit, the FW and RW DETECTORS, cooling FAN, EOM and the LOCKING ELECTRONICS.

- Set the DIODE DRIVER ACTIVE, DIODE TEC ACTIVE and RESONATOR TEC ACTIVE green LED's by pressing each associated button on the INTERLOCK CONTROLLER once. This allows the TEC cooling modules and DIODE LASER DRIVER to be activated.

- Turn the RESONATOR TEC POWER SUPPLY on.

- Turn the DIODE TEC POWER SUPPLY on and allow a few minutes for it to stabilise.

- Turn the NEWPORT LASER DIODE DRIVER on and turn its key switch to the on position.

- Ensure the current reading on the screen reads "0.0A". Else, turn the current control knob down to zero.

- Press the LDD button near the round current control knob on the right of the unit. This will turn on the green light near the button, indicating the unit is set to provide power to the Diode Laser.

2. 10 W LASER TURN ON/OFF PROCEDURE

- Turn the current knob to 25.50A **slowly**. Do not use any more current (further output power is unlikely to be achieved and misalignment of the laser could result). Turning the laser up to 25.50A should take several minutes (ie: do this slowly). The temperatures of the Diode Laser and SLAB are pre-set.

- Turn the NPRO on via the key switch. The temperature and current should be pre-set to suit the laser.

- Allow several minutes for the laser mode to stabilise.

Locking in manual setup

All instructions below refer to the LOCKING ELECTRONICS – the module under the INTERLOCK CONTROLLER.

- Ensure the mode switch is set to Manual (MAN).

- Ensure the HD ON switch is set to on (down) – this turns the HD PZT on.

** Important: The HD ON switch must be in the on position for both AUTO and MAN. operation. **

- The INT, HF ON and TEMP ON switches should be off (up) initially.

- Turn the OFFSET potentiometer on the LOCKING ELECTRONICS unit to change the DC OFFSET on the HV supply to drift the PZT location until the NPRO and 10W slave lasers lock. The reverse wave will turn off, changing the photodiode output from +V (unlocked) to zero (locked) (ie: The reverse wave will turn off as all power is in the forward direction). The RW=0 light should turn on. Once drift locked, switch the INT switch to on (down) (add in the integrator). Turn the HF ON switch on (down) (turns the HF PZT on).

- The ERROR BNC is the PDH error signal.

- Using an oscilloscope (or digital multimeter), measure the HD MON BNC signal. This needs to be set to zero while locked by changing the OFFSET potentiometer.

- Turn on the TEMP ON switch (this allows the LOCKING ELECTRONICS to change the slave temperature very slowly to keep the DC offset near zero, that is to keep the frequencies of the NPRO and slave matched).

2. 10 W LASER TURN ON/OFF PROCEDURE

- Note: The time constant of the TEMP ON electronics is several minutes. This switch must be manually operated and is not controlled by the AUTO LOCKER.

- The toggle switch can be shifted from MAN to automatic (AUTO).

Note: If in automatic mode, the position of the INT and HF ON are irrelevant. These switches are bypassed by the AUTO LOCKER.

- The AMPLITUDE sets the overall loop gain and is maximised. If excess noise appears on the PDH Error signal, decrease the AMPLITUDE setting to stop oscillations – if the mode matching is poor the gain needs to be reduced.

2. 10 W LASER TURN ON/OFF PROCEDURE

TURN OFF

- Switch the AUTO LOCKER switch to MAN.
- Switch the TEMP ON, HF ON and INT switches to their off positions.
- Reduce the NPRO current to 0A and turn the NPRO off.
- Turn the current knob on the NEWPORT LASER DIODE DRIVER down to 0A slowly. Turning the Diode Laser current down to 0A should take several minutes (ie: do this slowly).
- Press the LDD button on the NEWPORT LASER DIODE DRIVER and the green led should go off (indicating the Diode Laser is off). Turn the key switch off and the NEWPORT LASER DIODE DRIVER power switch off. Allow the laser to cool for several minutes.
- Turn the RESONATOR TEC POWER SUPPLY off.
- Turn the DIODE TEC POWER SUPPLY off.
- Turn each of the small toggle switches on the right of the SERVO LOCK POWER unit off (LED's turn off). Turn the SERVO LOCK POWER unit off (the switch on the left of the lowest silver unit in the LASER RACK).
- Turn the mains plug off.

(WARNING: always ensure this is plugged in to prevent ESD to the Diode Laser, even when switched off.)

IMPORTANT: If an interlock shutdown occurs, always ensure the current control knob on the NEWPORT LASER DIODE DRIVER is turned down to zero before turning the Diode Laser on again. Do not simply press the LDD button to reactivate the Diode Laser, otherwise the Diode Laser will be set to full power as soon as it is turned on, rather than ramped up slowly.

3. OPTICAL LAYOUT

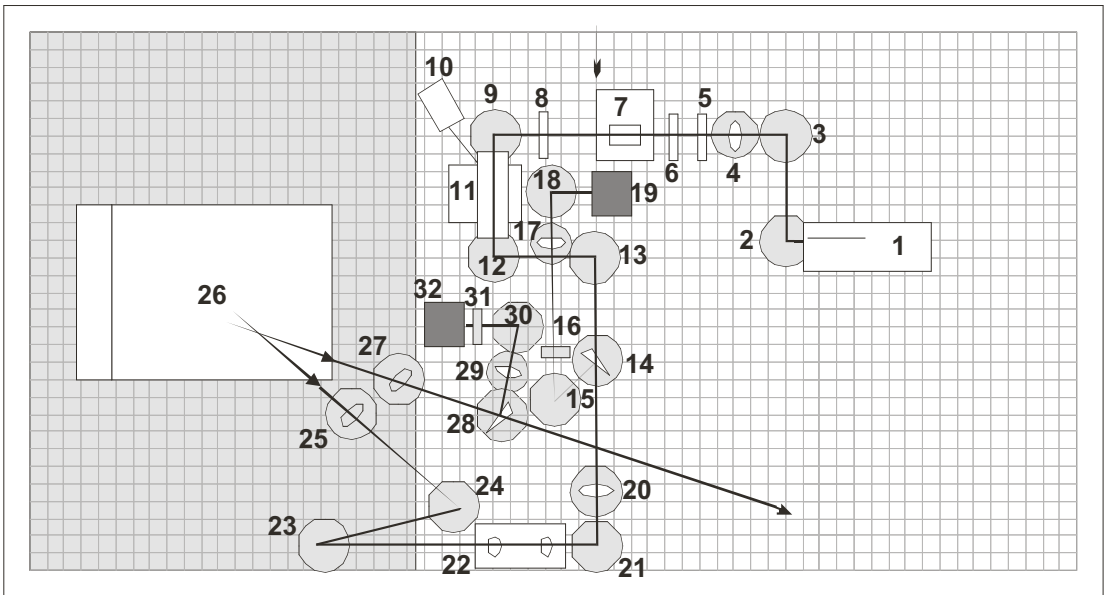

The optical layout for the injection-locked 10W laser consists of the following components:

1. Lightwave NPRO
2. YAG beam-steering mirror
3. YAG beam-steering mirror
4. 150mm AR-coated lens
5. L/4 plate
6. L/2 plate
7. ElectroOptic Modulator (EOM), New Focus Model # 4003M
8. L/2 plate
9. YAG beam-steering mirror
10. Reverse-wave beam dump
11. Faraday Isolator (FI), OFR Model # IO-5-1064-VHP
12. YAG beam-steering mirror
13. YAG beam-steering mirror
14. AR-coated wedge
15. YAG beam-steering mirror
16. Filter/filter holder (RW)
17. 100mm AR-coated lens
18. YAG beam-steering mirror
19. Reverse-wave detector (RW Det.)
20. 500mm AR-coated mode-matching lens
21. YAG beam-steering mirror
22. Periscope (76.2mm to 130mm)
23. YAG beam-steering mirror
24. YAG beam-steering mirror
25. 200mm AR-coated cylindrical lens
26. Air-cooled slave laser
27. 200mm AR-coated cylindrical lens
28. AR-coated wedge
29. 100mm AR-coated lens
30. YAG beam-steering mirror
31. Filter/filter holder (FW)
32. Forward-wave detector/ mixer (FW Det.)

- Components 1-22 : Beam height of 3 inches (76.2mm)
- Components 22-32 : Beam height of 130mm

4. LASER HEAD AND CONNECTIONS

The LASER HEAD contains the following components, which are all mounted on the integrated air-cooled base.

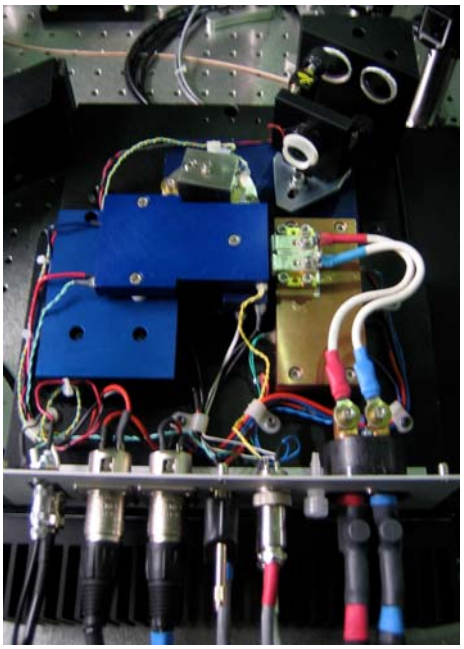

- DOUBLE DIODE BAR PACKAGE (CEO)
- DIODE COPPER BLOCK (Temperature controlled)
- PUMP REFLECTOR
- RESONATOR BASE (Temperature controlled)
- SLAB TOP BLOCK (Temperature controlled)
- HD RESONATOR MIRROR MOUNT/OUTPUT COUPLER
- HF RESONATOR MIRROR MOUNT / MAX R MIRROR
- THERMISTORS
- SLAB

DOUBLE DIODE BAR PACKAGE: Cutting Edge Optronics (CEO) Diode Laser package has two fast-axis collimated diode bars located side-by-side. The total available output power is 68W (using two 40W diode bars, lensing decreases the output power). (See schematic)

DIODE COPPER BLOCK: The DOUBLE DIODE BAR PACKAGE is bolted (using M4 bolts) onto the temperature controlled copper block. The DIODE TEC POWER SUPPLY drives two TEC's under the block. There are two thermistors mounted in this block, one used for the temperature control set point, while the other monitors the block temperature to ensure it remains within the working temperature range. Should this block become too hot or cold, the INTERLOCK CONTROLLER will turn off the NEWPORT LASER DIODE DRIVER.

PUMP REFLECTOR: The PUMP REFLECTOR is located parallel and behind the slab on the opposite side to the Diode Laser package. It reflects any pump light that is not absorbed on the first pass back into the slab to improve the efficiency.

RESONATOR BASE: The resonator base is temperature controlled using three TEC's connected in series, supplied by the RESONATOR TEC POWER SUPPLY. Two thermistors are mounted in the resonator base. One thermistor is used to set the base (slab) temperature, while the other is used to match the temperature of the top of the slab to the bottom of the slab.

4. LASER HEAD AND CONNECTIONS

SLAB: This laser uses a coplanar folded zigzag slab (CPFS) that has 10 TIR bounces/side. It has Brewster angled entrance/exit windows, is side-pumped and top/bottom cooled. The slab has no coatings. (See diagram below)

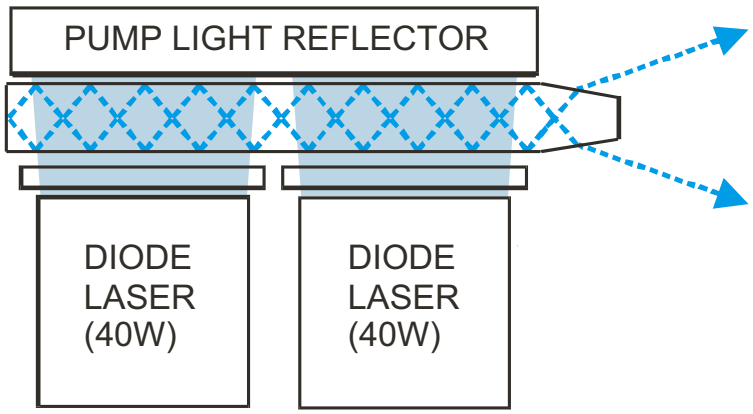

Side-pumping the slab using side-by-side diode bars on a single package.

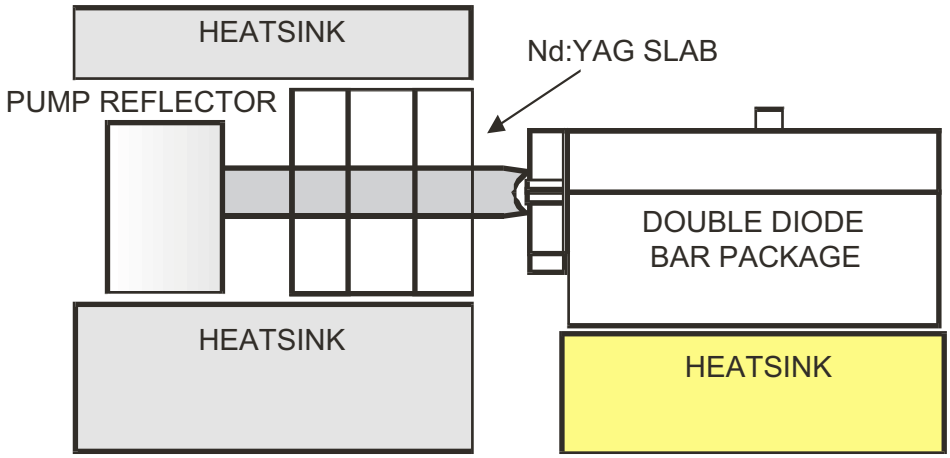

Top/bottom cooling of the slab, side-pumped using the double diode bar package.

SLAB TOP BLOCK: The top block clamps the top of the slab. It is connected to the LASER BASE via a TEC. The TEC is used to match the temperature of the top of the slab to the bottom. Two thermistors are mounted in this block, one directly above the slab for temperature stabilisation, and the other near the TEC, which is monitored by the INTERLOCK CONTROLLER. If the slab gets too hot or cold, the RESONATOR TEC POWER SUPPLY will turn off.

HD RESONATOR MIRROR MOUNT/OUTPUT COUPLER: A modified Lees (Linos) LM2 mount is used to hold the output coupler/PZT. The output coupler is a 90% reflectance, 5.00mCC optic, on a Piezomechanik PZT stack. (See details below).

4. LASER HEAD AND CONNECTIONS

HF RESONATOR MIRROR MOUNT / MAX R MIRROR: The HF mirror mount is a custom made stainless steel mount with adjustment in the Y-direction only. The maximum reflectivity (Max R) mirror is a custom coated mirror, with dimensions 9mm x 6.5mm and is attached to a small PZT.

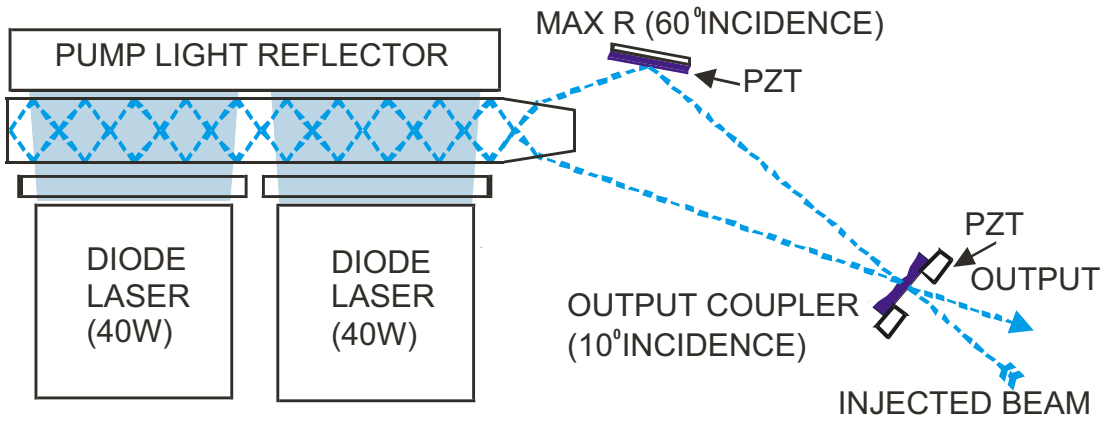

Travelling-wave resonator layout.

THERMISTORS: Temperature sensors used in the laser head are 100kOhm NTC (Negative Temperature Coefficient) thermistors.

Part Numbers:

TEC's:

Diode:	Melcor UT15-12-40-F2-T2-RTV	(x2)
Slab Top:	Melcor UT6-12-40-F1-T1-RTV	(x1)
Resonator Base:	Melcor UT6-7-30-F1-T2-RTV	(x3)

Optics:

MaxR Mirror:	BK7-9-6.5-3-MIRROR R=99.5% @ 1064nm (theta = 60^0, p-pol.)
Output Coupler:	PR1-1064-90-0725-5.00CC R=90% @ 1064nm (theta = 0^0) 5.00m Concave (0.75 inch diameter)

PZT's:

HFPZT (MaxR):	Ferroperm Piezoceramics Pz27
HDPZT (90%):	Piezomechanik HPST 1000/25-15/5 (PZT Stack)

4. LASER HEAD AND CONNECTORS

Schematic (Double Diode Bar Package)

- Diode package serial # 17820 used on the 10W Laser for TAMA.

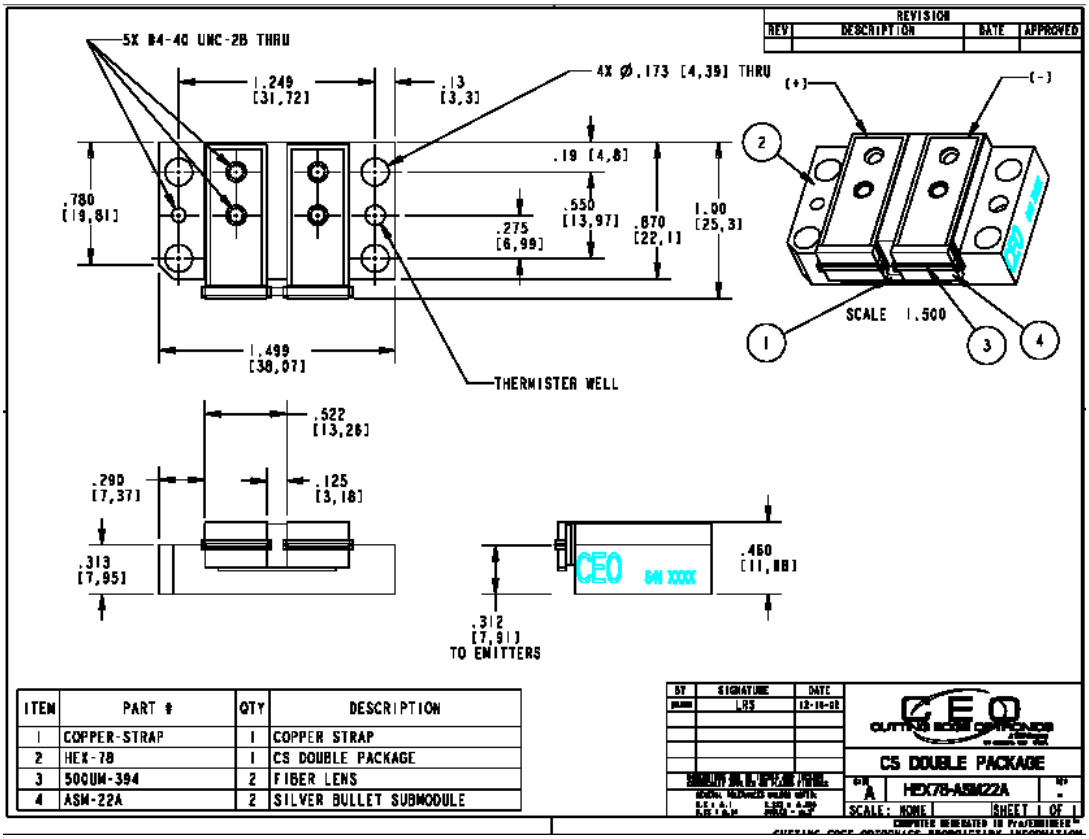

Cooling Fan:

The following fan is located in the base of the LASER RACK and is used for air-cooling the laser base via a flexible duct.

RS (Australia) Part # 504-928
Description: Slimline axial fan, 120mm frame, 100cft/min, 12V DC
Manufacturer: EBM PAPST
Model: 4312

5. LASER RACK LAYOUT

The laser rack consists of the following electronic units; each unit is removable from the rack. Input and Output cables are secured at the back of these units to a support frame preventing damage to the connectors.

- Newport Laser Diode Driver Model 5600
- Interlock Controller
- Locking Electroinics
- Resonator TEC Power Supply
- Diode TEC Power Supply
- RF/PICOLOG
- Servo Lock Power
- Mains Supply Module
- Cooling Fan / Diode TEC Transformer

This locking rack must remain GROUNDED AT ALL TIMES to prevent ESD to the diode laser, with the Mains Supply Module powering the entire LASER RACK.

A detailed description of each of these units is included in this document.

6. DESCRIPTION OF ELECTRONICS MODULES

This section describes each of the electronics modules in the LASER RACK, providing information about the function of the switches, LED's and connections, as well as schematics of the electronics.

6.1 NEWPORT LASER DIODE DRIVER MODEL 5600

For further information regarding the operation of the NEWPORT LASER DIODE DRIVER, including computer interfacing etc, please refer to the device manual.

6.2 INTERLOCK CONTROLLER

Front Panel

- EMERGENCY STOP (Push Button)
- SUPPLY FAIL (LED)
- RESET (Push Button)
- DIODE DRIVER ACTIVE (LED & RESET Button)
- DIODE TEC ACTIVE (LED & RESET Button)
- RESONATOR TEC ACTIVE (LED & RESET Button)
- FAULT RESET (Switch)
- FAULT STATUS (LEDs)
    - DIODE TEMP.
    - RESONATOR TEMP.
    - BASE TEMP.
    - REMOTE

EMERGENCY STOP: Activating this button will turn off the Newport Laser Diode Driver. This method of turning off the laser (pump diode) should only be used in an emergency, with the usual method for turning off the laser being described in the 10W LASER TURN ON/OFF PROCEDURE.

SUPPLY FAIL: This LED is illuminated when the supply power to the rack is turned off and then comes back on again. To reset, press the RESET switch. This will then allow operation of the INTERLOCK CONTROLLER. The purpose of this feature is to detect intermittent mains power conditions and prevent the laser being switched on and off repeatedly and rapidly.

RESET: Resetting this switch is necessary when the SUPPLY FAIL LED is illuminated. Once reset, the SUPPLY FAIL LED will cease to be illuminated and the INTERLOCK CONTROLLER can be operated.

DIODE DRIVER ACTIVE (RESET): The green LED will be illuminated when the RESET button below the LED is pushed once. It will not turn on if a fault exists, and will require this fault to be rectified before operation. Once illuminated, the NEWPORT LASER DIODE DRIVER can be operated.

DIODE TEC ACTIVE (RESET): The green LED will be illuminated when the RESET button below the LED is pushed once. It will not turn on if a fault exists, and will require this fault to be rectified before operation. Once illuminated, the DIODE TEC POWER SUPPLY can be operated.

RESONATOR TEC ACTIVE (RESET): The green LED will be illuminated when the RESET button below the LED is pushed once. It will not turn on if a fault exists, and will require this fault to be rectified before operation. Once illuminated, the RESONATOR TEC POWER SUPPLY can be operated.

6.2 INTERLOCK CONTROLLER

FAULT RESET: To clear any faults indicated by the orange FAULT STATUS LED's, press the toggle switch down once. If a fault remains, then there is a fault that needs to be addressed. Only once all faults have been cleared can each of the NEWPORT LASER DIODE DRIVER, DIODE TEC POWER SUPPLY and RESONATOR TEC POWER SUPPLY be operated.

FAULT STATUS LED's: Indicate that a fault needs to be addressed.

- **DIODE TEMP:** Indicates that the temperature of the Diode Laser copper block is outside its operating temperature range.
  Operation range: 12 ^{0}C - 45 ^{0}C
- **RESONATOR TEMP:** Indicates that the temperature of the resonator (or slab) is outside its operating temperature range.
  Operation range: 12 ^{0}C - 45 ^{0}C
- **BASE TEMP:** Indicates that the temperature of the air-cooled laser base is outside its operating range.
  Operation range: 12 ^{0}C - 50 ^{0}C
- **REMOTE:** This indicates that the remote switch has been triggered. Such a remote trigger could be a Reed switch on a door to an enclosure or similar.

These faults can only be cleared once the Diode/Resonator/Base are within their operating temperature range, or once the remote trigger has been reset.

→ Depending on the fault, the INTERLOCK CONTROLLER makes a decision about which modules should be shut down. This means that all three units will not necessarily be shut down when a fault is detected, only those directly affected.

6.2 INTERLOCK CONTROLLER

Rear Panel

- Inputs:
  - REMOTE (4-pin plug/socket)
  - LASER (D9 plug/socket)
- Outputs:
  - DIODE TEC (2-pin plug/socket)
  - RESONATOR TEC (2-pin plug/socket)
  - DIODE DRIVER (D9 plug/socket)
- Power/Others:
  - DIODE TEMP MON. (BNC)
  - RESONATOR TEMP MON. (BNC)
  - BASE TEMP MON. (BNC)
  - IEC (MAINS IN) (3-pin)

REMOTE: This two-pin connector is attached to the INTERLOCK CONTROLLER and can be connected to a Reed-type switch.

LASER: This connector is attached to the LASER HEAD via a cable and monitors three thermistors mounted within the LASER HEAD. These signals are used by the INTERLOCK CONTROLLER to monitor temperatures and detect faults that may require one or more of the control units to be turned off.

DIODE TEC: The output to the DIODE TEC POWER SUPPLY provides +5V signal when there is no fault. If there is a fault, the output is 0V and the DIODE TEC POWER SUPPLY unit will not operate. Therefore, this cable must be connected for the laser to be operated.

RESONATOR TEC: The output to the RESONATOR TEC POWER SUPPLY provides +5V signal when there is no fault. If there is a fault, the output is 0V and the RESONATOR TEC POWER SUPPLY unit will not operate. Therefore, this cable must be connected for the laser to be operated.

DIODE DRIVER: This output is connected to the NEWPORT LASER DIODE DRIVER. The NEWPORT LASER DIODE DRIVER provides +5V signal and tests for continuity between two pins on a D connector on the rear of the unit. Should it detect an open circuit, the driver is turned off. The INTERLOCK CONTROLLER uses an optical switch to create an open-circuit should a fault be detected, thus requiring the driver to be turned off. Therefore, the laser cannot be operated unless this cable is connected.

DIODE TEMP. MON: BNC output, used to monitor the temperature of the copper block on which the Diode Laser is mounted. This is usually connected to the PICOLOG A/D converter, allowing the temperature of the block to be monitored and logged. The temperature from the thermistor has been linearised, and the output voltage can be converted to ^{0}C using:

Diode Temp (^{0}C) = DiodeTempMon (V) * 10

6.2 INTERLOCK CONTROLLER

RESONATOR TEMP MON: BNC output, used to monitor the temperature of the resonator base (slab). This is usually connected to the PICOLOG A/D converter, allowing the temperature of the resonator base to be monitored and logged. The temperature from the thermistor has been linearised, and the output voltage can be converted to ^{0}C using:

Resonator Temp (^{0}C) = ResonatorTempMon (V) * 10

BASE TEMP MON: BNC output, used to monitor the temperature of the laser base (heatsink). This is usually connected to the PICOLOG A/D converter, allowing the temperature of the laser base to be monitored and logged. The temperature from the thermistor has been linearised, and thus, the output voltage can be converted to ^{0}C using:

Base Temp (^{0}C) = BaseTempMon (V) * 10

IEC: 100V AC with ground connection.

6.2 INTERLOCK CONTROLLER

Plug/Socket Pin connections

Remote 4-pin plug/socket

Pin#1	to reed switch	
Pin#2	n/c	
Pin#3	n/c	
Pin#4	to reed switch	(or bypass shunt between 1 and 4)

Laser D9 plug/socket (using 100kOhm NTC)

Pin#1	shield
Pin#2	diode-laser thermistor
Pin#3	diode-laser thermistor
Pin#4	slab thermistor
Pin#5	slab thermistor
Pin#6	base thermistor
Pin#7	base thermistor
Pin#8	n/c
Pin#9	n/c

Diode TEC 5V Interlock 2-pin plug/socket

Pin#1	Ground
Pin#2	+5V

Resonator TEC 5V Interlock 2-pin plug/socket

Pin#1	Ground
Pin#2	+5V

Diode Driver Interlock D9 plug/socket

Pin#1	connected (used by Newport driver)
Pin#2	connected (used by Newport driver, shield)
Pin#3	n/c
Pin#4	n/c
Pin#5	n/c
Pin#6	n/c
Pin#7	n/c
Pin#8	n/c
Pin#9	n/c

Nominal fuse for Interlock Controller: 100mA, 250V, M205

6.2 INTERLOCK CONTROLLER

Schematics

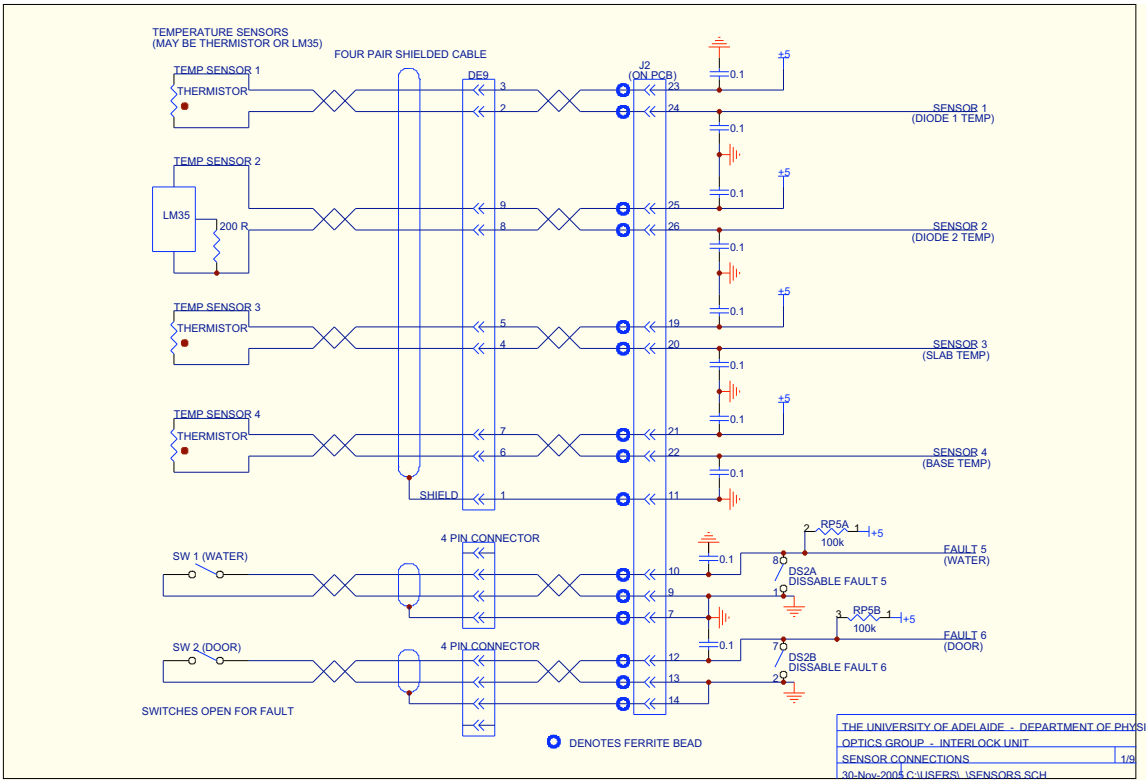

6.2 INTERLOCK CONTROLLER

Schematics

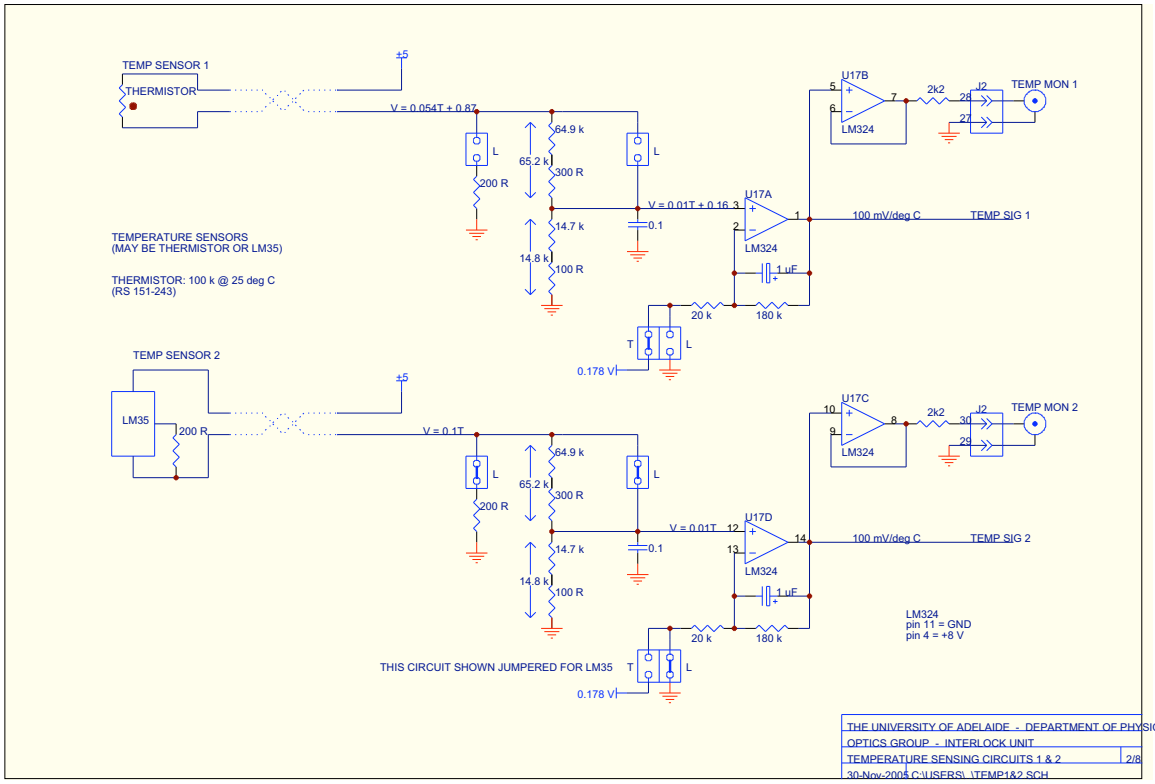

6.2 INTERLOCK CONTROLLER

Schematics

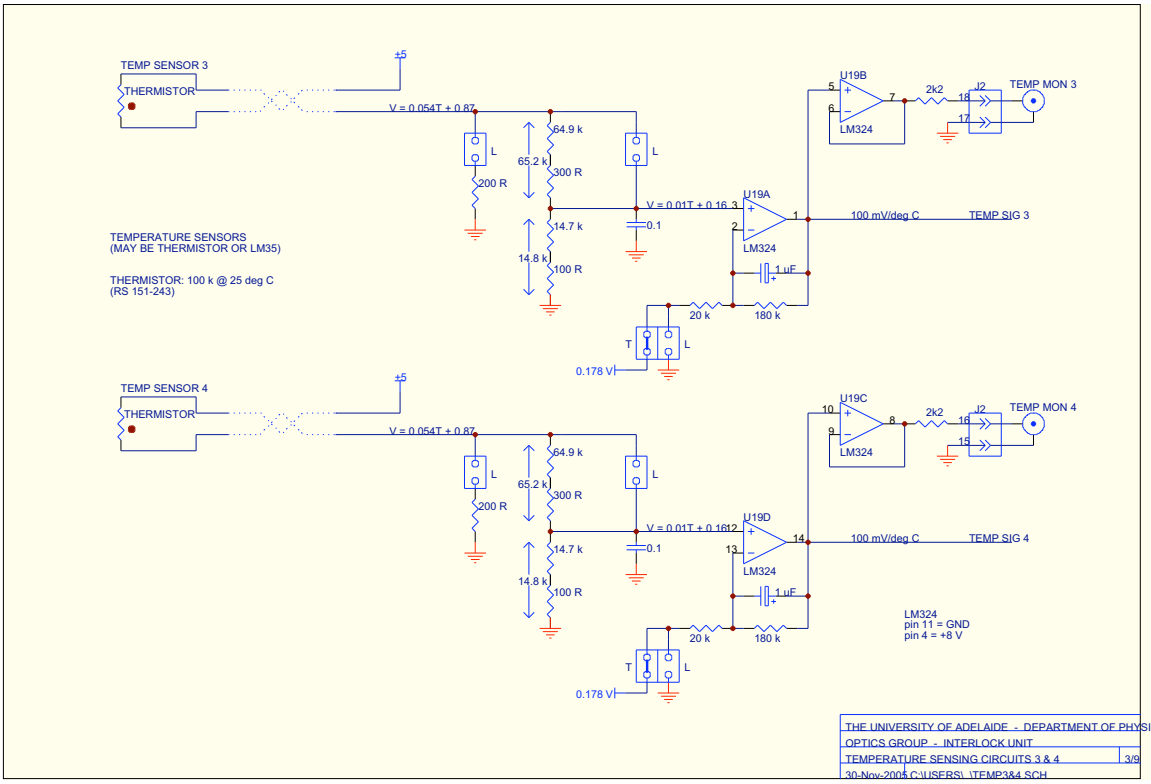

6.2 INTERLOCK CONTROLLER

Schematics

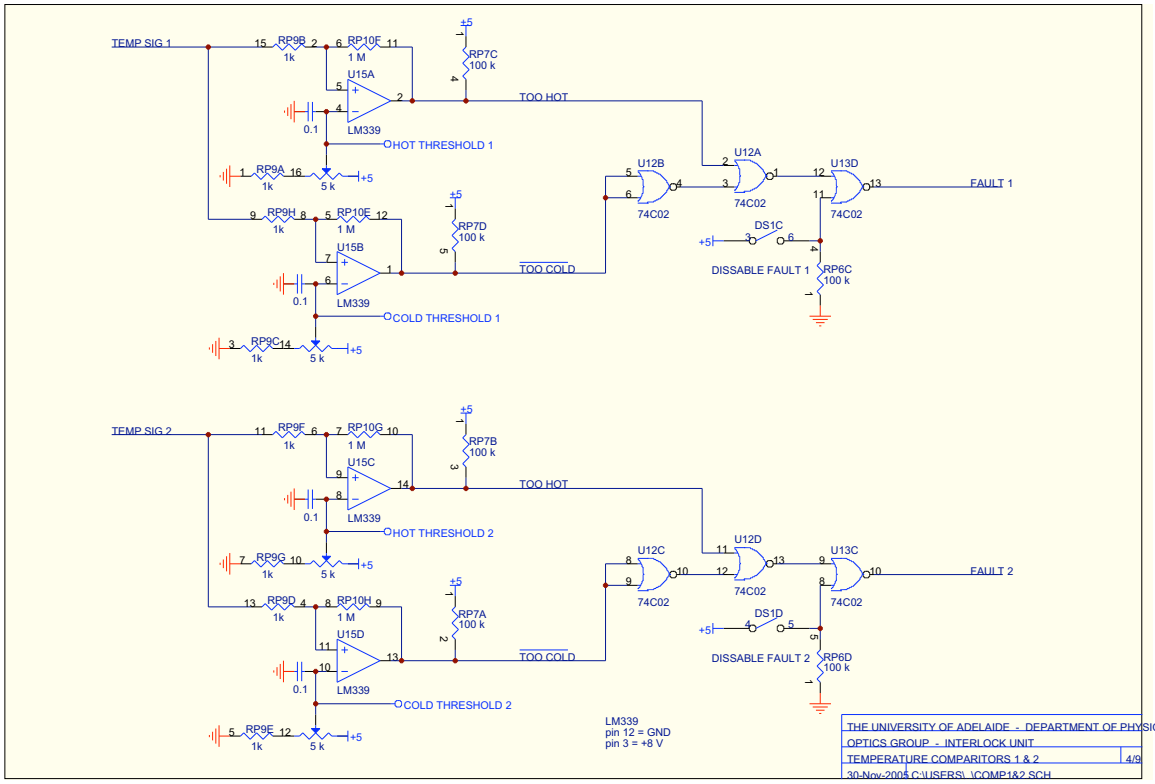

6.2 INTERLOCK CONTROLLER

Schematics

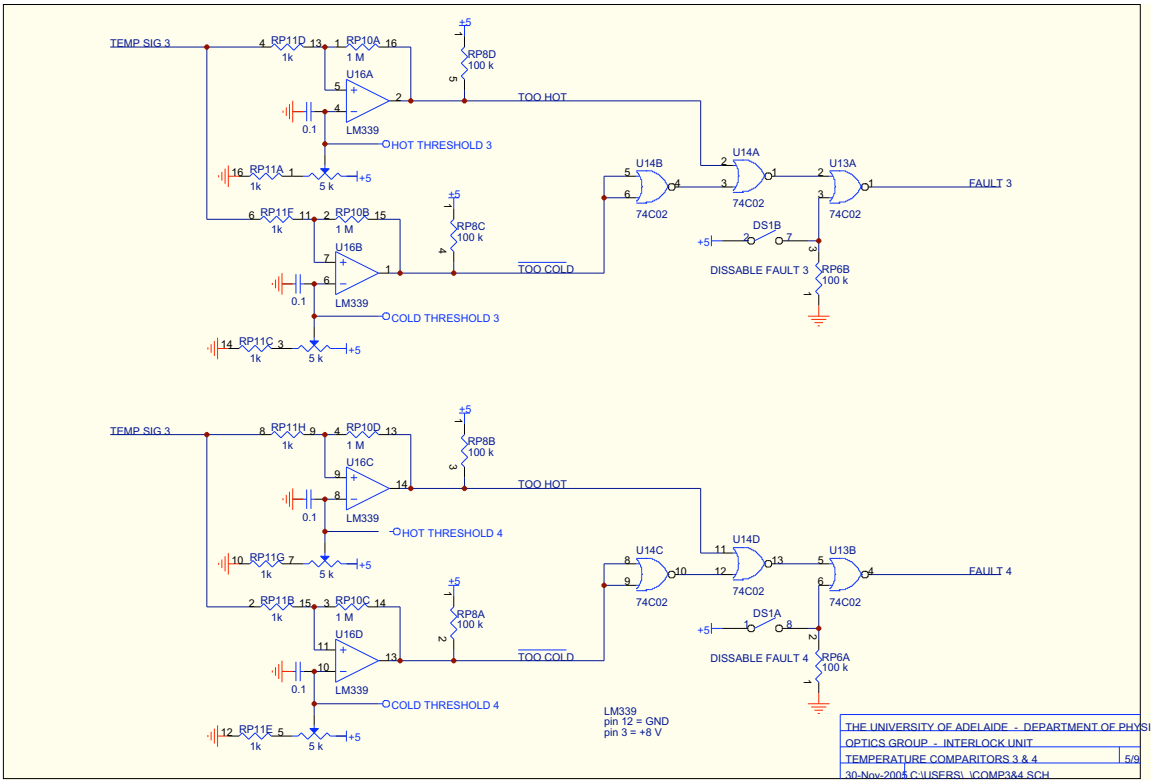

6.2 INTERLOCK CONTROLLER

Schematics

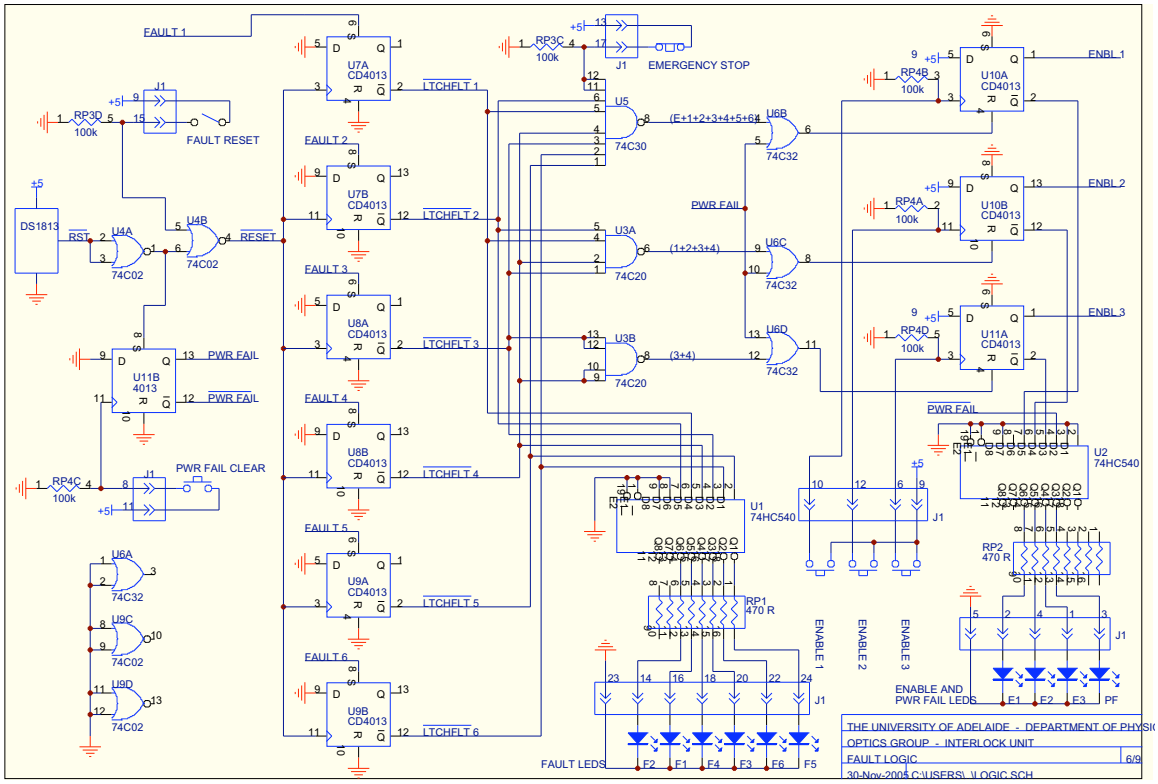

6.2 INTERLOCK CONTROLLER

Schematics

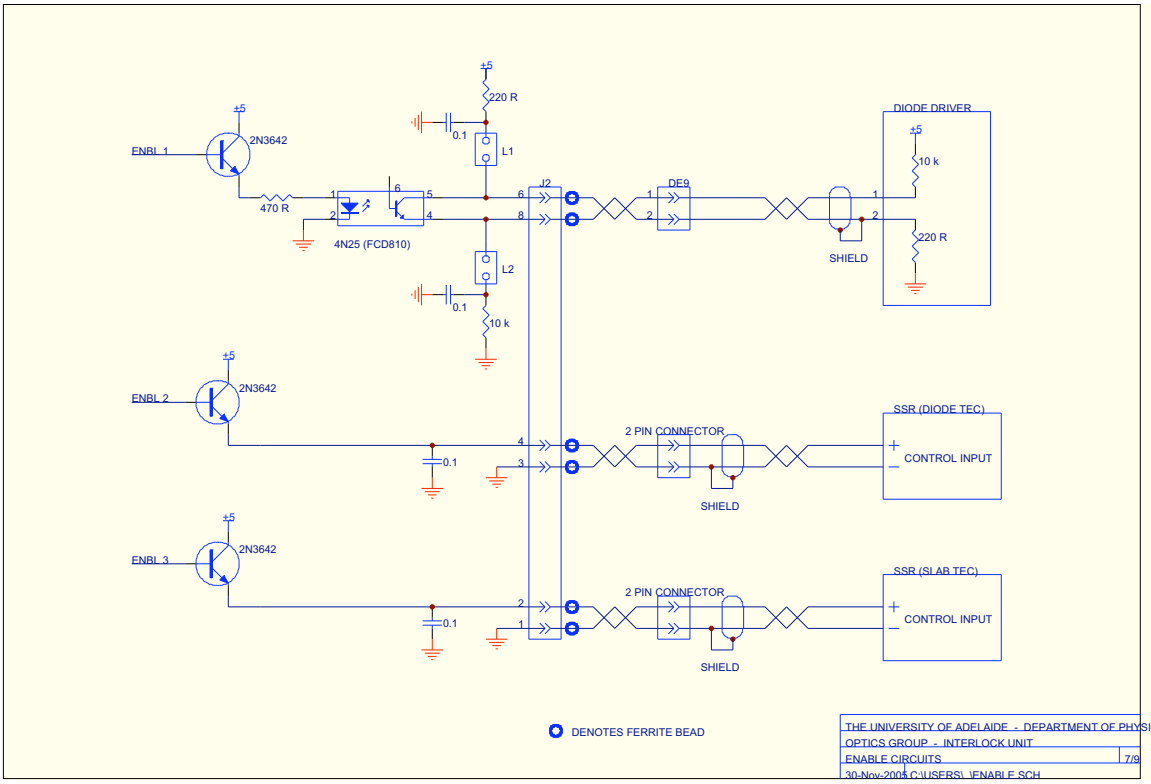

6.2 INTERLOCK CONTROLLER

Schematics

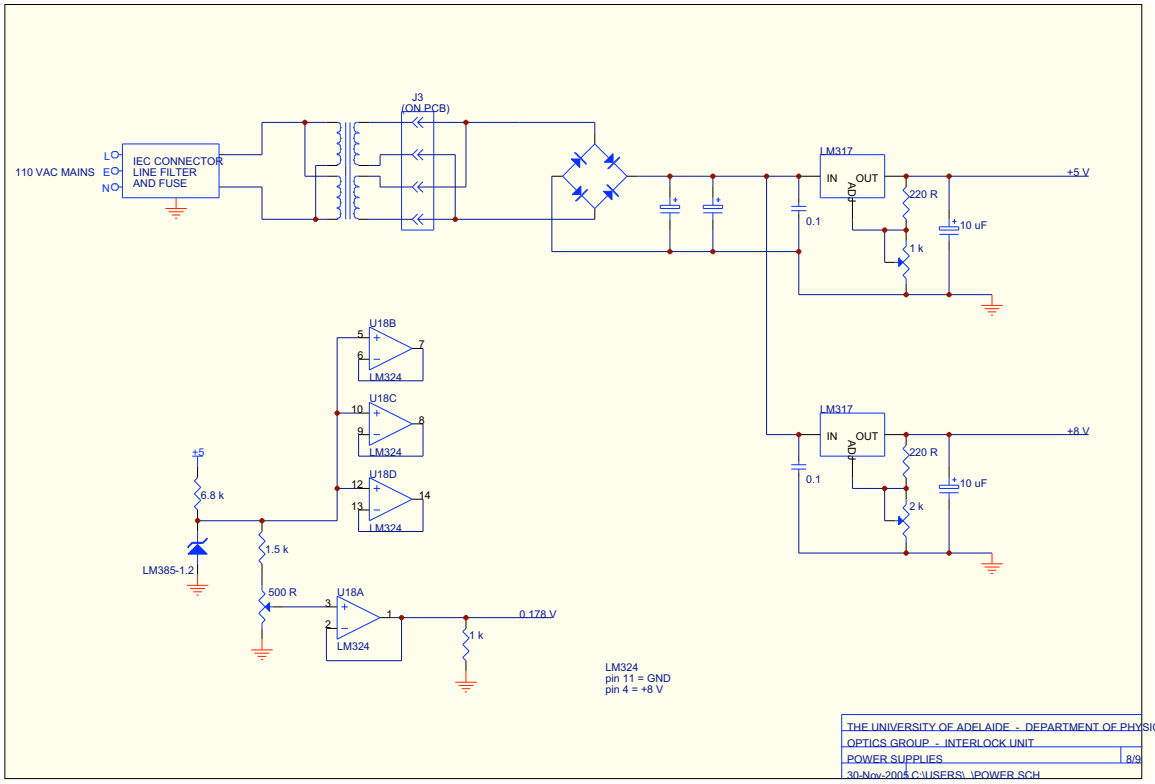

6.2 INTERLOCK CONTROLLER

Schematics

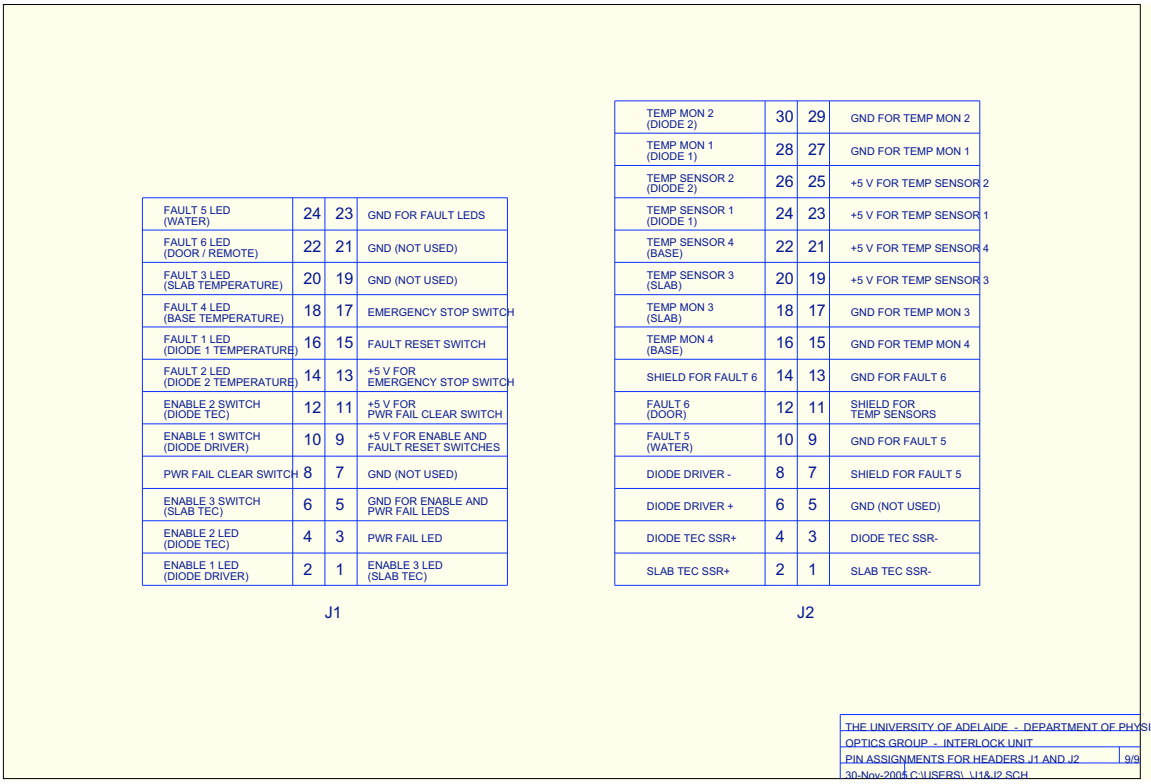

FAULT 5 LED (WATER)	24	23	GND FOR FAULT LEDS
FAULT 6 LED (DOOR / REMOTE)	22	21	GND (NOT USED)
FAULT 3 LED (SLAB TEMPERATURE)	20	19	GND (NOT USED)
FAULT 4 LED (BASE TEMPERATURE)	18	17	EMERGENCY STOP SWITCH
FAULT 1 LED (DIODE 1 TEMPERATURE)	16	15	FAULT RESET SWITCH
FAULT 2 LED (DIODE 2 TEMPERATURE)	14	13	+5 V FOR EMERGENCY STOP SWITCH
ENABLE 2 SWITCH (DIODE TEC)	12	11	+5 V FOR PWR FAIL CLEAR SWITCH
ENABLE 1 SWITCH (DIODE DRIVER)	10	9	+5 V FOR ENABLE AND FAULT RESET SWITCHES
PWR FAIL CLEAR SWITCH	8	7	GND (NOT USED)
ENABLE 3 SWITCH (SLAB TEC)	6	5	GND FOR ENABLE AND PWR FAIL LEDS
ENABLE 2 LED (DIODE TEC)	4	3	PWR FAIL LED
ENABLE 1 LED (DIODE DRIVER)	2	1	ENABLE 3 LED (SLAB TEC)

J1

TEMP MON 2 (DIODE 2)	30	29	GND FOR TEMP MON 2
TEMP MON 1 (DIODE 1)	28	27	GND FOR TEMP MON 1
TEMP SENSOR 2 (DIODE 2)	26	25	+5 V FOR TEMP SENSOR 2
TEMP SENSOR 1 (DIODE 1)	24	23	+5 V FOR TEMP SENSOR 1
TEMP SENSOR 4 (BASE)	22	21	+5 V FOR TEMP SENSOR 4
TEMP SENSOR 3 (SLAB)	20	19	+5 V FOR TEMP SENSOR 3
TEMP MON 3 (SLAB)	18	17	GND FOR TEMP MON 3
TEMP MON 4 (BASE)	16	15	GND FOR TEMP MON 4
SHIELD FOR FAULT 6	14	13	GND FOR FAULT 6
FAULT 6 (DOOR)	12	11	SHIELD FOR TEMP SENSORS
FAULT 5 (WATER)	10	9	GND FOR FAULT 5
DIODE DRIVER -	8	7	SHIELD FOR FAULT 5
DIODE DRIVER +	6	5	GND (NOT USED)
DIODE TEC SSR+	4	3	DIODE TEC SSR-
SLAB TEC SSR+	2	1	SLAB TEC SSR-

J2

THE UNIVERSITY OF ADELAIDE - DEPARTMENT OF PHYSI
OPTICS GROUP - INTERLOCK UNIT
PIN ASSIGNMENTS FOR HEADERS J1 AND J2 9/9
30-Nov-2005 C:\USERS\...\J1&J2.SCH

6.3 LOCKING ELECTRONICS

Front Panel

Locking:
- AUTO. / MAN. (Switch)
- HD ON (Switch)
- INT. (Switch)
- HF ON (Switch)
- TEMP. ON (Switch)
- HF GAIN (Trim pot – 10 turn)
- DIFF GAIN (Trim pot – 10 turn)
- LOOP GAIN (Trim pot – 10 turn)
- TEMP. GAIN (Trim pot – 10 turn)

Auto Locker:
- SCAN (Yellow LED)
- NO RW = 0 (Red LED)
- RW = 0 (Green LED)
- LOOP LOCKED (Green LED)
- RESET (Push button)

Monitors:
- ERROR (BNC)
- HD MON. (BNC)
- HF MON. (BNC)

HD PZT High Voltage Amplifier (SQV 1/1000)
- AMPLITUDE (Knob)
- OFFSET (Knob)
- LC DISPLAY

Locking:

AUTO. / MAN: This switch selects the method of locking. When the switch is in the manual position, locking can be achieved by using the SQV 1/1000 OFFSET knob to adjust the DC level to the HD PZT and following the manual locking procedure. With this switch in the automatic position, the laser can automatically acquire lock and close the appropriate switches. The INT and HF ON switches can be in either position when using the Automatic locking mode.

HD ON: The switch turns on the feedback to the High Dynamic (HD) range PZT. When the switch is in the up position, there is no feedback from the locking circuit to the HD PZT high voltage amplifier. Turning this switch to the down (or on) position will allow feedback to the HD PZT. This switch must remain in the down position for locking in both manual and automatic modes.

6.3 LOCKING ELECTRONICS

INT: When this switch is in the down (or on) position, the integrator is introduced into the HD PZT feedback circuit.

HF ON: When this switch is in the down (or on) position, the High Frequency (HF) PZT is engaged.

TEMP. ON: This switch provides slow feedback to the resonator temperature, using the RESONATOR TEC POWER SUPPLY. The temperature feedback increases the dynamic range of the locking by allowing the circuit to compensate for slow frequency drifts between the master and slave lasers. This switch must be in the down position to use this feature, as the temperature feedback is not controlled by the AUTO LOCKER.

HF GAIN: Trimpot used to adjust the High Frequency (HF) loop gain. Clockwise adjustment increases the HF loop gain. This gain has been pre-set.

DIFF GAIN: Trimpot used to adjust the differential gain of the High Dynamic (HD) range loop. Clockwise adjustment increases the differential gain. This gain has been pre-set.

LOOP GAIN: Trimpot used to adjust the overall gain of the HD loop. Clockwise adjustment increases the HD loop gain. This gain has been pre-set.

TEMP. GAIN: Trimpot used to adjust the gain of the temperature feedback to the RESONATOR TEC POWER SUPPLY. Clockwise adjustment increases the gain. This gain has been pre-set.

Auto Locker:

SCAN: When the yellow LED is illuminated, the auto-locker is scanning the HD PZT by applying a ramp voltage. It will continue to scan until the reverse-wave is suppressed. It will scan with increasing voltage over a region of approximately 200V and then scan back down.

NO RW = 0: If this red LED is illuminated, it indicates that the auto-locker has completed one full scan, and has failed to find a RW=0 event. The auto-locker will however continue to scan, attempting to find a lock. If the NO RW=0 LED remains illuminated, the operator may need to intervene and explore if there is a misalignment or some other problem.

RW = 0: Illumination of this green LED indicates that the auto-locker has found a HD PZT voltage where the reverse-wave is suppressed, and it is no longer scanning. If this is illuminated, then the reverse-wave is suppressed. This can be used to indicate when RW=0 when manual locking also. If it is not illuminated, then the reverse-wave is not suppressed and the slave laser is running bi-directional.

6.3 LOCKING ELECTRONICS

LOOP LOCKED: When the green LED is illuminated, the auto-locker has found RW = 0 and has switched the integrator into the circuit, the HF PZT and has reduced the DC offset at the HD MON port to be close to zero. Once this has been achieved, the LED will be illuminated. This implies that the laser has been successfully locked using the auto-locker.

RESET: Pressing this button will reset the auto-locker to its initial state. Once pressed, the operator is able to switch from manual to automatic mode without the laser losing lock.

Monitors:

ERROR: BNC output allows the user to connect to an oscilloscope and monitor the PDH error signal.

HD MON: BNC output allows the user to connect to an oscilloscope and monitor the signal from the locking card for the HD PZT loop. The buffered signal is identical to the signal to the SQV 1/1000 high voltage amplifier (inbuilt). The DC level should be kept close to zero, to prevent the high voltage amplifier from running out of dynamic range.

HF MON: BNC output allows the user to monitor the signal applied to the High Frequency (HF) PZT. Note: a voltage divider (1:1000) on the output is used.

HD PZT High Voltage Amplifier (SQV 1/1000)

The High Voltage Amplifier is a PiezoMechanik SQV 1/1000 Single Channel Amplifier +1000V Output.

(***Information from Piezomechanik Datasheet: Amplifiers, D/A Converters, Electronic HV-Switches for Piezonactuators***)

Input

Input:	+/- 5V (or +/- 10V, depending on Amplitude Potentiometer Setting. See below)
Input resistance:	10kOhm
Input connector:	BNC

Output

Voltage range:	0V to +1000V
Max. peak current/average current:	approx. 10mA
Gain:	200
Connector:	LEMOSA OS.250
Noise:	approx. 5mVpp with capacitive load (actuator)
Display:	LCD, 3 digits
Dimensions:	WxDxH 165x210x70mm
Weight:	approx.1.7kg

6.3 LOCKING ELECTRONICS

AMPLITUDE: This single turn potentiometer can be used to adapt the input signal to the working range of the amplifier. It makes it possible to use signal levels of 5V as well as 10V (see SQV 1/1000 specifications). The potentiometer determines the overall gain for the HD PZT feedback loop.

OFFSET: The SQV 1/1000 HV amplifier uses an offset potentiometer to manually set the DC output voltage over the full operating range. Thus, the amplifier can be used as an adjustable voltage supply when no external signal is applied. When an external signal is applied, the “Offset” voltage is superimposed automatically.
The potentiometer is used to change the DC voltage to the HD PZT to achieve locking when in the manual locking mode. When operating in the automatic mode, the DC level should initially be set to approximately 400V.

LC DISPLAY: 3-digit display indicates the approximate DC voltage to the HD PZT.

6.3 LOCKING ELECTRONICS

Rear Panel

- Inputs:
  - RW IN (BNC)
  - AUX IN (BNC)
  - DET IN (BNC)
- Outputs:
  - HV OUT (LEMO)
  - TEMP. OUT (BNC)
  - HF OUT (BNC)
  - PIC STATUS (BNC)
- Power/Others:
  - PIC PROGRAMMING JACK
  - DC POWER (D15)
  - LOGIC 5V (D9)
  - 100V (Fixed IEC female cable)

RW IN: This signal is from the REVERSE-WAVE DETECTOR and is used to indicate if the reverse-wave is on or off. The AUTO-LOCKER uses this input to determine if the slave laser is locked to the master. When the reverse-wave is suppressed, it would imply the laser is running only in the forward direction. This input is required for the AUTO-LOCKER to be operated.

AUX IN: Secondary input used for closed loop measurements. It allows the user to measure the transfer function of the circuit. Note: Normally not connected.

DET IN: The “IF” signal from the FORWARD-WAVE DETECTOR/MIXER is applied to this input. This supplies the PDH error signal used to lock the slave laser to the master. Active locking is achieved only when this input is connected.

HV OUT: The HV OUT is connected directly to the LASER HEAD, and drives the HD PZT. The output from the locking circuit drives the high voltage amplifier input (SQV 1/1000), and the output of the amplifier is used to lock the slave to the master laser.

TEMP. OUT: The BNC output is connected to the RESONATOR TEC POWER SUPPLY using coaxial cable, and is used to slowly adjust the resonator set temperature. It is used to assist in long-term injection locking by keeping the DC level on the HD PZT mid-range using low frequency feedback.

HF OUT: The HF OUT is connected to the LASER HEAD via a coaxial cable, and drives the HF PZT. The HF OUT is the output from the PA85 amplifier, and is used to increase the locking range by providing high frequency feedback to the slave resonator.

6.3 LOCKING ELECTRONICS

PIC STATUS: Output from the AUTO-LOCKER to indicate the state of PIC/AUTO-LOCKER. Note: Normally not connected.

PIC PROGRAMMING JACK: Used to re-program the PICAXE chip.

DC POWER: Supply for the LOCKING ELECTRONICS via a cable (with D15 connectors) from the SERVO LOCK POWER unit.

LOGIC 5V: Provides +5V power for the AUTO LOCKER via a cable (with D9 connectors) from the SERVO LOCK POWER unit.

100V: Provides 100V AC with ground connection for the SQV 1/1000 via the cable to the SERVO LOCK POWER unit.

6.3 LOCKING ELECTRONICS

Plug/Socket Pin connections

LOCKING CIRCUIT POWER (D15)

Pin # 1	+12V	(Locking card)
Pin # 2	0V	(Common Locking)
Pin # 3	-12V	(Locking card)
Pin # 4	Com +160V	(Com PA85)
Pin # 5	+160V	(PA85 power)
Pin # 6	n/c	
Pin # 7	Com -160V	(Com PA85)
Pin # 8	-160V	(PA85 power)
Pin # 9	Shield	
Pin #10	n/c	
Pin #11	n/c	
Pin #12	n/c	
Pin #13	n/c	
Pin #14	n/c	
Pin #15	n/c	

LOGIC +5V (D9)

Pin # 1	n/c	
Pin # 2	+5V	(Logic)
Pin # 3	n/c	
Pin # 4	0V	(Common Logic)
Pin # 5	n/c	
Pin # 6	n/c	
Pin # 7	n/c	
Pin # 8	n/c	
Pin # 9	n/c	

6.3 LOCKING ELECTRONICS

Schematics

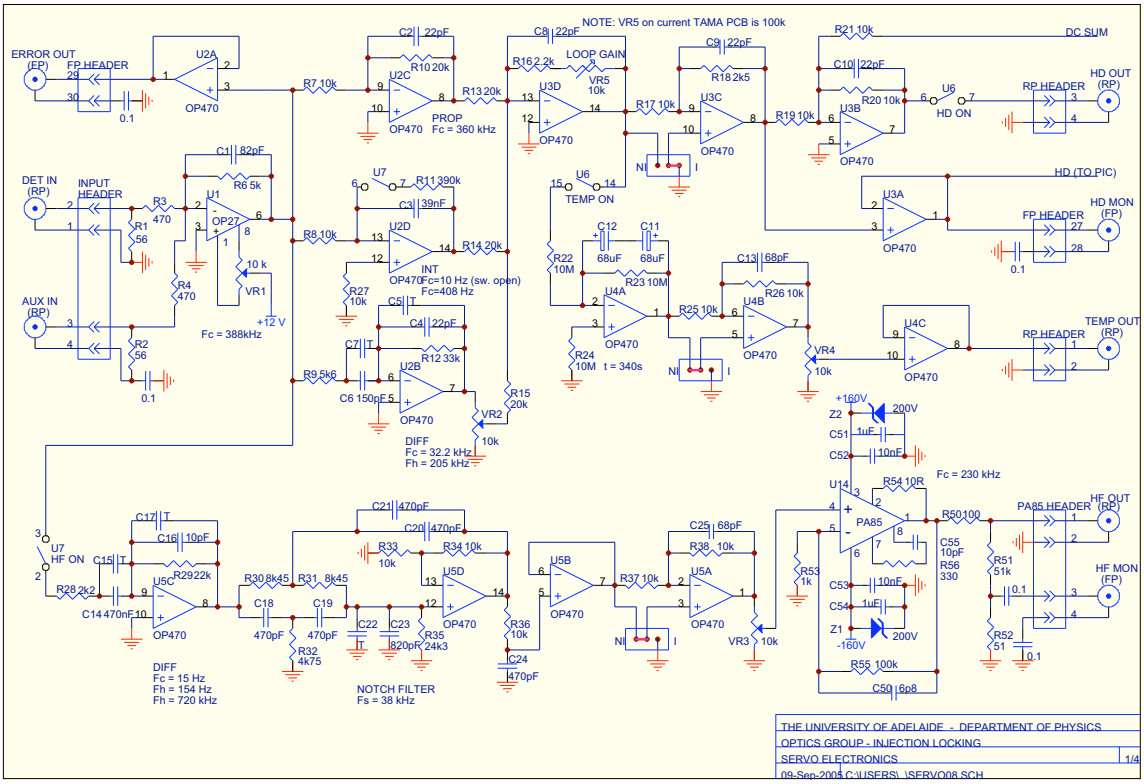

6.3 LOCKING ELECTRONICS

Schematics

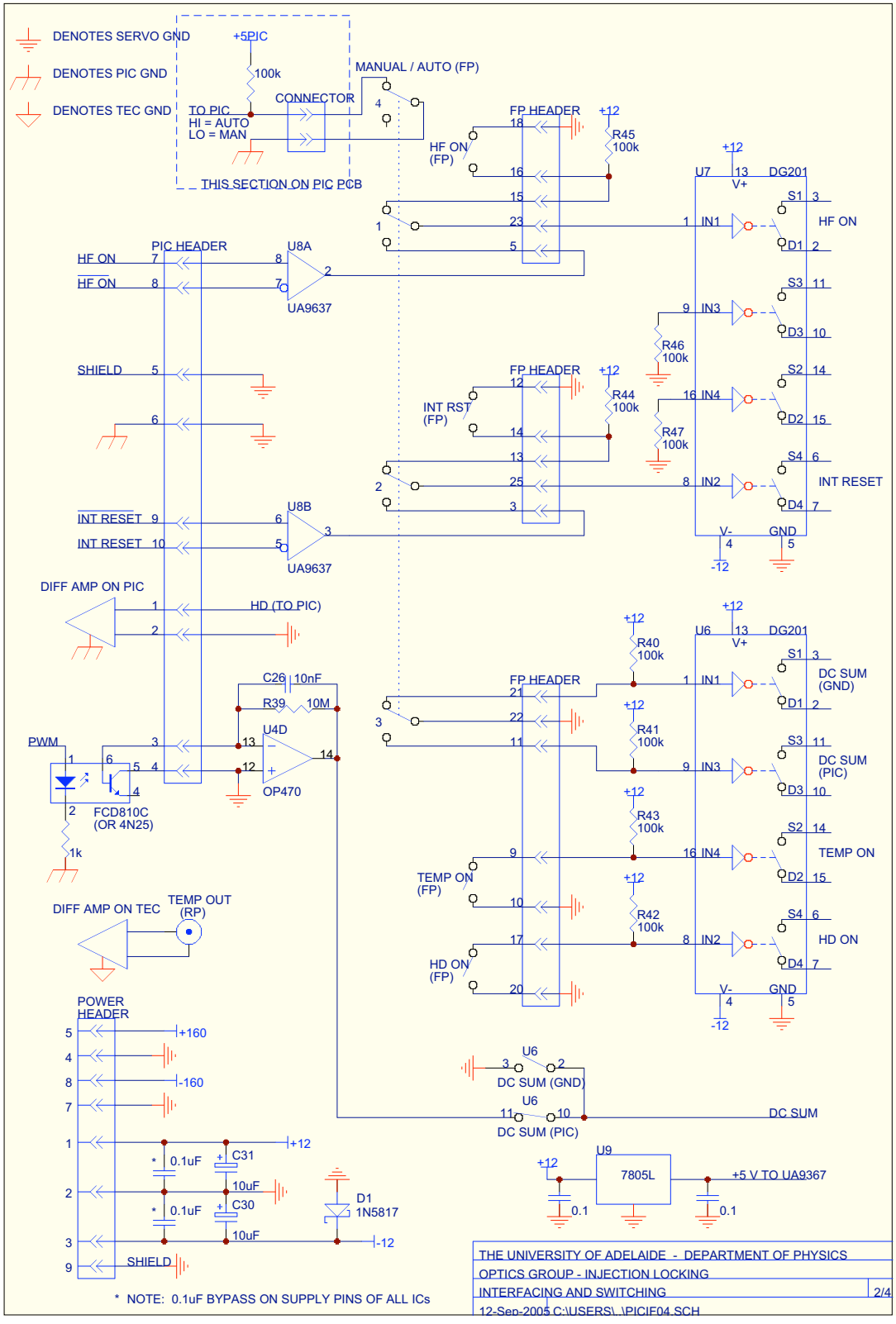

6.3 LOCKING ELECTRONICS

Schematics

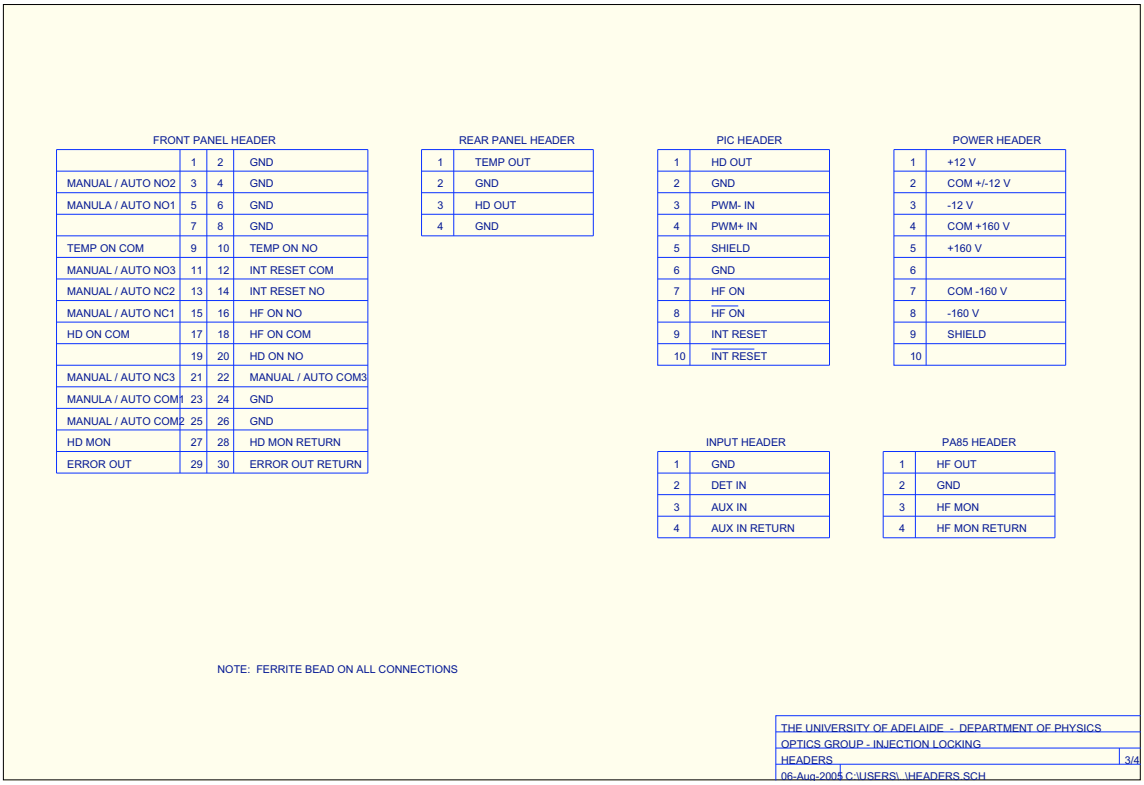

FRONT PANEL HEADER

	1	2	GND
MANUAL / AUTO NO2	3	4	GND
MANULA / AUTO NO1	5	6	GND
	7	8	GND
TEMP ON COM	9	10	TEMP ON NO
MANUAL / AUTO NO3	11	12	INT RESET COM
MANUAL / AUTO NC2	13	14	INT RESET NO
MANUAL / AUTO NC1	15	16	HF ON NO
HD ON COM	17	18	HF ON COM
	19	20	HD ON NO
MANUAL / AUTO NC3	21	22	MANUAL / AUTO COM3
MANULA / AUTO COM1	23	24	GND
MANUAL / AUTO COM2	25	26	GND
HD MON	27	28	HD MON RETURN
ERROR OUT	29	30	ERROR OUT RETURN

REAR PANEL HEADER

1	TEMP OUT
2	GND
3	HD OUT
4	GND

PIC HEADER

1	HD OUT
2	GND
3	PWM- IN
4	PWM+ IN
5	SHIELD
6	GND
7	HF ON
8	HF ON
9	INT RESET
10	INT RESET

POWER HEADER

1	+12 V
2	COM +/-12 V
3	-12 V
4	COM +160 V
5	+160 V
6	
7	COM -160 V
8	-160 V
9	SHIELD
10	

INPUT HEADER

1	GND
2	DET IN
3	AUX IN
4	AUX IN RETURN

PA85 HEADER

1	HF OUT
2	GND
3	HF MON
4	HF MON RETURN

NOTE: FERRITE BEAD ON ALL CONNECTIONS

THE UNIVERSITY OF ADELAIDE - DEPARTMENT OF PHYSICS
OPTICS GROUP - INJECTION LOCKING
HEADERS 3/4
06-Aug-2005 C:\USERS\ \HEADERS.SCH

6.3 LOCKING ELECTRONICS

Schematics

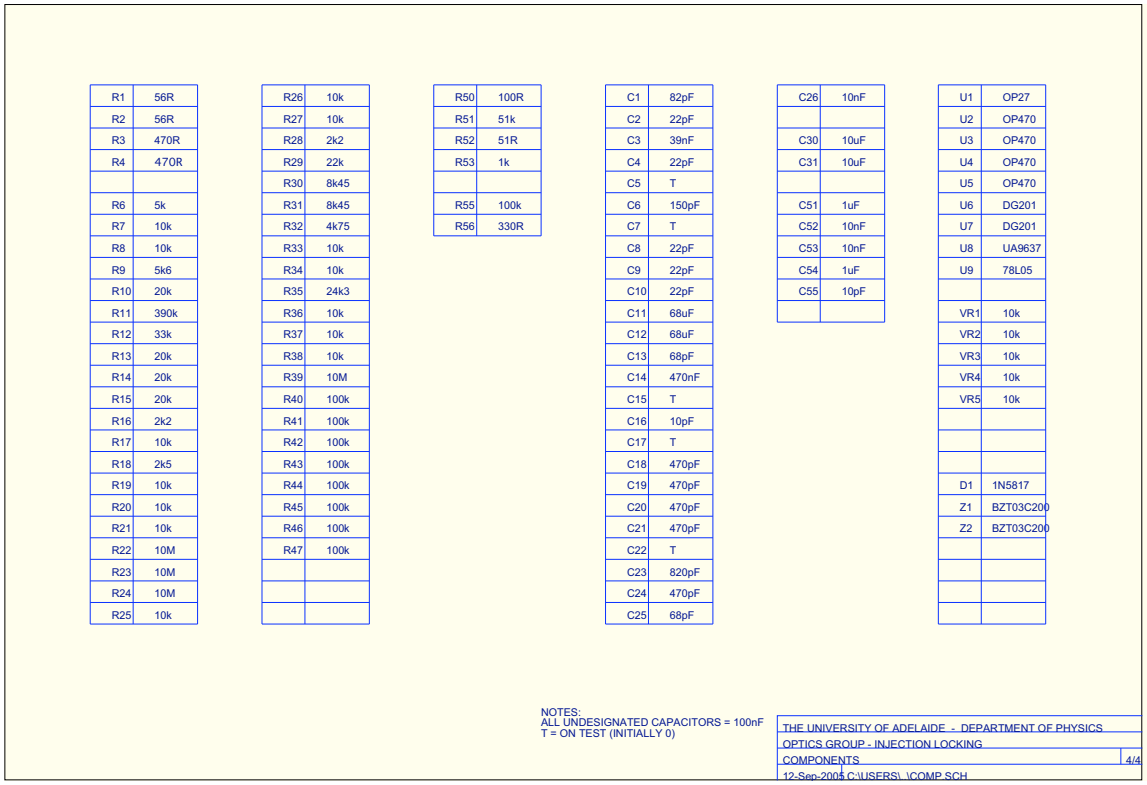

R1	56R
R2	56R
R3	470R
R4	470R
R6	5k
R7	10k
R8	10k
R9	5k6
R10	20k
R11	390k
R12	33k
R13	20k
R14	20k
R15	20k
R16	2k2
R17	10k
R18	2k5
R19	10k
R20	10k
R21	10k
R22	10M
R23	10M
R24	10M
R25	10k

R26	10k
R27	10k
R28	2k2
R29	22k
R30	8k45
R31	8k45
R32	4k75
R33	10k
R34	10k
R35	24k3
R36	10k
R37	10k
R38	10k
R39	10M
R40	100k
R41	100k
R42	100k
R43	100k
R44	100k
R45	100k
R46	100k
R47	100k

R50	100R
R51	51k
R52	51R
R53	1k
R55	100k
R56	330R

C1	82pF
C2	22pF
C3	39nF
C4	22pF
C5	T
C6	150pF
C7	T
C8	22pF
C9	22pF
C10	22pF
C11	68uF
C12	68uF
C13	68pF
C14	470nF
C15	T
C16	10pF
C17	T
C18	470pF
C19	470pF
C20	470pF
C21	470pF
C22	T
C23	820pF
C24	470pF
C25	68pF

C26	10nF
C30	10uF
C31	10uF
C51	1uF
C52	10nF
C53	10nF
C54	1uF
C55	10pF

U1	OP27
U2	OP470
U3	OP470
U4	OP470
U5	OP470
U6	DG201
U7	DG201
U8	UA9637
U9	78L05
VR1	10k
VR2	10k
VR3	10k
VR4	10k
VR5	10k
D1	1N5817
Z1	BZT03C200
Z2	BZT03C200

NOTES:
ALL UNDESIGNATED CAPACITORS = 100nF
T = ON TEST (INITIALLY 0)

THE UNIVERSITY OF ADELAIDE - DEPARTMENT OF PHYSICS
OPTICS GROUP - INJECTION LOCKING
COMPONENTS 4/4
12-Sep-2005 C:\USERS\ \COMP.SCH

6.3 LOCKING ELECTRONICS

Schematic (Auto Locker)

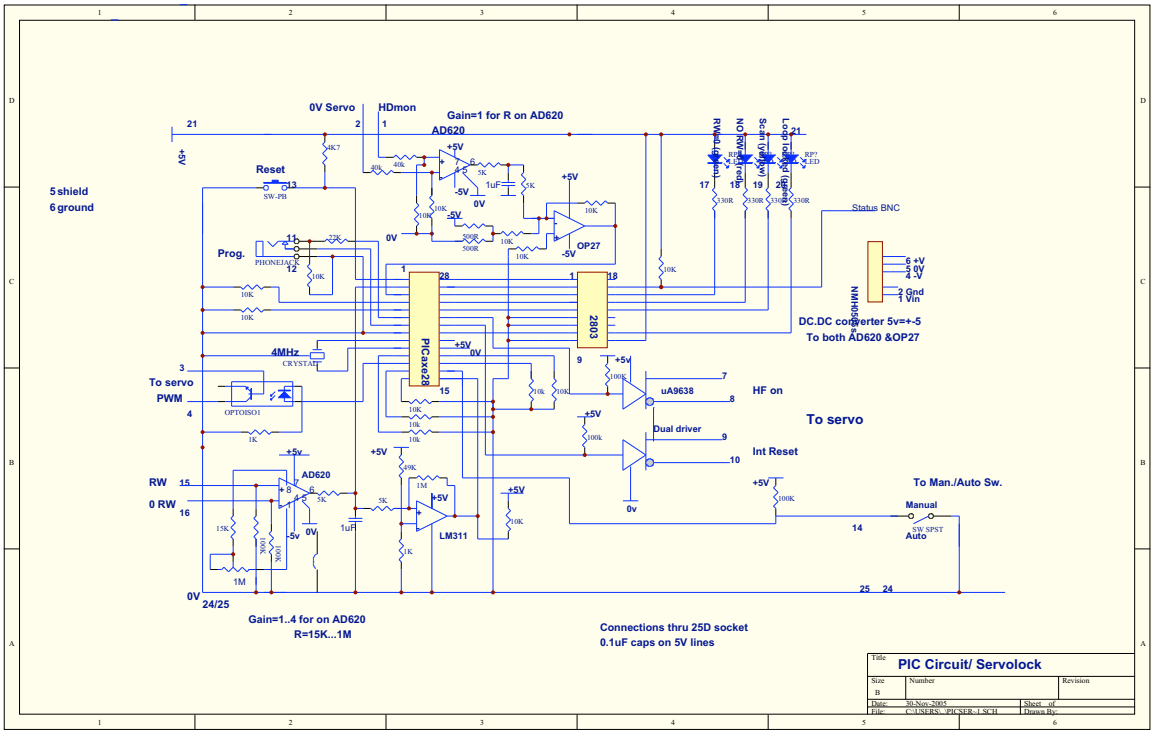

6.3 LOCKING ELECTRONICS

Auto Locking PIC Program

The PICAXE-28 Programming Editor was used to write the following program to the chip:

(10W Auto Locker . bas)

```
        symbol LOOP_LOCKED_LED = 0          ; loop-locked LED at output 0
        symbol INT_SW = 1                   ; integrator switch at output 1
        symbol NO_HF_SW = 2                 ; HF loop switch at output 2
        symbol SCANNING_LED = 3             ; scanning LED at output 3
        symbol NO_RW_ZERO_LED = 4           ; RW=0 did not occur LED at output 4
        symbol RW_ZERO_LED = 5              ; RW=0 LED at output 5
        symbol STATUS = 6                   ; STATUS (for TAMA) at output 6

manual:
        switchoff LOOP_LOCKED_LED           ; loop-locked LED off
        switchoff INT_SW                    ; reset integrator
        switchon NO_HF_SW                   ; open HF loop
        switchoff SCANNING_LED              ; not scanning
        switchoff NO_RW_ZERO_LED            ; switch off RW=0 did not occur LED
        switchoff STATUS                    ; set STATUS no lock

loop1:                                      ; wait for AUTO switch (FIRST TIME)
        if pin4 = 0 then switchon_rw_eq_0   ; if RW=0 then switch on RW=0 LED
        switchoff RW_ZERO_LED
        if pin5 = 1 then scan               ; AUTO switch closed but RW=/0
        goto loop1

switchon_rw_eq_0:
        switchon RW_ZERO_LED                ; RW=0
        if pin5 = 1 then close_loop         ; RW=0 and AUTO switch closed
        goto loop1

scan:
        switchoff STATUS                    ; set STATUS no lock
        switchoff LOOP_LOCKED_LED           ; loop-locked LED off
        switchoff INT_SW                    ; reset integrator
        switchon NO_HF_SW                   ; open HF loop
        switchoff RW_ZERO_LED               ; switch off RW=0 LED
        switchon SCANNING_LED
scan_loop:
        let b3 = 1
        debug b3
        for w0 = 200 to 800 step 10
                debug w0
                pwmout 1,199,w0             ; pwm period = (199+1) us, on-time = (w0/4) us
                pause 100                   ; wait 100 ms
                if pin4 = 0 then zero_hdmon
        next w0
        for w0 = 800 to 0 step -10
                debug w0
                pwmout 1,199,w0
                pause 100
                if pin4 = 0 then zero_hdmon
        next w0
        for w0 = 0 to 200 step 10
                debug w0
                pwmout 1,199,w0
                pause 100
                if pin4 = 0 then zero_hdmon
        next w0
        switchon NO_RW_ZERO_LED             ; no RW=0 interrupt!
        pause 3000                          ; wait 3s
        switchoff NO_RW_ZERO_LED
        goto scan_loop

zero_hdmon:
        let b4 = 1
        debug b4
        switchon RW_ZERO_LED
        readadc 1, b1                       ; read HD MON
```

6.3 LOCKING ELECTRONICS

```
        debug b1
        if b1 < 120 then hdmon_too_low          ; HD MON too low (less than -150 mV)
        if b1 > 140 then hdmon_too_high         ; HD MON too high greater than 150 mV)
        goto close_loop                         ; HD MON OK

hdmon_too_low:                                  ; try increasing HD MON by increasing w0
        let b5 = 1
        debug b5
        if pin4 = 1 then scan                   ; check RW=0 still
        let w0 = w0 + 1                         ; now use finer steps
        debug w0
        pwmout 1,199,w0
        pause 100                               ; wait 100 ms
        readadc 1, b2                           ; read HD MON
        debug b2
        if b2 < b1 then decrease_w0_1           ; HD MON decreased so try decreasing w0
        if b2 >= 120 then close_loop            ; HD MON close to 0
        if w0 = 800 then close_loop     ; can't increase w0 further so close loop with HD MON /= 0
        goto hdmon_too_low                      ; it worked so try a bit more

hdmon_too_high:                                 ; try decreasing HD MON by increasing w0
        let b6 = 1
        debug b6
        if pin4 = 1 then scan                   ; check RW=0 still
        let w0 = w0 + 1                         ; now use finer steps
        debug w0
        pwmout 1,199,w0
        pause 100
        readadc 1, b2                           ; read HD MON
        debug b2
        if b2 > b1 then decrease_w0_2           ; HD MON increased so try decreasing w0
        if b2 <=140 then close_loop             ; HD MON close to 0
        if w0 = 800 then close_loop     ; can't increase w0 further so close loop with HD MON /= 0
        goto hdmon_too_high                     ; it worked so try a bit more

decrease_w0_1:                                  ; increasing w0 failed so try decreasing w0
        let b7 = 1
        debug b7
        if pin4 = 1 then scan                   ; check RW=0 still
        let w0 = w0 - 1
        debug w0
        pwmout 1,199,w0
        pause 100
        readadc 1, b2                           ; read HD MON
        if b2 >=120 then close_loop             ; HD MON close to 0
        if w0 = 0 then close_loop       ; can't decrease w0 further so close loop with HD MON /=0
        goto decrease_w0_1                      ; it worked so try a bit more

decrease_w0_2:
        let b8 = 1
        debug b8
        if pin4 = 1 then scan                   ; check RW=0 still
        let w0 = w0 - 1
        debug w0
        pwmout 1,199,w0
        pause 100
        readadc 1,b2                            ; read HD MON
        if b2 <=135 then close_loop             ; HD MON close to 0
        if w0 = 0 then close_loop       ; can't decrease w0 further so close loop with HD MON /=0
        goto decrease_w0_2                      ; it worked so try a bit more
close_loop:
        if pin4 = 1 then scan
        switchoff SCANNING_LED                  ; scanning stopped
        switchon INT_SW                         ; switch in integrator
        switchoff NO_HF_SW                      ; close HF loop
        switchon LOOP_LOCKED_LED                ; loop locked
        switchon STATUS                         ; set STATUS locked
loop2:
        if pin4 = 1 then scan                   ; wait forever for RW/=0
        if pin5 = 0 then manual                 ; wait forever for MANUAL switch
        goto loop2
        end
```

6.4 RESONATOR TEC POWER SUPPLY

Front panel

- MAINS SWITCH
- TEMP. OFFSET
- SET TEMP.
- TOP ERROR
- BOTTOM ERROR
- +/- 15V

MAINS SWITCH: This switch provides power the unit, provided the INTERLOCK CONTROLLER has supplied a +5V signal to the internal relay. If the INTERLOCK CONTROLLER detects a fault that requires the RESONATOR TEC POWER SUPPLY to be turned off, the unit will not function until such time that the detected fault has been corrected.

TEMP. OFFSET: This 10-turn potentiometer allows the user to adjust the temperature offset between the top and bottom of the slab. This can be used to correct astigmatic thermal lensing. See 10W SLAVE LASER OPERATIONAL SETTINGS for this preset value.

SET TEMP: This 10-turn potentiometer is used to set the temperature of the resonator base. Please note, changing the slab temperature will change the frequency of the slave laser with respect to the NPRO and decrease the locking range. Operating the slab temperature too low will result in excess heating of the resonator base, thus making cooling the laser more difficult.

TOP ERROR: Error signal of the temperature servo for the top of the slab. This is connected to a BNC feed-through and then connected to the PICOLOG A/D converter.

BOTTOM ERROR: Error signal of the temperature servo for the resonator base (bottom of the slab). This is connected to a BNC feed-through and then connected to the PICOLOG A/D converter.

+/- 15V: When these LED's are illuminated, the PID temperature servo is active.

6.4 RESONATOR TEC POWER SUPPLY

Rear panel

- Inputs:
  - 5V INTERLOCK (2-pin plug/socket)
  - THERMISTOR (8-pin plug/socket)
  - TEMP. OFFSET (BNC)
- Outputs:
  - RESONATOR TEC (4-pin plug/socket)
  - 4-PIN MONITOR CABLE (Hardwired 4-pin)
- Power/Others:
  - IEC (MAINS IN) (3-pin)

5V INTERLOCK: This 2-pin input cable is connected to the INTERLOCK CONTROLLER and allows the unit to drive the TEC's. If the INTERLOCK CONTROLLER provides a +5V signal to the relay within this unit, operation is allowed. If the INTERLOCK CONTROLLER detects a problem (for example a temperature fault) that requires this unit to be turned off, the +5V is switched off, thus turning off the drive current to the TEC's. The RESONATOR TEC POWER SUPPLY cannot be operated unless connected to the INTERLOCK CONTROLLER.

THERMISTOR: The THERMISTOR input cable (8-pin connector) is connected to the LASER HEAD, connecting the RESONATOR TEC POWER SUPPLY to three thermistors mounted in the LASER HEAD. A thermistor is mounted in the resonator base, and is used to set the temperature of the slab. The other two thermistors are mounted directly above and below the slab, in equivalent positions. This allows the temperature of the top of the slab to match to the temperature of the bottom of the slab. The top temperature servo is faster than the resonator (bottom of the slab) servo.

TEMP OFFSET: BNC input connected to the LOCKING ELECTRONICS (TEMP. OUT) and is used to feed back to the resonator set temperature. This assists in long-term injection-locking by keeping the DC level on the HD PZT mid-range. If this feedback is not being used (or if this cable is disconnected), then a 50 Ohm terminator should be used to short the temp offset.

RESONATOR TEC: This output (4-pin connector) is connected to the LASER HEAD, and drives the TEC's for the resonator base and the top of slab.

MONITOR CABLE: This cable is connected to the PICOLOG A/D converter unit and provides signals to monitor the top/bottom TEC voltages (4-pin output).

IEC: 100V AC with ground connection.

6.4 RESONATOR TEC POWER SUPPLY

Plug/Socket Pin connections

5V Interlock 2-pin plug/socket

Pin#1	Ground
Pin#2	+5V

Thermistor 8-pin plug/socket (using 100kOhm NTC)

Pin#1	Primary top slab thermistor
Pin#2	Primary top slab thermistor
Pin#3	Following top slab thermistor
Pin#4	Following top slab thermistor
Pin#5	N/C
Pin#6	Resonator Base thermistor
Pin#7	Resonator Base thermistor
Pin#8	N/C

Resonator TEC 4-pin plug/socket

Pin#1	Top slab (+ve)
Pin#2	Top slab (-ve)
Pin#3	Resonator Base (-ve)
Pin#4	Resonator Base (+ve)

4-pin Monitor Cable/plug (Hardwired to unit)

Pin#1	see plug
Pin#2	see plug
Pin#3	see plug
Pin#4	see plug

Nominal fuse for Resonator TEC Power Supply: 1.5A, 250V, 3AG

6.4 RESONATOR TEC POWER SUPPLY

Schematic (Bottom)

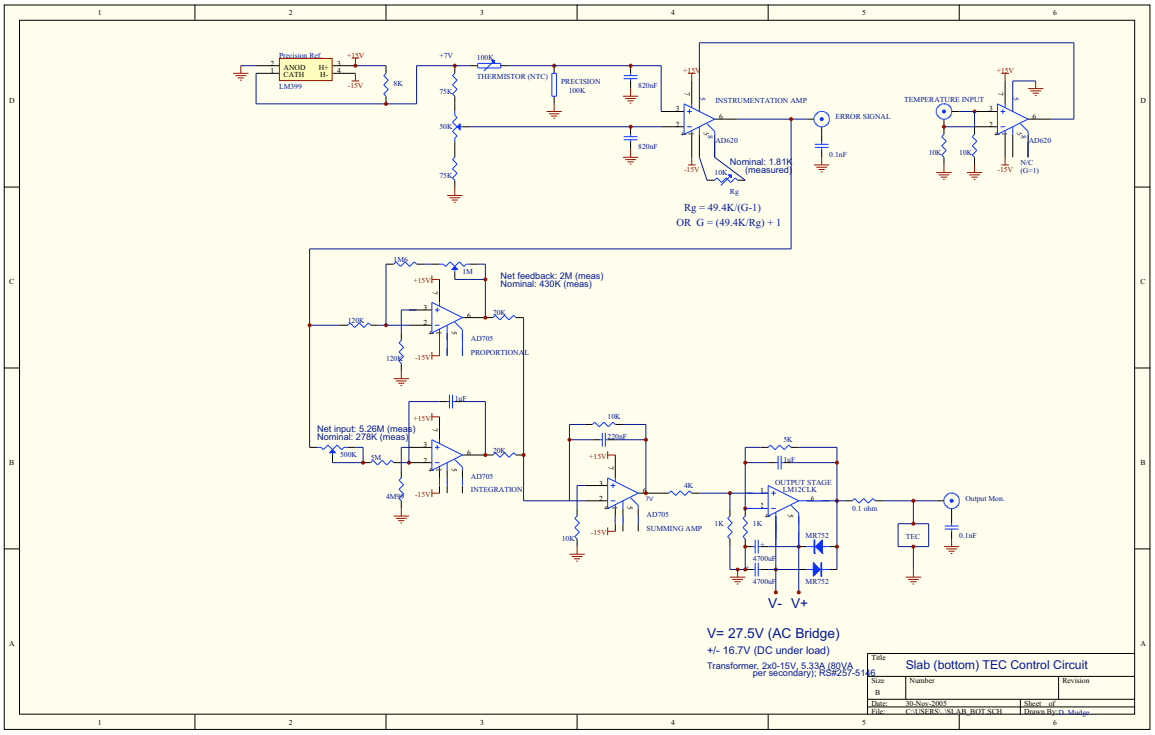

6.4 RESONATOR TEC POWER SUPPLY

Schematic (Top)

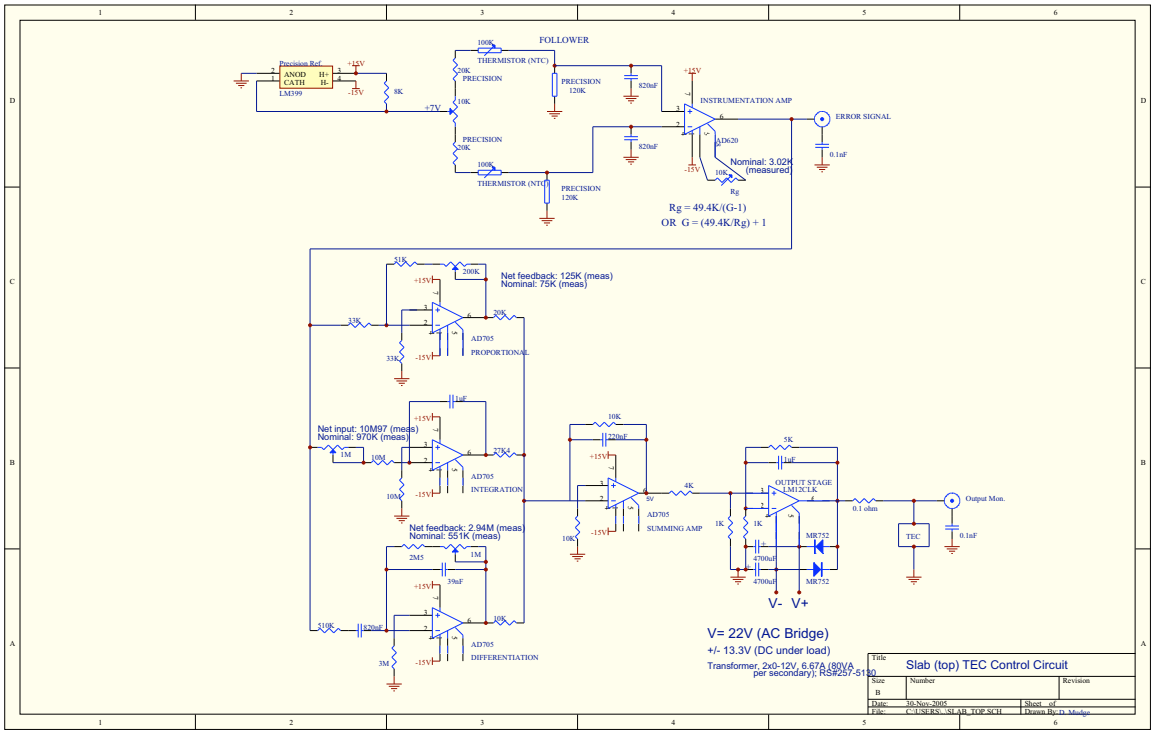

6.5 DIODE TEC POWER SUPPLY

Front Panel

- MAINS SWITCH
- SET TEMP.
- ERROR
- +/- 15V

MAINS SWITCH: This switch provides power to the unit, provided the INTERLOCK CONTROLLER has supplied a +5V signal to the internal relay. If the INTERLOCK CONTROLLER detects a fault that requires the DIODE TEC POWER SUPPLY to be turned off, the unit will not function until such time that the detected fault has been corrected.

SET TEMP: This 10-turn potentiometer is used to set the temperature of the copper block on which the Diode Laser is mounted.

ERROR: Error signal of the temperature servo for the Diode Laser copper block.

+/- 15V: When these LED's are illuminated, it indicates the temperature servo is active.

6.5 DIODE TEC POWER SUPPLY

Rear Panel

- Inputs:
  - 5V INTERLOCK (2-pin plug/socket)
  - THERMISTOR (4-pin plug/socket)
- Outputs:
  - DIODE TEC (3-pin plug/socket)
  - MONITOR CABLE (Hardwired 3-pin)
- Power/Others:
  - IEC OUT TO TRANSFORMER
  - FEMALE IEC FROM TRANSFORMER (x2)
  - IEC (MAINS IN) (3-pin)

5V INTERLOCK: This 2-pin input cable is connected to the INTERLOCK CONTROLLER and allows the unit to be operated. The INTERLOCK CONTROLLER provides +5V to the relay within this unit, allowing operation. If the INTERLOCK CONTROLLER detects a problem, the +5V is switched off, turning off the DIODE TEC POWER SUPPLY. The DIODE TEC POWER SUPPLY cannot be operated unless connected to the INTERLOCK CONTROLLER.

THERMISTOR: The THERMISTOR input cable (4-pin connector) connects the DIODE TEC POWER SUPPLY to the thermistor in the copper block on which the Diode Laser package is mounted in the LASER HEAD. This allows the temperature and output wavelength of the Diode Laser to be controlled.

DIODE TEC: This output (3-pin connector) is connected to the LASER HEAD, and powers two TEC's to temperature stabilise and cool the Diode Laser copper block. It provides the feedback for the temperature control of the copper block. Each TEC is independently supplied by one of the dual output driver stages of the DIODE TEC POWER SUPPLY.

MONITOR CABLE: This cable is connected to the PICOLOG A/D converter unit and provides signals to monitor the Diode Laser TEC voltages (3-pin output).

IEC OUT TO TRANSFORMER: This cable provides mains power for the TRANSFORMER box that is located in the bottom of the LASER RACK.

FEMALE IEC FROM TRANSFORMER (2 Connectors): These cables provide the lower voltage AC power from the TRANSFORMER box for the two DIODE TEC POWER SUPPLY output stages.

IEC: 100V AC with ground connection.

6.5 DIODE TEC POWER SUPPLY

Plug/Socket Pin connections

5V interlock 2-pin plug/socket

Pin#1	Ground
Pin#2	+5V

Thermistor 4-pin plug/socket (using 100 kOhm NTC)

Pin#1	Thermistor (common)
Pin#2	n/c
Pin#3	Thermistor (+ve)
Pin#4	n/c

Diode TEC 3-pin plug/socket

Pin#1	Supply for TEC #1
Pin#2	Supply for TEC #2
Pin#3	Ground

3-pin Monitor Cable/plug (Hardwired to unit)

Pin#1	see connector
Pin#2	see connector
Pin#3	see connector

Nominal fuse for Diode TEC Power Supply: 5A, 250V, 3AG (Delay)

6.5 DIODE TEC POWER SUPPLY

Schematic

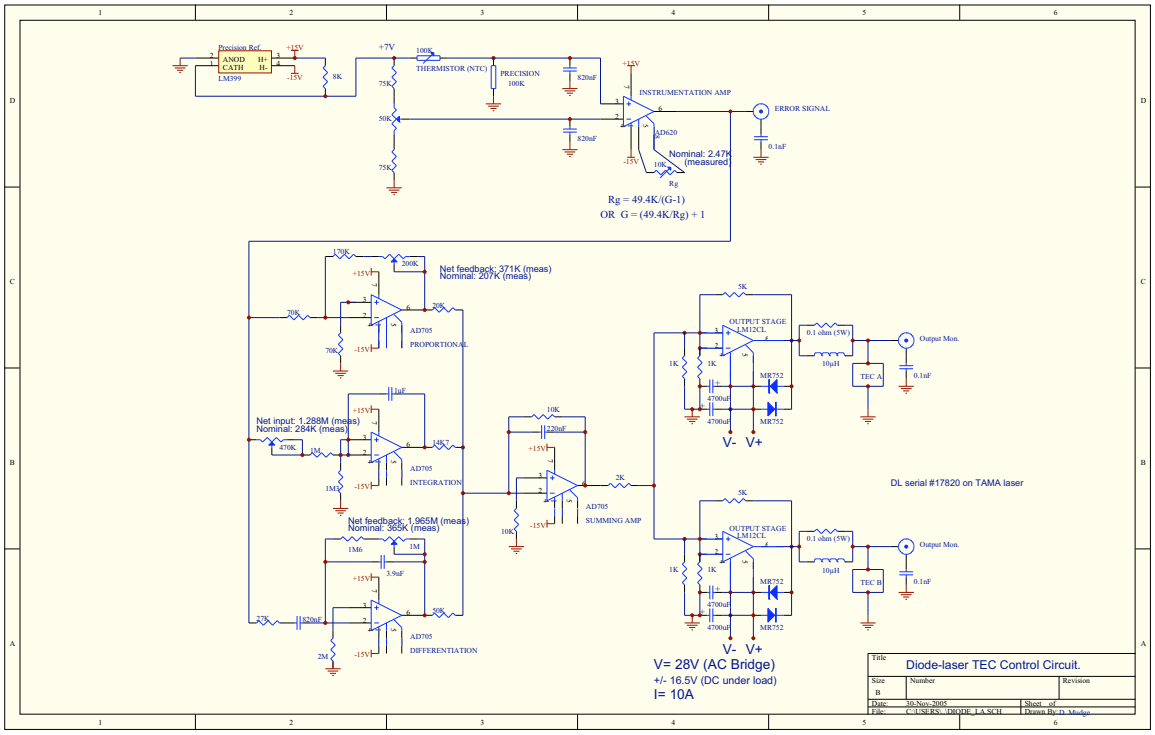

6.6 RF / PICOLOG

Front Panel

- ON/OFF SWITCH (Switch)
- LED (Red LED)
- PICOLOG (25-pin connector)

ON/OFF SWITCH: This switch provides power to the level shifter buffer interface electronics, required for operation of the PICOLOG A/D converter unit. This switch must be turned on to monitor signals from the laser.

LED: Illumination of this red LED indicates that the level shifter buffer interface electronics for the PICOLOG A/D converter is powered.

PICOLOG: The 25-pin connector can be used to connect the monitoring computer to the PICOLOG A/D converter by using a parallel port cable (the A/D converter is built into the unit).

Rear Panel

- Inputs:
  - RF POWER (D9)
  - DL ERR (BNC)
  - SLT ERR (BNC)
  - SLB ERR (BNC)
  - DL TEMP MON (BNC)
  - RES TEMP MON (BNC)
  - BASE TEMP MON (BNC)
  - POWER METER (BNC)
  - DL VTEC (3-pin plug/socket)
  - SLAB VTEC (4-pin plug/socket)
  - N/C (BNC)
- Outputs:
  - LOCAL OSC. (BNC)
  - EOM (Cable with Grommet)
- Power/Others:
  - IEC (MAINS IN) (3-pin)

RF POWER: This supplies +12V from the SERVO LOCK POWER unit for the RF electronics. The switch on the SERVO LOCK POWER unit determines if the RF electronics is powered.

DL ERR: Error signal of the temperature servo for the Diode Laser copper block, this PICOLOG A/D converter input is connected to the DIODE TEC POWER SUPPLY.

SLT ERR: Error signal of the temperature servo for the top of the slab, this input is connected to the RESONATOR TEC POWER SUPPLY.

6.6 RF / PICOLOG

SLB ERR: Error signal of the temperature servo for the resonator base (bottom of the slab), this PICOLOG A/D converter input is connected to the RESONATOR TEC POWER SUPPLY.

DL TEMP MON: Temperature of the copper block on which the Diode Laser is mounted, this PICOLOG A/D converter input is connected to the INTERLOCK CONTROLLER.

RES TEMP MON: Temperature of the resonator base (slab), this PICOLOG A/D converter input is connected to the INTERLOCK CONTROLLER.

BASE TEMP MON: Temperature of the laser base (heatsink), this PICOLOG A/D converter input is connected to the INTERLOCK CONTROLLER.

POWER METER: This input to the PICOLOG A/D converter can be connected to a power meter monitoring port (max. 2.5V full scale output), allowing the output laser power to be monitored and logged.

DL VTEC: Allows the output voltages for the Diode Laser TEC's to be monitored. This PICOLOG A/D converter input is connected to the DIODE TEC POWER SUPPLY.

SLAB VTEC: Allows the output voltages for the top/bottom TEC's to be monitored. This PICOLOG A/D converter input is connected to the RESONATOR TEC POWER SUPPLY.

LOCAL OSC: The LOCAL OSC is a pickoff from the 150MHz RF source from the RF electronics. This output is connected to the FORWARD-WAVE DETECTOR "LO IN" BNC input.

EOM: The EOM is supplied with the 150MHz RF drive signal from this port and adds 150MHz sidebands to the Master Laser (NPRO) light.

IEC: 100V AC with ground connection.

6.6 RF / PICOLOG

PICOLOG

The purpose of this unit is to allow a simple computer interface to monitor (or log) the performance of the laser. It is a useful tool when setting servo electronics, and for detecting the cause of an INTERLOCK CONTROLLER shutdown.

Model: Pico ADC-11 10 bit A/D converter

Internet: http://www.picotech.com/

The Pico A/D converter has eleven channels – each has an input range of 0-2.5V. However, most of the signals produced by the laser are bi-polar and up to +/-15V in magnitude. Therefore, level shifter buffer interface electronics are used to set the full scale range of the appropriate signal to a maximum of 2.5V, and shift the zero level to approximately 1.25V (ie: midrange) in the case of a bi-polar signal. The Pico A/D converter is mounted within the RF/PICOLOG unit.

Important: The switch on the front of the RF/PICOLOG unit needs to be turned on (red LED is illuminated) for the level shifter buffer interface electronics to be powered. This switch must therefore be turned on to monitor signals from the laser. If the PICOLOG is not being monitored by a computer, this switch can be either on or off (it will not effect the laser performance or damage the A/D converter).

Note: The RF electronics in this module is supplied with power from the SERVO LOCK POWER unit and not via the switch on the front panel of the RF/PICOLOG unit (the switch is for the PICOLOG A/D converter level shifter buffer interface electronics only).

The following table contains the A/D channel number, Input Signal, Wire colour (internal wiring), A/D input pin, expected Input Range of the input signal, and the measured Pico signal resulting from the nominated Input Range.

6.6 RF / PICOLOG

A/D Chann. #	Input Voltage Signal	Wire colour (A/D pin)	Input Range	Pico Signal
1	Diode-laser temp. (err)	pink (3)	±15V	0.0678-1.9408V
2	Slab top temp. (error)	brown (4)	±15V	0.0702-1.9408V
3	Slab bottom temp. (err)	green (5)	±15V	0.0653-1.9383V
4	Diode-laser V(TEC)	orange (6)	±10V	0.1624-1.9115V
5	Slab top V(TEC)	grey (7)	± 8V	0.1923-1.928V
6	Slab bottom V(TEC)	yellow (8)	± 8V	0.1996-1.9261V
7	Diode-laser monitor temp.	aqua (9)	0-5V	0-2.4976V
8	Slab monitor temperature	white (10)	0-5V	0-2.4976V
9	Base monitor temperature	purple (11)	0-4.992V	0-2.5000V
10	Laser power meter	red (12)	0-1.25V	0-1.25V
11	Air temp. (thermistor)	blue (13)	2-50°C	2.5-0.45V

Channel 11 monitors the air temperature using a thermistor mounted inside the RF/Picolog unit.

The following table provides conversion formulae (resulting from calibration measurements). Thus, for example, assuming a voltage of 0.8V is measured on A/D channel 1 (using the computer software provided), then the Diode-laser temp. (err) signal = 16.00495*(0.8)-16.07697 = -3.27301V.

A/D Chann. #	PicoLog conversion
1	16.00495*(Pico)-16.07697 V
2	16.0329*(Pico)-16.11737 V
3	16.01782*(Pico)-16.03174 V
4	11.43179*(Pico)-11.85662 V
5	9.21586*(Pico)-9.76673 V
6	9.27128*(Pico)-9.85409 V
7	(2.00432*(Pico)-0.00773)*10 °C
8	(2.00457*(Pico)-0.0071)*10 °C
9	(1.99851*(Pico)-0.00461)*10 °C
10	0-FSD W
11	(3887.1/(ln[R/32650]+14.238))-273 °C (‡)

‡ R=(30E+3*Pico)/(5-Pico)

Nominal fuse for PICOLOG: 100mA, 250V

6.6 RF / PICOLOG

RF

Within the rack is the RF mounting plate. This plate is electrically isolated from the unit case, and is connected to a +12V input floating supply from the SERVO LOCK POWER unit. It provides the 150MHz RF drive signal for the EOM, as well as a pickoff of this signal for the mixer within the FORWARD-WAVE DETECTOR.

The RF system (within the RF/PICOLOG RACK) is electrically floating, to avoid ground loops, and is grounded through the SQV 1/1000 High voltage amplifier.

This plate consists of the following components:

TUNABLE VOLTAGE SOURCE: Used to tune the input voltage to the VOLTAGE CONTROLLED OSCILLATOR, such that it produces the required 150MHz RF output to drive the EOM.

VOLTAGE CONTROLLED OSCILLATOR: (Mini-Circuits ZOS-200)
The TUNABLE VOLTAGE SOURCE output (approximately +8V in this instance) is used as the input to the VOLTAGE CONTROLLED OSCIALLATOR. The VOLTAGE CONTROLLED OSCILLATOR produces a 150MHz with has an output power of +10dBm. And requires +12V supply voltage for operation.

6dB ATTENUATOR: Connects the VOLTAGE CONTROLLED OSCIALLATOR to the RF AMPLIFIER, attenuating the input to the appropriate level.

RF AMPLIFIER: (Mini-Circuits ZHL-2010)
This low noise, medium-high power RF amplifier is used to amplify the output from the VOLTAGE CONTROLLED OSCILLATOR (which is attenuated by the 6dB ATTENUATOR). It uses SMA connectors, and requires +12V supply voltage. The amplifier has a nominal gain of 20dB. This output signal is used to connect to the EOM and “LO IN” input to the FORWARD-WAVE DETECTOR.

DIRECTIONAL COUPLER: (Mini-Circuits ZFDC-20-3)
The DIRECTIONAL COUPLER is used to provide a 150MHz LO pickoff for the FORWARD-WAVE DETECTOR. The -27dB pickoff of the EOM signal is connected to the “LO IN” input of the FORWARD-WAVE DETECTOR, providing it with a +7dBm RF signal for the double balanced mixer (Mini-Circuits SBL-1). The other port of the DIRECTIONAL COUPLER supplies the EOM.

6.7 SERVO LOCK POWER

Front Panel

- MAINS (Switch)
- AUTO LOCK (LED & Switch)
- FW DET. (LED & Switch)
- RW DET. (LED & Switch)
- FAN (LED & Switch)
- E.O.M. (LED & Switch)
- LOCKING (LED & Switch)

MAINS: The MAINS switch supplies power to the various power supplies. Turning on the MAINS switch provides power to the SQV 1/1000 High Voltage Amplifier in the LOCKING ELECTRONICS rack.

AUTO LOCK: When this switch is in the down (or on) position the red LED will illuminate and provide power to the AUTO LOCKER in the LOCKING ELECTRONICS rack. The AUTO LOCKER is only required to be powered when using the LOCKING ELECTRONICS in the Auto mode.

FW DET: When the FW DET switch is in the down (or on) position the red LED illuminates and provides power to the FORWARD-WAVE DETECTOR. This detector is required to be powered when locking the laser in either Automatic or Manual modes.

RW DET: When the RW DET switch is in the down (or on) position the red LED illuminates and provides power to the REVERSE-WAVE DETECTOR. This detector is required to be powered when locking the laser in the Automatic mode (not specifically required for manual mode except as a locking indicator).

FAN: The fan switch powers the laser base cooling fan. This fan is located in the bottom of the LASER RACK and cools the laser base via a flexible duct. This cooling fan MUST be on whenever the laser is operated.

E.O.M.: With the Electro Optic Modulator (EOM) switch in the down (or on) position, the red LED is illuminated and provides power for the 150MHz RF Signal Generator and RF Amplifier. This is located in the unlabelled brown electronics module, situated between the DIODE TEC POWER SUPPLY and the SERVO LOCK POWER unit in the LASER RACK. With the EOM switch in the down (or on) position, a 150MHz drive signal is applied to the EOM (located on the optical table) and adds 150MHz sidebands to the Master Laser (NPRO) light.

LOCKING: With the LOCKING switch in the down (or on) position, the red LED illuminates and provides power to the LOCKING ELECTRONICS. This is necessary to be powered when locking the laser in either the Automatic or Manual modes.

6.7 SERVO LOCK POWER

Rear Panel

- Inputs:
  - 100V AC (IEC plug)
- Outputs:
  - LOCKING CIRCUIT POWER (D15)
  - RF POWER (D9)
  - FANS (D9)
  - LOGIC (D9)
  - FW DETECTOR (DC Jack)
  - RW DETECTOR (DC Jack)
  - HIGH VOLTAGE AMPLIFIER (Female IEC socket)

LOCKING CIRCUIT POWER: A D15 cable supplies the power to the injection-locking card and connects to the LOCKING ELECTRONICS rack. It supplies the +/-12V required for the locking card itself, as well as +/-160V for the HF PZT amplifier (PA85).

RF POWER: A cable (with D9 connectors) supplies +12V for the RF electronics.

FANS: The supply cable (with D9 connectors) is connected to the fan for air-cooling the LASER BASE. The 12V fan is located in the bottom of the LASER RACK.

LOGIC: This cable (with D9 connectors) is connected to the LOCKING ELECTRONICS rack and supples +5V for the auto-locking circuit.

FW DETECTOR: DC Jack that supplies +12V for the FORWARD-WAVE DETECTOR, located on the optical table.

RW DETECTOR: DC Jack that supplies +12V for the REVERSE-WAVE DETECTOR, located on the optical table.

HIGH VOLTAGE AMPLIFIER: Female IEC, used to supply 100V AC power for the HD PZT High Voltage Amplifier. The amplifier (SQV 1/1000) is located in the LOCKING ELECTRONICS rack. When the front panel MAINS SWITCH is turned on, the High Voltage Amplifier is powered.

6.7 SERVO LOCK POWER

Plug/socket Pin connections

LOCKING CIRCUIT POWER (D15)

-	Pin # 1	+12V	(Locking card)
-	Pin # 2	0V	(Common Locking)
-	Pin # 3	-12V	(Locking card)
-	Pin # 4	Com +160V	(Com PA85)
-	Pin # 5	+160V	(PA85 power)
-	Pin # 6	n/c	
-	Pin # 7	Com -160V	(Com PA85)
-	Pin # 8	-160V	(PA85 power)
-	Pin # 9	Shield	
-	Pin #10	n/c	
-	Pin #11	n/c	
-	Pin #12	n/c	
-	Pin #13	n/c	
-	Pin #14	n/c	
-	Pin #15	n/c	

LOGIC +5V (D9)

-	Pin # 1	n/c	
-	Pin # 2	+5V	(Logic)
-	Pin # 3	n/c	
-	Pin # 4	0V	(Logic)
-	Pin # 5	n/c	
-	Pin # 6	n/c	
-	Pin # 7	n/c	
-	Pin # 8	n/c	
-	Pin # 9	n/c	

RF POWER (D9)

-	Pin # 1	+12V
-	Pin # 2	0V
-	Pin # 3	n/c
-	Pin # 4	n/c
-	Pin # 5	n/c
-	Pin # 6	n/c
-	Pin # 7	n/c
-	Pin # 8	n/c
-	Pin # 9	n/c

6.7 SERVO LOCK POWER

FANS (D9)

- Pin # 1 n/c
- Pin # 2 n/c
- Pin # 3 n/c
- Pin # 4 0V
- Pin # 5 +12V
- Pin # 6 n/c
- Pin # 7 n/c
- Pin # 8 n/c
- Pin # 9 n/c

FW DETECTOR (DC Jack)

- Centre +12V
- Outer Shell 0V

RW DETECTOR (DC Jack)

- Centre +12V
- Outer Shell 0V

HIGH VOLTAGE AMPLIFIER (Female IEC socket)

- Switched 100V AC

Nominal fuses for SERVO LOCK POWER: 2 x 2A, 250V
2 x 0.5A, 250V (delay)

6.7 SERVO LOCK POWER

Schematic

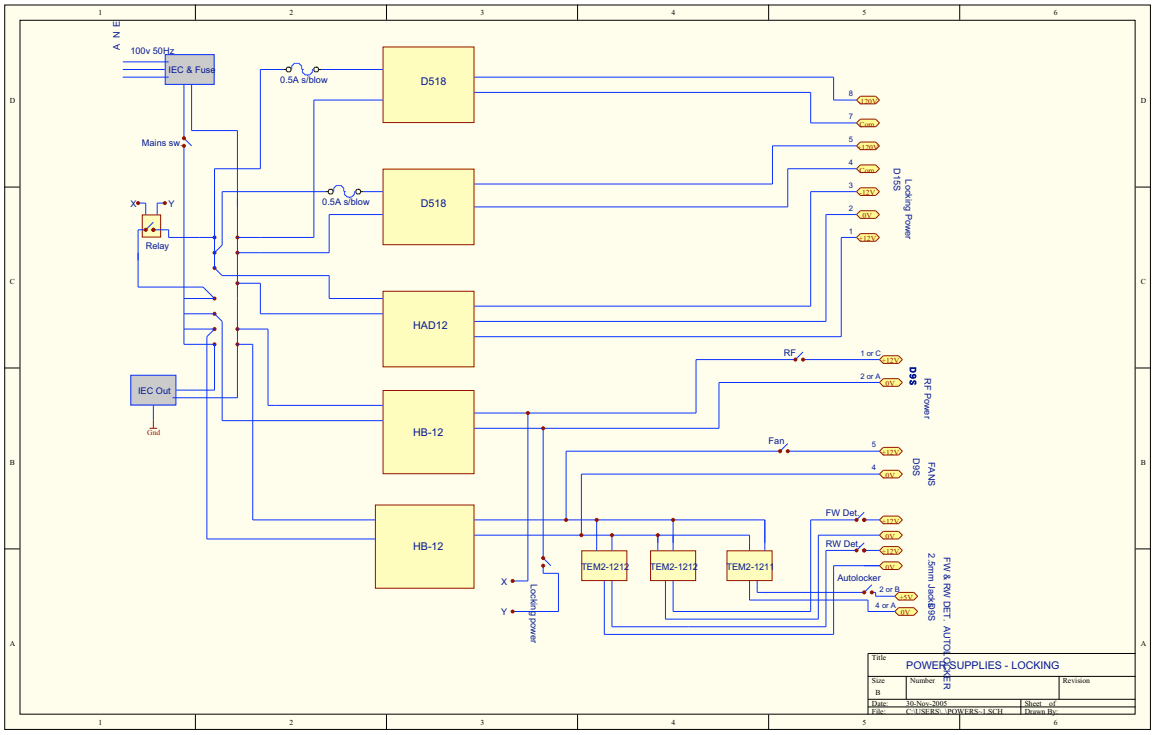

7. DETECTORS

FORWARD-WAVE DETECTOR (FW DET)

The FORWARD-WAVE DETECTOR is powered by the SERVO LOCK POWER unit, which provides +12V when the switch is in the down (or on) position. The forward-wave slave laser output is aligned to the photodiode. The DC level generated by this photodiode can be measured using the “MONITOR” BNC on the FW Detector. Within the detector box is a double balanced mixer (Mini-circuits SBL-1), with the photodiode output as the “RF” input to this mixer. The local oscillator “LO” pickoff (+7dBm level) from the 150MHz RF Source connects to the detector box via the “LO IN” BNC input, while the “IF OUT” output of the mixer is connected to the DET IN on the LOCKING ELECTRONICS rack.

The “IF OUT” provides the Pound-Drever-Hall (PDH) locking signal used to lock the slave laser to the master laser.

When aligning the FORWARD-WAVE DETECTOR, the following unlocked “MONITOR” BNC DC level should be used:

MONITOR DC level = **200 - 300 mV**

(This level should be measured with the master laser blocked, hence the slave laser is running in both the forward and reverse directions)

This detector box is electrically isolated from the optical table. A delrin spacer is used between the diecast box and the pedestal post to provide isolation.

REVERSE-WAVE DETECTOR (RW DET)

The REVERSE-WAVE DETECTOR is powered by the SERVO LOCK POWER unit, which provides +12V when the switch is in the down (or on) position. The reverse-wave slave laser output is aligned to the photodiode. The DC level is measured using the BNC on the detector box.

When aligning this reverse-wave detector, the following “REVERSE OUT” BNC DC level should be used:

REVERSE OUT DC level = **300 – 500mV**

(This level should be measured with the master laser blocked, hence the slave laser is running in both the forward and reverse directions)

This detector box is electrically isolated from the optical table. A delrin spacer is used between the diecast box and the pedestal post to provide isolation.

7. DETECTORS

Schematics

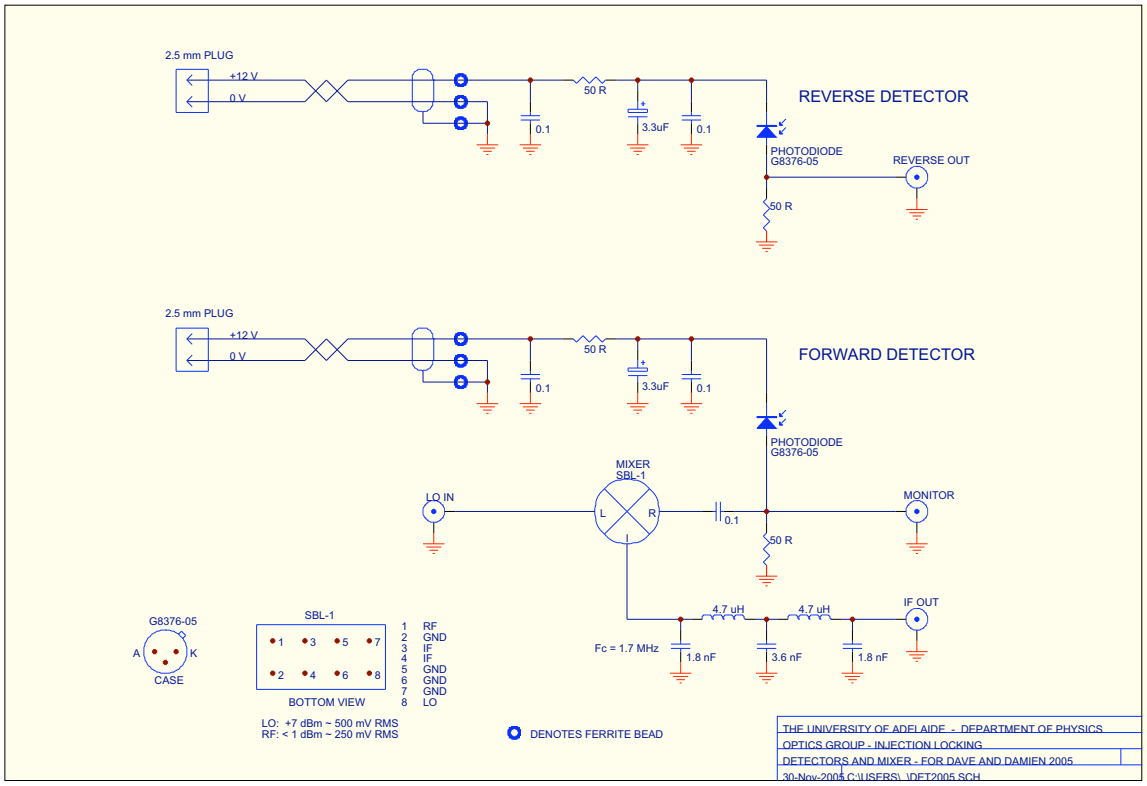

8. MODE MATCHING

Details of the master to slave mode-matching

The first waist in the system after the NPRO is produced by the 150mm focal length lens (component # 4 in the optical setup). The waist size is approximately 590microns ($2w_0$) and is located between the EOM (component #7) and the L/2 plate (component #8) and is matched into the slave laser using a 500mm AR-coated lens (component #20). The slave laser has a waist size of approximately 900 microns ($2w_0$), and located approximately 175mm inside the slave laser measured from the forward-wave cylindrical optic (component #27).

Suggested method for alignment of master to slave laser

- Operate the master laser just above threshold (with the slave laser off).
- Align an iris or metal plate (with a small hole in it) to the master laser beam axis at two locations between mirror mount 23 and the isolator (with a distance of approximately 0.5-1.0m between them)
  Note: These must be located between the slave laser and the isolator.
- Turn the master laser off.
- Turn the slave laser on, just above threshold.
- Use mirror mounts 23 and 24 to translate and align the slave laser axis such that it is co-axial to both of the iris's (or metal plates).
- This should coarsely align the master laser to the slave laser, without burning any components inside the 10 W slave laser (eg: PZT insulation, wires, etc) due to master laser misalignment.
- Detect using a CCD (or similar) a fraction of the forward wave at a distance from the slave laser (as far as possible from the slave laser).
- Using either mirror mount 23 or 24, carefully adjust the master and slave laser beams to ensure they overlap.
- For improved results, monitor the overlap of the master and slave beams at two different locations in the forward wave (separated by as much distance as practical). This will allow mirror mounts 23 and 24 to be adjusted such that the master and slave laser spots overlap at both locations.
- The master and slave lasers should now be aligned.
- To test alignment, turn the HD ON switch on the LOCKING ELECTRONICS to the off position (that is, no HD feedback).

- Change the offset on the HD PZT. Short term drift locking should be observed (assuming the temperatures of the master and slave laser gain media are similar).

- If the slave laser spot moves significantly on the CCD between the unlocked and locked state, the alignment needs to be improved.

- Once drift locking is observed with stable beam pointing, feedback can be employed to long-term injection-lock the laser.

9. BEAM QUALITY

The beam quality of the laser was measured once installed at TAMA300, using the Coherent ModeMaster. Below is a sample measurement.

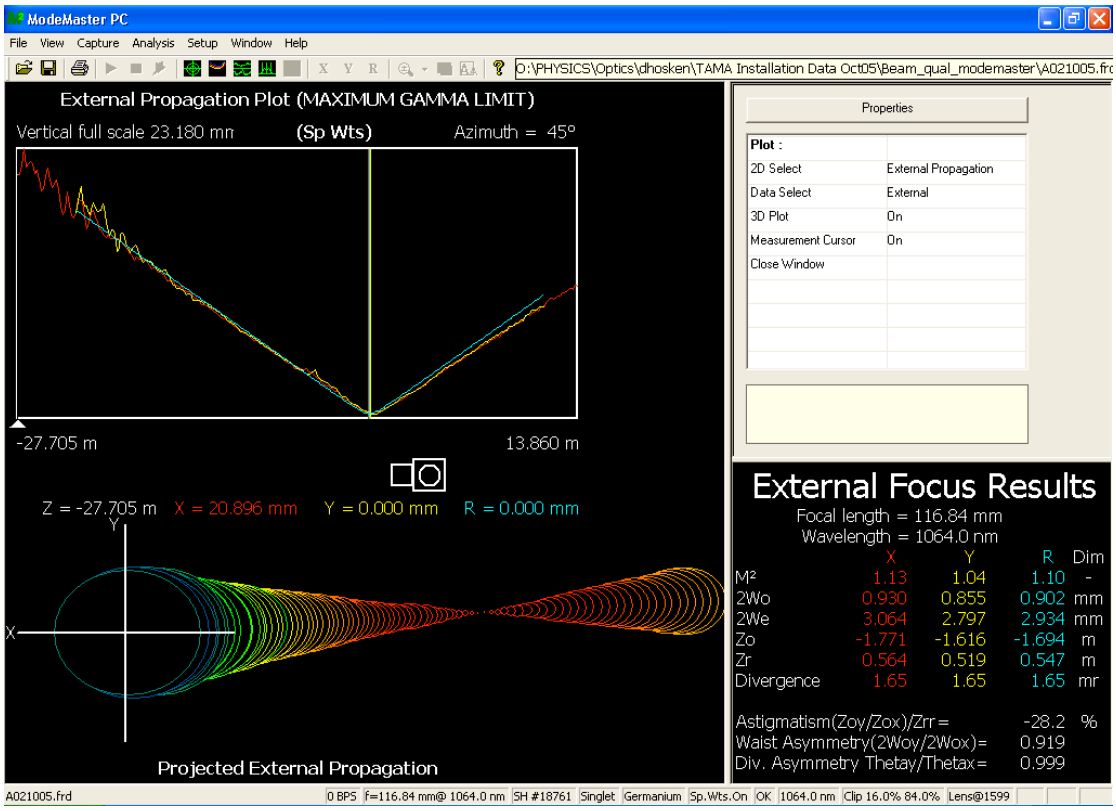

EXTERNAL FOCUS RESULTS

(Averaged of several collimated slave laser output results from the ModeMaster)

	X	Y	R	Dim
M^2	1.13	1.06	1.11	-
2Wo	0.932	0.850	0.901	mm
2We	3.055	2.858	2.956	mm
Zo	-1.767	-1.618	-1.691	m
Zr	0.564	0.504	0.541	m
Divergence	1.65	1.69	1.67	mr

Distance from the ModeMaster to the slave laser waist position (for the above measurements) is approximately: 1607mm.

*** Slave laser waist position is approximately 175mm inside the slave laser as measured from the forward-wave cylindrical optic (Component #27 on OPTICAL LAYOUT) ***

Note: We believe that the measurement of the M^2_x may be artificially higher than the actual value, due to a spurious secondary reflection.

Bibliography

[1] K. S. Thorne, "Gravitational-wave research: Current status and future prospects," *Rev. Mod. Phys.*, vol. 52, pp. 285–297, Apr. 1980.

[2] A. Abramovici, W. E. Althouse, R. W. P. Drever, Y. G. Gursel, S. Kawamura, F. J. Raab, D. Shoemaker, L. Sievers, R. E. Spero, K. S. Thorne, R. E. Vogt, R. Weiss, S. E. Whitcomb, and M. E. Zucker, "LIGO: The Laser Interferometer Gravitational-Wave Observatory," *Science*, vol. 256, pp. 325–333, Apr. 1992.

[3] R. A. Hulse and J. H. Taylor, "Discovery of a pular in a binary system," *Astrophys. J.*, vol. 195, pp. L51–L53, Jan. 1975.

[4] J. H. Taylor and J. M. Weisberg, "Further experimental tests of relativistic gravity using the binary pulsar PSR 1913+16," *Astrophys. J.*, vol. 345, pp. 434–450, Oct. 1989.

[5] S. A. Hughes, S. Marka, P. L. Bender, and C. J. Hogan, "New physics and astronomy with the new gravitational-wave observatories," Tech. Rep. P010029-00-D, LIGO Project, 2001. http://www.ligo.caltech.edu/docs/P/P010029-00.pdf.

[6] L. Ju, D. G. Blair, and C. Zhao, "Detection of gravitational waves," *Rep. Prog. Phys.*, vol. 63, pp. 1317–1427, 2000.

[7] B. C. Barish and R. Weiss, "LIGO and the detection of gravitational waves," *Phys. Today*, vol. 52, pp. 44–50, Oct. 1999.

[8] B. C. Barish, "The Laser Interferometer Gravitational-Wave Observatory LIGO," *Adv. Space Res.*, vol. 25, no. 6, pp. 1165–1169, 2000.

[9] V. Fafone, "Resonant-mass detectors: status and perspectives," *Classical Quant. Grav.*, vol. 21, pp. S377–S383, 2004.

[10] L. Baggio, M. Bignotto, M. Bonaldi, M. Cerdonio, L. Conti, P. Falferi, N. Liguori, A. Marin, R. Mezzena, A. Ortolan, S. Poggi, G. A. Prodi, R. Salemi, G. Soranzo, L. Taffarello, R. Vedovato, A. Vinante, S. Vitale, and J. P. Zendri, "3-Mode Detection for Widening the Bandwidth of Resonant Gravitational Wave Detectors," *Phys. Rev. Lett.*, vol. 94, pp. 241101–1 – 241101–4, Jun. 2005.

[11] M. Cerdonio, "Recent progress and medium term prospectives of "bars" and "spheres"." Talk presented at the 6th Edoardo Amaldi Conference on Gravitational Waves, 20 Jun. 2005.

[12] P. Astone *et al.*, "Search for gravitational wave bursts by the network of resonant detectors," *Classical Quant. Grav.*, vol. 19, pp. 1367–1375, 2002.

[13] B. Abbott *et al.*, "Detector description and performance for the first coincidence observations between LIGO and GEO," *Nucl. Instrum. Meth. A*, vol. 517, pp. 154–179, Jan. 2004.

[14] B. C. Barish, "First Generation Interferometers," *AIP Conf. Proc.*, vol. 575, pp. 3–14, 2001.

[15] G. Heinzel, A. Freise, H. Grote, K. Strain, and K. Danzmann, "Dual recycling for GEO 600," *Classical Quant. Grav.*, vol. 19, pp. 1547–1553, Mar. 2002.

[16] F. J. Raab, "The status of laser interferometer gravitational-wave detectors," *J. Phys.: Conf. Ser.*, vol. 39, pp. 25–31, 2006.

[17] B. Willke *et al.*, "The GEO 600 gravitational wave detector," *Classical Quant. Grav.*, vol. 19, no. 7, pp. 1377–1387, 2002.

[18] J. R. Smith *et al.*, "Commissioning, characterization and operation of the dual-recycled GEO 600," *Class. Quantum. Grav.*, vol. 21, pp. S1737–S1745, Oct. 2004.

[19] R. Passaquieti, "Virgo an Interferometer for Gravitational Wave Detection," *Nucl. Phys. B- Proc. Sup*, vol. 85, pp. 241–247, 2000.

[20] M. Ando *et al.*, "Stable Operation of a 300-m Laser Interferometer with Sufficient Sensitivity to Detect Gravitational-Wave Events within Our Galaxy," *Phys. Rev. Lett.*, vol. 86, pp. 3950–3954, Apr. 2001.

[21] C. Zhao *et al.*, "Gingin High Optical Power Test Facility," *J. Phys.: Conf. Ser.*, vol. 32, pp. 368–373, 2006.

[22] T. Creighton, "Advanced LIGO: Sources and astrophysics," *Classical Quant. Grav.*, vol. 20, pp. S853–S869, Sep. 2003.

[23] A. Weinstein *et al.*, "Advanced LIGO Optical Configuration and Prototyping Effort," *Classical Quant. Grav.*, vol. 19, no. 7, pp. 1575–1584, 2002.

[24] P. Fritschel, "Second generation instruments for the Laser Interferometer Gravitational Wave Observatory (LIGO)." LIGO Publication P020016-00-R, Sep. 2002. http://www.ligo.caltech.edu/docs/P/P020016-00.pdf.

[25] E. Gustafson, D. Shoemaker, K. Strain, and R. Weiss, "LSC White Paper on Detector Research and Development." LIGO Technical Note T990080-00-D, Sep. 1999. http://www.ligo.caltech.edu/docs/T/T990080-00.pdf.

[26] K. Kuroda *et al.*, "Large-Scale Cryogenic Gravitational Wave Telescope," *Int. J. Mod. Phys. D*, vol. 8, no. 5, pp. 557–579, 1999.

[27] K. Danzmann and A. Rüdiger, "LISA technology - concept, status, prospects," *Classical Quant. Grav.*, vol. 20, pp. S1–S9, 2003.

[28] J. Hough, D. Robertson, H. Ward, and P. McNamara, "LISA - The Interferometer," *Adv. Space Res.*, vol. 32, no. 7, pp. 1247–1250, 2003.

[29] N. Seto, S. Kawamura, and T. Nakamura, "Possibility of Direct Measurement of the Acceleration of the Universe Using 0.1 Hz Band Laser Interferometer Gravitational Wave Antenna in Space," *Phys. Rev. Lett.*, vol. 87, pp. 221103–1 –221103–4, Nov. 2001.

[30] P. King, R. Savage, and S. Seel, "(Infrared) Pre-stabilized Laser (PSL) Design Requirements." LIGO Technical Note T970080-09-D, Jun. 1997. http://www.ligo.caltech.edu/docs/T/T970080-09.pdf.

[31] "Target Specifications: LIGO 10-W Laser." LIGO Engineering Documentation E970055-01-D, Jun. 1997. http://www.ligo.caltech.edu/docs/E/E970055-01.pdf.

[32] D. Ottaway, T. Rutherford, R. Savage, P. Veitch, and B. Willke, "LIGO Pre-stabilized Laser Conceptual Design." LIGO Technical Note T000036-07-W, Nov. 2000. http://www.ligo.caltech.edu/docs/T/T000036-07.pdf.

[33] T. J. Kane and R. L. Byer, "Monolithic, unidirectional single-mode Nd:YAG ring laser," *Opt. Lett.*, vol. 10, pp. 65–67, Feb. 1985.

[34] T. Day, E. K. Gustafson, and R. L. Byer, "Sub-Hertz Relative Frequency Stabilization of Two-Diode Laser-Pumped Nd"YAG Lasers Locked to a Fabry-Perot Interferometer," *IEEE J Quantum Elect.*, vol. 28, pp. 1106–1117, Apr. 1992.

[35] I. Freitag, I. Kröpke, A. Tünnerman, and H. Welling, "Electrooptically fast tunable miniature diode-pumped Nd:YAG ring laser," *Opt. Commun.*, pp. 371–376, Sep. 1993.

[36] A. D. Farinas, E. K. Gustafson, and R. L. Byer, "Frequency and intensity noise in an injection-locked, solid-state laser," *J. Opt. Am. B*, vol. 12, pp. 328–334, 1995.

[37] F. Bondu, P. Fritschel, C. N. Man, and A. Brillet, "Ultrahigh-spectral-purity laser for the VIRGO experiment," *Opt. Lett.*, vol. 21, pp. 582–584, Apr. 1996.

[38] F. Siefert, P. Kwee, M. Heurs, B. Willke, and K. Danzmann, "Laser power stabilization for second-generation gravitational wave detectors," *Opt. Lett.*, vol. 31, pp. 2000–2002, Jul. 2006.

[39] A. E. Siegman, *Lasers*. Sausalito, California: University Science Books, 1986.

[40] P. Fritschel, "DC Readout for Advanced LIGO." Technical Plenary Session of the LIGO Scientific Collaboration meeting, Hannover, Germany, Aug. 2003. http://www.ligo.caltech.edu/docs/G/G030460-00/G0304060-00.pdf.

[41] K. Somiya, Y. Chen, S. Kawamura, and N. Mio, "Frequency noise and intensity noise of next-generation gravitational-wave detectors with RF/DC readout schemes," *Phys. Rev. D*, vol. 73, pp. 122005–1 – 122005–17, 2006.

[42] G. Mueller, "Beam jitter coupling in advanced LIGO," *Opt. Express*, vol. 13, pp. 7118–7132, Sep. 2005.

[43] W. Koechner, *Solid-State Laser Engineering*. Berlin: Springer-Verlag, 5th ed., 1999.

[44] A. K. Sridharan, S. Saraf, S. Sinha, and R. L. Byer, "Zigzag slabs for solid-state laser amplifiers: Batch fabrication and parasitic oscillation suppression," *Appl. Optics*, vol. 45, pp. 3340–3351, May 2006.

[45] A. E. Siegman, "Lasers without photons - or should it be lasers with too many photons?," *Appl. Phys. B-Lasers O*, vol. 60, pp. 247–257, 1995.

[46] S. Saraf, K. Urbanek, R. L. Byer, and P. J. King, "Quantum noise measurements in a continuous-wave laser-diode-pumped Nd:YAG saturated amplifier," *Opt. Lett.*, vol. 30, pp. 1195–1197, May 2005.

[47] W. M. Tulloch, T. S. Rutherford, E. H. Huntington, R. Ewart, C. C. Harb, B. Willke, E. K. Gustafson, M. M. Fejer, R. L. Byer, S. Rowan, and J. Hough, "Quantum noise in a continuous-wave laser-diode-pumped Nd:YAG linear optical amplifier," *Opt. Lett.*, vol. 23, pp. 1852–1854, Dec. 1998.

[48] I. Freitag and H. Welling, "Investigation on Amplitude and Frequency Noise of Injection-Locked Diode-Pumped Nd:YAG Lasers," *Appl. Phys. B-Lasers O*, vol. 58, pp. 537–543, 1994.

[49] D. J. Hosken, D. Mudge, C. Hollitt, K. Takeno, P. J. Veitch, M. W. Hamilton, and J. Munch, "Development of Power Scalable Lasers for Gravitational Wave Interferometry," *Prog. Theor. Phys. Supp.*, vol. 151, pp. 216–220, May 2003.

[50] M. I. Nathan, "Semiconductor Lasers," *Appl. Optics*, vol. 5, pp. 1514–1528, Oct. 1966.

[51] T. Y. Fan and R. L. Byer, "Diode Laser-Pumped Solid-State Lasers," *IEEE J. Quantum Electron.*, vol. 24, pp. 895–912, Jun. 1988.

[52] U. Brauch and M. Schubert, "Comparison of lamp and diode pumped cw Nd:YAG slab lasers," *Opt. Commun.*, vol. 117, pp. 116–122, May 1995.

[53] S. A. Payne *et al.*, "Diode Arrays, Crystals, and Thermal Management for Solid-State lasers," *IEEE J. Selected Topics in Quantum Electron.*, vol. 3, pp. 71–81, Feb. 1997.

[54] M. Frede, B. Schulz, R. Wilhelm, P. Kwee, F. Seifert, B. Willke, and D. Kracht, "Fundamental mode, single-frequency laser amplifier for gravitational wave detectors," *Opt. Express*, vol. 15, pp. 459–465, Jan. 2007.

[55] M. Ostermeyer, P. Kappe, R. Menzel, and V. Wulfmeyer, "Diode-pumped Nd:YAG master oscillator power amplifer with high pulse rate energy, excellent beam quality, and frequency-stabilized master oscillator as a basis for next-generation lidar system," *Appl. Optics*, vol. 44, pp. 582–590, Feb. 2005.

[56] S. T. Yang, J. Imai, M. Oka, N. Eguchi, and S. Kubota, "Frequency-stabilized, 10-W continuous-wave, laser-diode end pumped, injection-locked Nd:YAG laser," *Opt. Lett.*, vol. 21, pp. 1676–1678, Oct. 1996.

[57] D. Kracht, M. Frede, R. Wilhelm, and C. Fallnich, "Comparison of crystalline and ceramic composite Nd:YAG for high power diode end-pumping," *Opt. Express*, vol. 13, pp. 6212–6216, Aug. 2005.

[58] M. Ostermeyer and R. Menzel, "34-Watt flash-lamp-pumped single-rod Nd"YAG laser with 1.2*DL beam quality via special resonator design," *Appl. Phys. B-Laser O*, vol. 65, pp. 669–671, 1997.

[59] K. Takeno, T. Ozeki, S. Moriwaki, and N. Mio, "100 W, single-frequency operation of an injection-locked Nd:YAG laser," *Opt. Lett.*, vol. 30, pp. 2110–2112, Aug. 2005.

[60] M. Frede, R. Wilhelm, M. Brendel, C. Fallnich, F. Seifert, B. Willke, and K. Danzmann, "High power fundamental mode Nd:YAG laser with efficient birefringence compensation," *Opt. Express*, vol. 12, pp. 3581–3589, Jul. 2004.

[61] M. Frede, R. Wilhelm, D. Kracht, and C. Fallnich, "Nd:YAG ring laser with 213 W linearly polarized fundamental mode output power," *Opt. Express*, vol. 13, pp. 7516–7519, Sep. 2005.

[62] D. Kracht, R. Wilhelm, M. Frede, K. Dupre, and L. Ackermann, "407 W End-pumped Multi-segmented Nd:YAG Laser," *Opt. Express*, vol. 13, pp. 10140–10144, Dec. 2005.

[63] J. M. Eggleston, T. J. Kane, K. Kuhn, J. Unternahrer, and R. L. Byer, "The Slab Geometry Laser - Part I: Theory," *IEEE J Quantum Elect.*, vol. 20, pp. 289–301, Mar. 1984.

[64] J. Richards and A. McInnes, "Versatile, efficient, diode-pumped miniature slab laser," *Opt. Lett.*, vol. 20, pp. 371–373, Feb. 1995.

[65] R. J. Shine, Jr., A. J. Alfrey, and R. L. Byer, "40-W cw, TEM_{00}-mode, diode-laser-pumped, Nd:YAG miniature-slab laser," *Opt. Lett.*, vol. 20, pp. 459–461, Mar. 1995.

[66] D. J. Ottaway, P. J. Veitch, M. W. Hamilton, C. Hollitt, D. Mudge, and J. Munch, "A Compact Injection-Locked Nd:YAG Laser for Gravitational Wave Detection," *IEEE J Quantum Elect.*, vol. 34, pp. 2006–2009, Oct. 1998.

[67] D. Mudge, P. J. Veitch, J. Munch, D. J. Ottaway, and M. W. Hamilton, "High-Power Diode-Laser-Pumped CW Solid-State Lasers Using Stable-Unstable Resonators," *IEEE J. Selected Topics in Quantum Electron.*, vol. 3, pp. 19–25, Feb. 1997.

[68] A. D. Farinas, E. K. Gustafson, and R. L. Byer, "Design and characterization of a 5.5-W, cw, injection-locked, fiber-coupled, laser-diode-pumped Nd:YAG miniature-slab laser," *Opt. Lett.*, vol. 19, pp. 114–116, Jan. 1994.

[69] T. S. Rutherford, W. M. Tulloch, E. K. Gustafson, and R. L. Byer, "Edge-Pumped Quasi-Three-Level Slab Lasers: Design and Power Scaling," *IEEE J Quantum Elect.*, vol. 36, no. 2, pp. 205–219, 2000.

[70] T. S. Rutherford, W. M. Tulloch, S. Sinha, and R. L. Byer, "Yb:YAG and Nd:YAG edge-pumped slab lasers," *Opt. Lett.*, vol. 26, pp. 986–988, Jul. 2001.

[71] G. D. Goodno, S. Palese, J. Harkenrider, and H. Injeyan, "Yb:YAG power oscillator with high brightness and linear polarization," *Opt. Lett.*, vol. 26, pp. 1672–1674, Nov. 2001.

[72] H. Injeyan and C. S. Hoefer, "End pumped zig-zag slab laser gain medium." United States Patent 6,094,297, 25 Jul. 2000.

[73] T. J. Kane, R. C. Eckardt, and R. L. Byer, "Reduced Thermal Focusing and Birefringence in Zig-Zag Slab Geometry Crystalline Lasers," *IEEE J. Quantum Elect.*, vol. 19, pp. 1351–1354, Sep. 1983.

[74] I. Zawischa, K. Plamann, C. Fallnich, H. Welling, H. Zellmer, and A. Tünnermann, "All-solid-state neodymium-based single-frequency master-oscillator fiber power-amplifier system emitting 5.5 W of radiation at 1064 nm," *Opt. Lett.*, vol. 24, pp. 469–471, Apr. 1999.

[75] S. Höfer, A. Liem, J. Limpert, H. Zellmer, A. Tünnermann, S. Unger, S. Jetschke, H. R. Müller, and I. Freitag, "Single-frequency master-osillator fiber power amplifer system emitting 20 W of power," *Opt. Lett.*, vol. 26, pp. 1326–1328, Sep. 2001.

[76] A. Liem, J. Limpert, H. Zellmer, and A. Tünnermann, "100-W single-frequency master-oscillator fiber power amplifier," *Opt. Lett.*, vol. 28, pp. 1537–1539, Sep. 2003.

[77] Y. Jeong *et al.*, "Single-frequency, single-mode, plane-polarized ytterbium-doped fiber master oscillator power amplifier source with 264 W of output power," *Opt. Lett.*, vol. 30, pp. 459–461, Mar. 2005.

[78] M. Hildebrandt, M. Frede, P. Kwee, B. Willke, and D. Kracht, "Single-frequency master-oscillator photonic crystal fiber amplifier with 148 W output power," *Opt. Express*, vol. 14, pp. 11071–11076, Nov. 2006.

[79] J. P. Koplow, D. A. V. Kliner, and L. Goldberg, "Single-mode operation of a coiled multimode fiber amplifer," *Opt. Lett.*, vol. 25, pp. 442–444, Apr. 2000.

[80] T. Dascalu, N. Pavel, and T. Taira, "90 W continuous-wave diode edge-pumped microchip composite Yb:$Y_3Al_5O_{12}$ laser," *Appl. Phys. Lett.*, vol. 83, pp. 4086–4088, Nov. 2003.

[81] Y. Liao, R. J. D. Miller, and M. R. Armstrong, "Pressure tuning of thermal lensing for high-power scaling," *Opt. Lett.*, vol. 24, pp. 1343–1345, Oct. 1999.

[82] C. Stewen, K. Contag, M. Larionov, A. Giesen, and H. Hügel, "A 1-kW CW Thin Disc Laser," *IEEE J. Sel. Top. Quantum Elect.*, vol. 6, pp. 650–657, Jul. 2000.

[83] R. Abbott and P. King, "(Infrared) Pre-stabilized Laser (PSL) Final Design." LIGO Technical Note T990025-00-D, Mar. 1999. http://www.ligo.caltech.edu/docs/T/T990025-00.pdf.

[84] B. Willke, N. Uehara, E. K. Gustafson, R. L. Byer, P. J. King, S. U. Seel, and R. I. Savage, Jr, "Spatial and temporal filtering of a 10-W Nd:YAG laser with a Fabry-Perot ring-cavity premode cleaner," *Opt. Lett.*, vol. 23, pp. 1704–1706, Nov. 1998.

[85] J. Rollins, D. Ottaway, M. Zucker, and R. Weiss, "Solid-state laser intensity stabilization at the 10^{-8} level," *Opt. Lett.*, vol. 29, pp. 1876–1878, Aug. 2004.

[86] I. Zawischa, M. Brendel, K. Danzmann, C. Fallnich, M. Kirchner, S. Nagano, V. Quetschke, H. Welling, and B. Willke, "The GEO 600 Laser System," *Classical Quant. Grav.*, vol. 19, pp. 1775–1781, 2002.

[87] F. Bondu, A. Brillet, F. Cleva, H. Heitmann, M. Loupias, C. N. Man, H. Trinquet, and the VIRGO Collaboration, "The VIRGO injection system," *Classical Quant. Grav.*, vol. 19, no. 7, pp. 1829–1833, 2002.

[88] F. Acernese *et al.*, "The Virgo interferometric gravitational antenna," *Opt. Laser Eng.*, vol. 45, pp. 478–487, 2007.

[89] S. Nagano *et al.*, "Development of a light source with an injection-locked Nd:YAG laser and a ring-mode cleaner for the TAMA 300 gravitational-wave detector," *Rev. Sci. Instrum.*, vol. 73, pp. 2136–2142, May 2002.

[90] S. Nagano *et al.*, "Development of a multistage laser frequency stabilization for an interferometric gravitational-wave detector," *Rev. Sci. Instrum.*, vol. 74, pp. 4176–4183, Sep. 2003.

[91] K. Takeno, *Development of a 100-W Nd:YAG Laser Using the Injection Locking Technique for Gravitational Wave Detectors.* PhD thesis, University of Tokyo, 2006.

[92] B. Willke, K. Danzmann, C. Fallnich, M. Frede, M. Heurs, P. King, D. Kracht, P. Kwee, R. Savage, F. Seifert, and R. Wilhelm, "Stabilized High Power Laser for Advanced Gravitational Wave Detectors," *J. Phys.: Conf. Ser.*, vol. 32, pp. 270–275, 2006.

[93] K. Takeno, T. Ozeki, S. Moriwaki, and N. Mio, "Development of a 100- W, single-frequency Nd:YAG laser for large-scale cryogenic gravitational wave telescope," *J. Phys.: Conf. Ser.*, vol. 32, pp. 276–281, 2006.

[94] D. Mudge, M. Ostermeyer, D. J. Ottaway, P. J. Veitch, J. Munch, and M. W. Hamilton, "High-power Nd:YAG lasers using stable-unstable resonators," *Class. Quantum Grav.*, vol. 19, pp. 1783–1792, Mar. 2002.

[95] A. McInnes and J. Richards, "Thermal Effects in a Coplanar-Pumped Folded-Zigzag Slab Laser," *IEEE J. Quantum Elect.*, vol. 32, pp. 1243–1252, Jul. 1996.

[96] D. Mudge, D. Hosken, P. Veitch, and J. Munch, "Adelaide High Power Laser Development." LIGO Scientific Collaboration Meeting, Livingston, LA, USA, Mar. 2004. http://www.ligo.caltech.edu/docs/G/G040068-00/G040068-00.pdf.

[97] D. Mudge, M. Ostermeyer, P. J. Veitch, J. Munch, B. Middlemiss, D. J. Ottaway, and M. W. Hamilton, "Power Scalable TEMoo CW Nd:YAG Laser with Thermal Lens Compensation," *IEEE J. Selected Topics in Quantum Electron.*, vol. 6, pp. 643–649, Jul./Aug. 2000.

[98] D. Mudge, *A High Power Scalable Diode-Laser-Pumped CW Nd:YAG Laser Using a Stable-Unstable Resonator.* PhD thesis, The University of Adelaide, 2000.

[99] D. J. Ottaway, P. J. Veitch, C. Hollitt, D. Mudge, M. W. Hamilton, and J. Munch, "Frequency and intensity noise of an injection-locked Nd:YAG ring laser," *Appl. Phys. B-Lasers O*, vol. 71, pp. 163–168, Jun. 2000.

[100] D. Ottaway, *Medium Power Stable Lasers for High Precision Metrology.* PhD thesis, The University of Adelaide, 1998.

[101] D. Shoemaker, R. Schilling, L. Schnupp, W. Winkler, K. Maischberger, and A. Rüdiger, "Noise behavior of the Garching 30-meter prototype gravitational-wave detector," *Phys. Rev. D*, vol. 38, pp. 423–432, Jul. 1988.

[102] D. I. Robertson, E. Morrison, J. Hough, S. Killbourn, B. J. Meers, G. P. Newton, N. A. Robertson, K. A. Strain, and H. Ward, "The Glasgow 10 m prototype laser interferometric gravitational wave detector," *Rev. Sci. Instrum.*, vol. 66, pp. 4447–4452, Sep. 1995.

[103] R. Barillet, A. Brillet, R. Chiche, F. Cleva, L. Latracht, and C. N. Man, "An injection-locked Nd:YAG laser for the interferometric detection of gravitational waves," *Meas. Sci. Technol.*, vol. 7, pp. 162–169, Feb. 1996.

[104] F. L. Pedrotti and L. S. Pedrotti, *Introduction to Optics.* New Jersey, USA: Prentice-Hall, 2nd ed., 1996.

[105] S. H. Wang, C. J. Tay, C. Quan, and H. M. Shang, "Collimating of diverging laser diode beam using graded-index optical fiber," *Opt. Laser Eng.*, vol. 34, pp. 121–127, Sep. 2000.

[106] F. Barone, E. Calloni, A. Grado, R. D. Rosa, L. D. Fiore, L. Milano, and G. Russo, "High accuracy digital temperature control for a laser diode," *Rev. Sci. Instrum.*, vol. 66, pp. 4051–4054, Aug. 1995.

[107] C. C. Bradley, J. Chen, and R. G. Hulet, "Instrumentation for the stable operation of laser diodes," *Rev. Sci. Instrum.*, vol. 61, pp. 2097–2101, Aug. 1990.

[108] K. Ogata, *Modern Control Engineering*. New Jersey, USA: Prentice-Hall, 4th ed., 2002.

[109] MELCOR, Trenton, NJ, USA, *Thermoelectric Handbook*.

[110] G. K. McMillan, *Tuning and Control Loop Performance : A Practitioner's Guide*. North Carolina, USA: The Instrument Society of America, 2nd ed., 1990.

[111] R. Sundar, K. Ranganathan, and A. K. Nath, "Performance studies of diode-side-pumped CW Nd:YAG laser in copper coated optical pump cavity," *Opt. Laser Technol.*, vol. 39, pp. 1426–1431, Oct. 2007.

[112] N. Hodgson and H. Weber, *Optical Resonators: Fundamentals, Advanced Concepts and Applications*. London: Springer-Verlag, 1997.

[113] S. A. Amarande and M. J. Damzen, "Measurement of the thermal lens of grazing-incidence diode-pumped Nd:YVO4 laser amplifier," *Opt. Commun.*, vol. 265, pp. 306–313, 2006.

[114] J. E. Murray, "Pulsed Gain and Thermal Lensing of Nd:$LiYF_4$," *IEEE J. Quantum Elect.*, vol. QE-19, pp. 488–491, Apr 1983.

[115] V. Michau, F. de Rougemont, and R. Frey, "Mirror number dependence in a prism- or grating- tuned ring laser cavity," *Appl. Optics*, vol. 25, pp. 2037–2038, July 1986.

[116] D. Ottaway *Personal Communication*.

[117] P. W. Milonni and J. H. Eberly, *Lasers*. USA: John Wiley Sons, Inc., 1988.

[118] Sciopt Enterprises, P.O. Box 20637, San Jose, CA 95160 USA, *Paraxia - Resonator and Optics Programs*, 2.0 ed., 1992.

[119] E. C. Guyer and D. L. Brownell, eds., *Handbook of Applied Thermal Design*. PA, USA: Taylor and Francis, 1999.

[120] ScillaSoft Consulting, NJ, USA, *AZTEC - A Thermoelectric Design/Selection Guide*, 2001. Version 2.0 H (Program).

[121] V. Karaganov, M. Law, M. Kaesler, D. G. Lancaster, and M. R. Taylor, "Engineering Development of a Directed IR Countermeasure Laser," *Proc. SPIE*, vol. 5615, pp. 48–53, 2004.

[122] A. D. Hays, G. Witt, N. Martin, D. DiBiase, and R. Burnham, "Ultra-compact diode-pumped solid-state lasers," *Proc. SPIE*, vol. 2380, pp. 88–94, 1995.

[123] Synrad, Inc., WA, USA, *Synrad Firestar T Series Lasers*, Aug. 2004. http://www.synrad.com/tseries/tseries.pdf , Brochure.

[124] R. C. Powell, *Physics of Solid-State Laser Materials*. New York, USA: Springer-Verlag, 1998.

[125] H. W. Ott, *NOISE REDUCTION TECHNIQUES IN ELECTRICAL SYSTEMS*. USA: John Wiley Sons, Inc., 2nd ed., 1988.

[126] P. Horowitz and W. Hill, *The Art of Electronics*. NY, USA: Cambridge University Press, 2nd ed., 1998.

[127] Lattice Semiconductor Corporation, *Analog Layout and Grounding Techniques*, Sep 1999. Application note: an6012-01.

[128] T. Williams, *The Circuit Designer's Companion*. Great Britain: Butterworth-Heinemann Ltd., 1991.

[129] A. C. Eckbreth, "Coupling Considerations for Ring Resonators," *IEEE J. Quantum Elect.*, vol. 11, pp. 796–798, Sep. 1975.

[130] P. B. Chapple, "Beam waist and M^2 measurement using a finite slit," *Opt. Eng.*, vol. 33, pp. 2461–2466, Jul. 1994.

[131] Spiricon Inc., UT, USA, *M^2-101*, Jun. 1995. Version 5.10 (Part No. 10582-001, Rev A).

[132] I. Freitag, D. Golla, S. Knoke, W. Schone, H. Zellmer, A. Tunnermann, and H. Welling, "Amplitude and frequency stability of a diode-pumped Nd:YAG laser operating at a single-frequency continuous-wave output power of 20 W," *Opt. Lett.*, vol. 20, pp. 462–464, Mar. 1995.

[133] R. Adler, "A Study of Locking Phenomena in Oscillators," *P. IEEE*, vol. 61, pp. 1380–1385, Oct. 1973.

[134] E. D. Black, "An introduction to Pound-Drever-Hall laser frequency stabilization," *Am. J. Phys.*, vol. 69, pp. 79–87, Jan. 2001.

[135] R. W. P. Drever, J. L. Hall, F. V. Kowalski, J. Hough, G. M. Ford, A. J. Munley, and H. Ward, "Laser Phase and Frequency Stabilization Using an Optical Resonator," *Appl. Phys. B*, vol. 31, pp. 97–105, Feb. 1983.

[136] M. W. Hamilton, "An introduction to stabilized lasers," *Contemp. Phys.*, vol. 30, pp. 21–33, Jan. 1989.

[137] D. Z. Anderson, "Alignment of resonant optical cavities," *Appl. Optics*, vol. 23, pp. 2944–2949, Sep. 1984.

[138] H. Kogelnik and T. Li, "Laser Beams and Resonators," *Appl. Optics*, vol. 5, pp. 1550–1567, Oct. 1966.

[139] P. W. McNamara, H. Ward, and J. Hough, "Laser frequency stabilisation for LISA: Experimental progress," *Adv. Space Res.*, vol. 25, pp. 1137–1141, 2000.

[140] C. D. Nabors, A. D. Farinas, T. Day, S. T. Yang, E. K. Gustafson, and R. L. Byer, "Injection locking of a 13-W cw Nd:YAG ring laser," *Opt. Lett.*, vol. 14, pp. 1189–1191, Nov. 1989.

[141] Piezomechanik GmbH, Munich, Germany, *Piezo-Mechanics: An Introduction*, Sep. 2003.

[142] Piezomechanik GmbH, Munich, Germany, *Piezo-Mechanical and Electrostrictive Stack and Ring Actuators: Product Range and Technical Data*, Oct. 2006.

[143] G. F. Franklin, J. D. Powell, and A. Emami-Naeini, *Feedback Control of Dynamic Systems*. USA: Pearson Prentice Hall, 5th ed., 2006.

[144] S. Timoshenko, D. H. Young, and W. Weaver, Jr, *Vibration Problems in Engineering*. USA: John Wiley Sons, Inc., 4th ed., 1974.

[145] Loctite Corporation, CT, USA, *Technical Data Sheet: Loctite Hysol Product E-30CL*, Aug. 2001.

[146] Ferroperm Piezoceramics A/S, Denmark, *Ferroperm Catalogue*, May 2003.

[147] R. C. Dorf and R. H. Bishop, *Modern Control Systems*. New Jersey, USA: Pearson Prentice Hall, 10th ed., 2005.

[148] A. B. Williams and F. J. Taylor, *Electronic Filter Design Handbook*. NY, USA: McGraw-Hill Inc., 3rd ed., 1995.

[149] B. J. J. Slagmolen, *Direct Measurement of the Spectral Distribution of Thermal Noise*. PhD thesis, The Australian National University, 2004.

[150] Piezomechanik GmbH, Munich, Germany, *Amplifiers, D/A Converters, Electronic HV-Switches for Piezoactuators*, Nov. 1998.

[151] Apex Microtechnology Corporation, Tucson, USA, *Datasheet: High Voltage Power Operational Ampliers, PA85 PA85A*, Jan. 1998.

[152] Revolution Education Ltd, Bath, UK, *PICAXE Manual www.picaxe.co.uk*, 2004. picaxe-manual1.pdf.

[153] R. Abbott and P. King, "Control System Design for the LIGO Pre-Stabilized Laser." LIGO Publication P010037-00-C, Nov. 2001. http://www.ligo.caltech.edu/docs/P/P010037-00.pdf.

[154] E. H. Huntington, B. C. Buchler, C. C. Harb, T. C. Ralph, D. E. McClelland, and H. A. Bachor, "Feedback control of the intensity noise of injection locked lasers," *Opt. Commun.*, vol. 145, pp. 359–366, Jan. 1998.

[155] M. Heurs, T. Meier, V. M. Quetschke, B. Willke, I. Freitag, and K. Danzmann, "Intensity and frequency noise reduction of a Nd:YAG NPRO via pump light stabilisation," *Appl. Phys. B - Lasers O.*, vol. 85, pp. 79–84, Jul. 2006.

[156] C. C. Harb, M. B. Gray, H. A. Bachor, R. Schilling, P. Rottengatter, I. Freitag, and H. Welling, "Suppression of the Intensity Noise in a Diode-Pumped Neodymium:YAG Nonplanar Ring Laser," *IEEE J Quantum Elect.*, vol. 30, pp. 2907–2913, Dec. 1994.

[157] T. J. Kane, "Intensity Noise in Diode-Pumped Single-Frequency Nd:YAG Lasers and its Control by Electronic Feedback," *IEEE Photonic. Tech. L.*, vol. 2, pp. 244–245, Apr. 1990.

[158] M. Heurs, V. M. Quetschke, B. Willke, and K. Danzmann, "Simultaneously suppressing frequency and intensity noise in a Nd:YAG nonplanar ring oscillator by means of the current-lock technique," *Opt. Lett.*, vol. 29, pp. 2148–2150, Sep. 2004.

[159] C. C. Harb, T. C. Ralph, E. H. Huntington, I. Freitag, D. E. McClelland, and H. A. Bachor, "Intensity-noise properties of injection-locked lasers," *Phys. Rev. A*, vol. 54, pp. 4370–4382, Nov. 1996.

[160] T. C. Ralph, C. C. Harb, and H. A. Bachor, "Intensity noise of injection-locked lasers: Quantum theory using a linearized input-output method," *Phys. Rev. A*, vol. 54, pp. 4359–4369, Nov. 1996.

[161] New Focus, Inc., Santa Clara, CA, USA, *Models 1801 and 1811 High-Speed Photoreceivers User's Manual.* 180413 Rev. F.

[162] E. H. Huntington, T. C. Ralph, and I. Zawischa, "Sources of phase noise in an injection-locked solid-state laser," *J. Opt. Soc. Am. B*, vol. 17, pp. 280–292, Feb. 2000.

[163] Hewlett Packard, CA, USA, *Understanding and Measuring Phase Noise in the Frequency Domain*, Oct. 1976. Application Note 207.

[164] C. Zhao, J. Degallaix, L. Ju, Y. Fan, D. G. Blair, B. J. J. Slagmolen, M. B. Gray, C. M. M. Lowry, D. E. McClelland, D. J. Hosken, D. Mudge, A. Brooks, J. Munch, P. J. Veitch, M. A. Barton, and G. Billingsley, "Compensation of Strong Thermal Lensing in High-Optical-Power Cavities," *Phys. Rev. Lett.*, vol. 96, p. 231101(4), Jun. 2006.

[165] C. Zhao, L. Ju, Y. Fan, S. Gras, B. J. J. Slagmolen, H. Miao, P. Barriga, D. G. Blair, D. J. Hosken, A. F. Brooks, P. J. Veitch, D. Mudge, and J. Munch, "Observation of three-mode parametric interactions in long optical cavities," *Phys. Rev. A*, vol. 78, p. 023807(6), Aug. 2008.

[166] M. R. Spiegel and J. Liu, *Schaum's Outline Series MATHEMATICAL HANDBOOK OF FORMULAS AND TABLES.* Singapore: McGraw-Hill International, 2nd ed., 1999.